UNIVERSITY OF ADELAIDE

PHYSICS DEPARTMENT

A STUDY OF PHOTOGRAPHIC IMAGES USING FOURIER TECHNIQUES

by

Rowland Edmund Little, B.Sc. Tech.
(WEAPONS RESEARCH ESTABLISHMENT, SALISBURY, S.A.)

THESIS SUBMITTED FOR THE
M.SC. DEGREE

1965

STATEMENT

I herewith state that this thesis does not contain any material which has been accepted for the award of any other degree or diploma in any University, or any material previously published or written by any other person, except when due reference is made in the text of the thesis.

Signed

TABLE OF CONTENTS

STUDY OF PHOTOGRAPHIC IMAGES USING FOURIER TECHNIQUES

SUMMARY

An optical Fourier analyser for analysing transparency functions has been constructed and found to give accurate results. A detailed description of the instrument, an adaption of a Michelson interferometer, including the mechanical units and electronic circuits used, is given.

An attempt to establish the amount of harmonics present when recording sine wave objects on the straight portion of the H & D curve of the photographic emulsion has been made. There are limitations to the validity of this treatment but for low contrast objects a good estimation of the harmonic content can be made. Working in terms of transmitted intensity it is shown that a simple theory, similar to that used in the design of audio power amplifiers, can be used to calculate the harmonic content of sine wave images. The results obtained from this theory are compared with those predicted from the straight part of the H & D curve and the values measured with the apparatus.

A method for calculating the frequency response of photographic emulsions is established and the response of four Ilford emulsions is measured.

Some applications of the instrument are suggested and discussed.

CHAPTER I

FOURIER METHODS AS APPLIED TO OPTICAL IMAGE FORMATION AND PHOTOGRAPHY

I.1 Introduction

In 1946 considerable impetus was given to the subject of assessing optical systems when Duffieux(1), suggested applying to them the same Fourier techniques which had already proved of great value in communication theory. Essentially, in terms of the electrical analogy, this meant considering an optical system as a passive network and deriving its transfer function to describe how it treated sine wave inputs, in this case of varying spatial frequency.

That optical systems could be considered in this fashion and a transfer function derived was quickly proved, both theoretically and practically. The advantage of this approach is that it gives an objective method for assessing an optical system which correlates well with subjective appraisals. Many of the rather puzzling observations in optics which had hitherto remained unexplained, for example reversal of contrast in the images of line gratings of certain frequencies, were now quite easily understood.

Since any incoherent object can be considered as a suitable combination of sine wave gratings of various frequencies, contrast and orientation, it is possible, knowing the transfer function of the system under investigation, to predict the form of the image of various simple objects e.g. slits and edges, and thus an assessment of the imaging properties of the system can be readily made. The term simple objects is used to imply that these objects have Fourier spectra which are one dimensional and easily deduced mathematically.

I.2 The object and image as a superposition of cosine-wave gratings

The final image produced by an optical instrument may be considered in a number of ways. It is possible, for example, to analyse it in terms of star images or, alternatively, to regard it as a superposition of cosine-wave gratings. A study of photographic images based on point sources was made by G. Haase and M. Muller (1960) (2) and the possibilities offered by information theory have also been considered. Making a number of assumptions the information content of a photographic image may be assessed numerically, as by Linfoot (1955) (3), but this approach is rather complicated and unfortunately its results are not easily interpreted in a useful manner. Finally one may specify the distribution of intensity in the image by its Fourier transform assuming that it is composed of incoherent cosine-wave gratings of intensity.

Consider an aerial image formed by a photographic lens. The light intensity usually varies in it in two dimensions, so that a function of two variables has to be used to represent the distribution of intensity. Let $B'_o\ (\xi'_o, \eta'_o)$ represent this distribution with reference to a rectangular set of coordinates (ξ'_o, η'_o) in the image plane (figure 1.1). Then $B'_o\ (\xi'_o, \eta'_o)$ will have a two-dimensional Fourier transform given by :

$$b'_o\ (S_o, t_o) = \iint B'_o\ (\xi'_o, \eta'_o) \exp\left\{-i\,2\pi\,(\xi'_o\, S_o + \eta'_o\, t_o)\right\} d\,\xi'_o\, d\,\eta'_o \qquad 1.1$$

which after a rotation of **axes** (ξ'_o, η'_o) through an angle $=\ \tan^{-1}$ (t_o/S_o) and putting $R = (S_o^2 + t_o^2)^{\frac{1}{2}}$ may be written :

$$b'_o\ (S_o, t_o) = \int \left\{ \int B'\ (\xi', \eta')\, d\,\eta' \right\} \exp\,(-i\,2\pi\,\xi' R)\, d\,\xi' \qquad 1.2$$

$B'\ (\xi', \eta')$ is simply the intensity function referred to the new axis and R the spatial frequency. If the integrated intensity along the η axis is denoted by :

$$B'\ (\xi') = \int B'\ (\xi', \eta')\, d\,\eta' \qquad 1.3$$

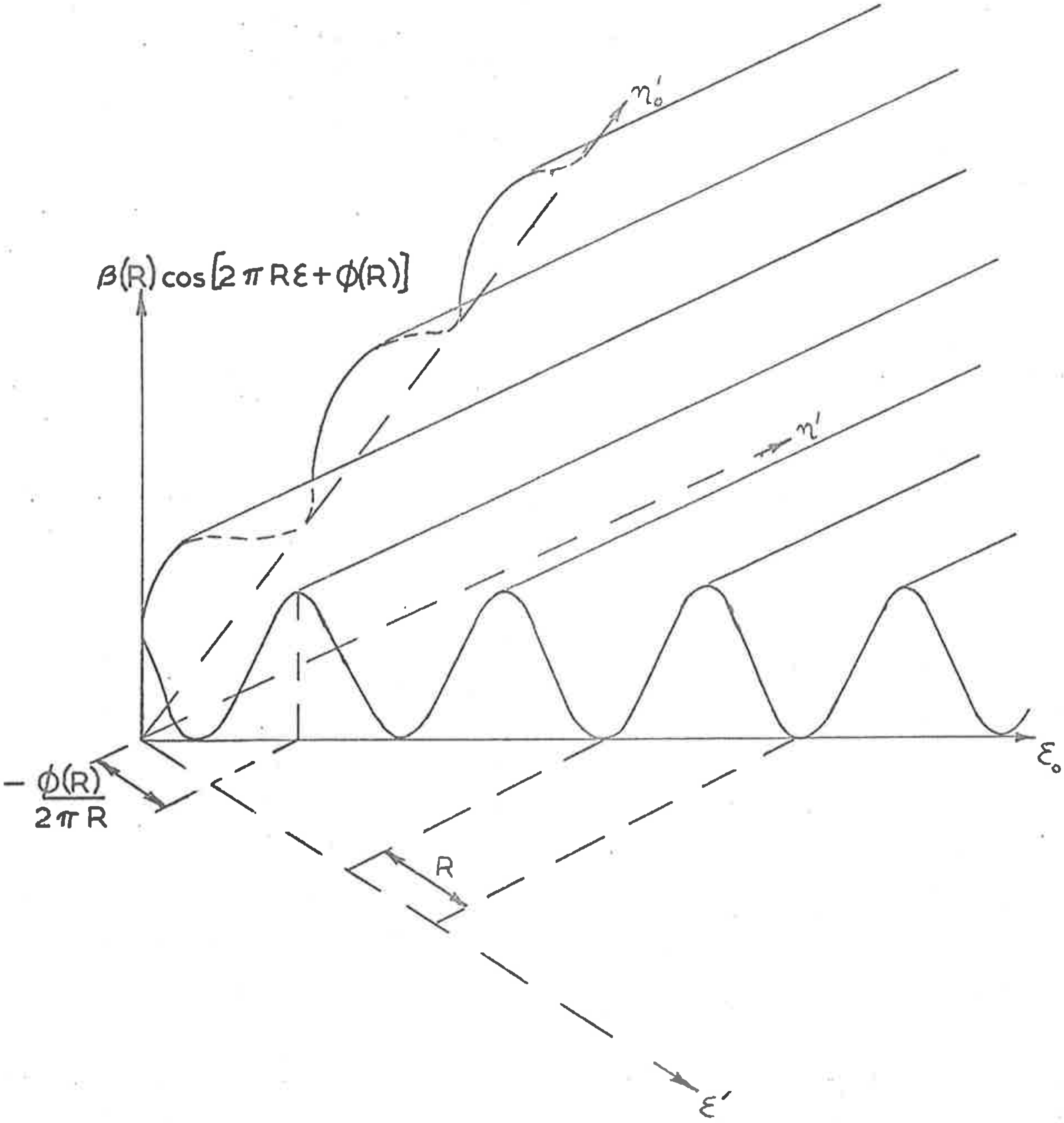

FIGURE 1.1

the two dimensional transform $b'_o\,(S_o, t_o)$ may be seen to be obtainable from the one dimensional transform :

$$b'\,(R) = \int B\,(\xi')\,\exp\,(-i\,2\,\pi\,R\,\xi')\,d\,\xi' \qquad 1.4$$

when this is known as a function of R for different azimuths ψ, since $b'\,(R) = b'_o\,(R\,\mathrm{Cos}\,\psi,\ R\,\mathrm{Sin}\,\psi)$. This interpretation shows that any object and image may be regarded as a superposition of cosinusoidal line gratings of variable opacity of different wavelength frequency and orientation (figure 1.1).

This representation of the aerial image shows that to evaluate image quality it should be sufficient to know how different spatial frequencies in different azimuths for each image point are transferred by the optical system from the object to the image plane.

I.3 The frequency response of lens systems

Any aerial image may be considered as a suitable combination of cosine-wave gratings. Assume a grating like object across which the intensity varies according to the formula (figure 1.2)

$$B\,(\xi) = \alpha + \beta\,\mathrm{Cos}\,2\,\pi\,R\,\xi \qquad 1.5$$

Its image will have an intensity distribution of the form :

$$B'\,(\xi') = \alpha' + \beta'\,\mathrm{Cos}\left\{2\,\pi\,R\,\xi' + \theta\,(R)\right\} \qquad 1.6$$

Two conditions must be fulfilled to obtain this result. Firstly, the system should be isoplanatic, which requires the aberrations to change slowly over the image plane. Secondly, the intensity distribution in the image should be found by the simple addition of the intensities produced by each elementary area of the object, this means that the illumination must be incoherent.

If these two conditions hold, the optical system may be placed in that class known as linear systems.

Formally a linear system may be described in the following manner.

Let I (u), the input to a physical system, denote a function depending on the value of some quantity u, and let 0 (u′) be the resulting output specified by its dependence on u′. The conditions for linearity are that two inputs $I_1(u)$, $I_2(u)$ which give separately outputs $0_1(u')$, $0_2(u')$ will give an output $0_1(u') + 0_2(u')$ for an input $I_1(u) + I_2(u)$ or symbolically :

$$I_1(u) + I_2(u) \rightarrow 0_1(u') + 0_2(u') \qquad 1.7$$

If the input is "delayed" by a quantity u_o, the output is similarly "delayed", in symbols

$$I\ (u - u_o) \rightarrow 0\ (u' - u_o) \qquad 1.8$$

If these two conditions are fulfilled the system is linear. In image forming systems condition (1.7) requires the object to be incoherent and (1.8) expresses the isoplanatic condition.

The contrast in the object cosine-wave (1.5) is measured by the ratio β/α, figure 1.2, and that in the image by β'/α'. The ratio of the image **and the object contrast** is denoted by T (R, ψ), where ψ is the azimuthal angle between the lines of the grating and the meridian plane of the optical system forming the image. Thus $T\ (R, \psi) = (\beta'/\alpha')/(\beta/\alpha)$. The maxima of (1.6) are displaced laterally relative to those of (1.5) by an amount $\xi = -\theta\ (R)/2\pi R$.

These two quantities may be usefully combined to form a single complex number, namely :

$$D\ (R, \psi) = T\ (R, \psi) \exp i\, \theta\ (R, \psi) \qquad 1.9$$

This complex number is referred to as the frequency response of the system. If D (R, ψ) is known for any given region of the image plane as a function of spatial frequency R and azimuth ψ, then the image forming properties of the optical system are completely specified. It is now possible to multiply the amplitude of each object cosine-wave grating by T (R, ψ) and shift its position by an amount $\delta\xi' \doteq -\theta\ (R, \psi)/2\pi R$

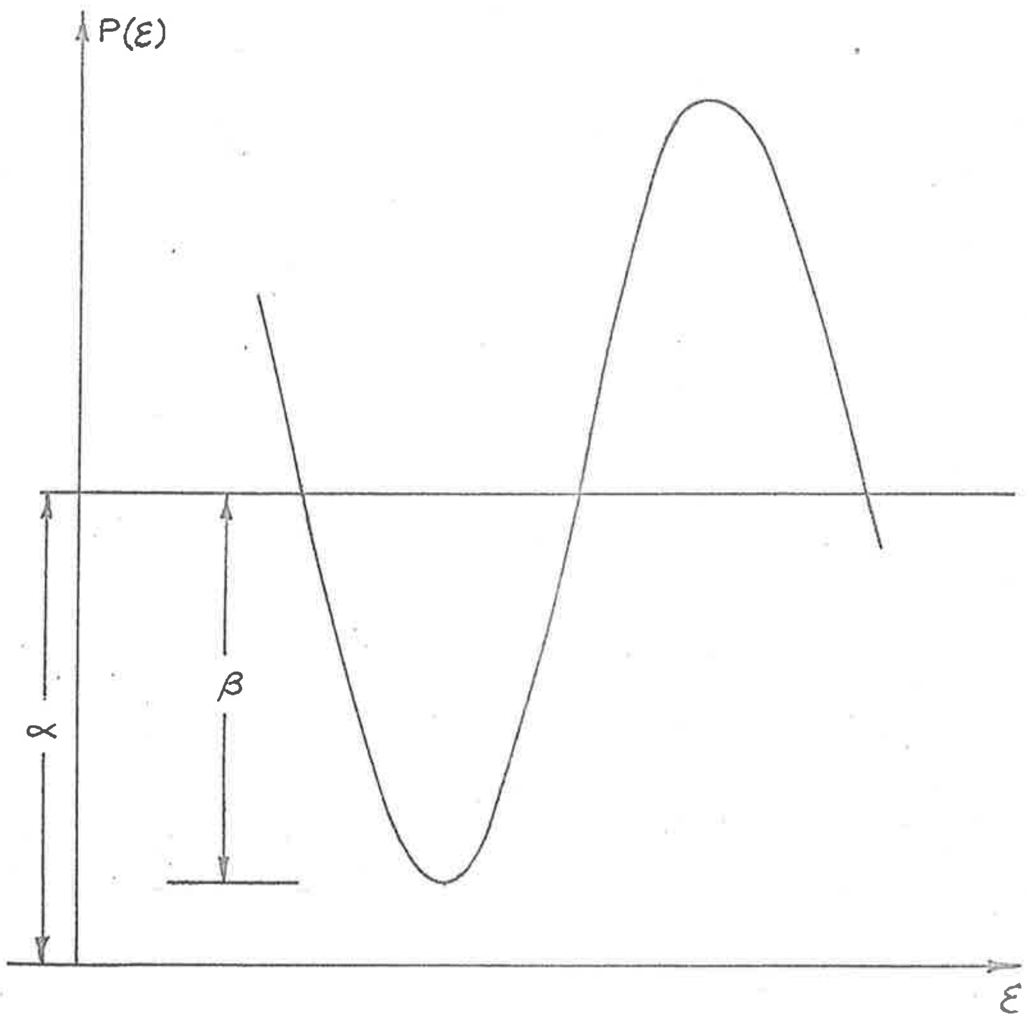

FIGURE 1.2

This is illustrated in figure 1.3.

The contrast transfer function T (R, ψ) is identically equal to unity, when R = 0. It will fall to zero at a certain spatial frequency, R_{max}, which is called the limit of resolution. Contrast, usually reversed, may appear in the image at frequencies greater than R_{max} giving rise to spurious resolution.

The frequency response in the presence of defect of focus has been calculated by Hopkins(4) (1955), for astigmatism by De(5) (1955), and for spherical aberration and coma by Goodbody(6) (1959). Many of these results have been verified by K.G. Birch(7) (1960) using a scanning method. An automatically recording interferometer has also been used by D. Kelsall(8) (1959). This is used in monochromatic light and besides T (R, ψ), the phase shift θ (R) has been measured in some cases.

I.4 Frequency response as applied to photographic image recording

The application of frequency response methods to the actual recording of an aerial image, specified in terms of its Fourier transform, by a photographic emulsion presents several peculiarities. Firstly the problem is simplified since under most conditions, excluding very large incidence angles of the image forming light, no spatial phase shift takes place between the incident cosine-wave and recorded cosine-wave. Unfortunately the problem is complicated by the non linear properties of the photographic emulsion. These non linearities are present due to the relationship between exposure and resulting density which is characteristic of all photographic materials. If the input signal is described in the symbolic manner of (1.7), the two inputs correspond to variations of light intensity expressed in terms of exposure, the output signal corresponds to transmitted intensity. The effect of the two exposures will not **ever** give a transmitted intensity equal to the sum of the intensities obtained from the two inputs acting separately.

DISTRIBUTION OF INTENSITY IN THE IMAGE OF A COSINE GRATING.

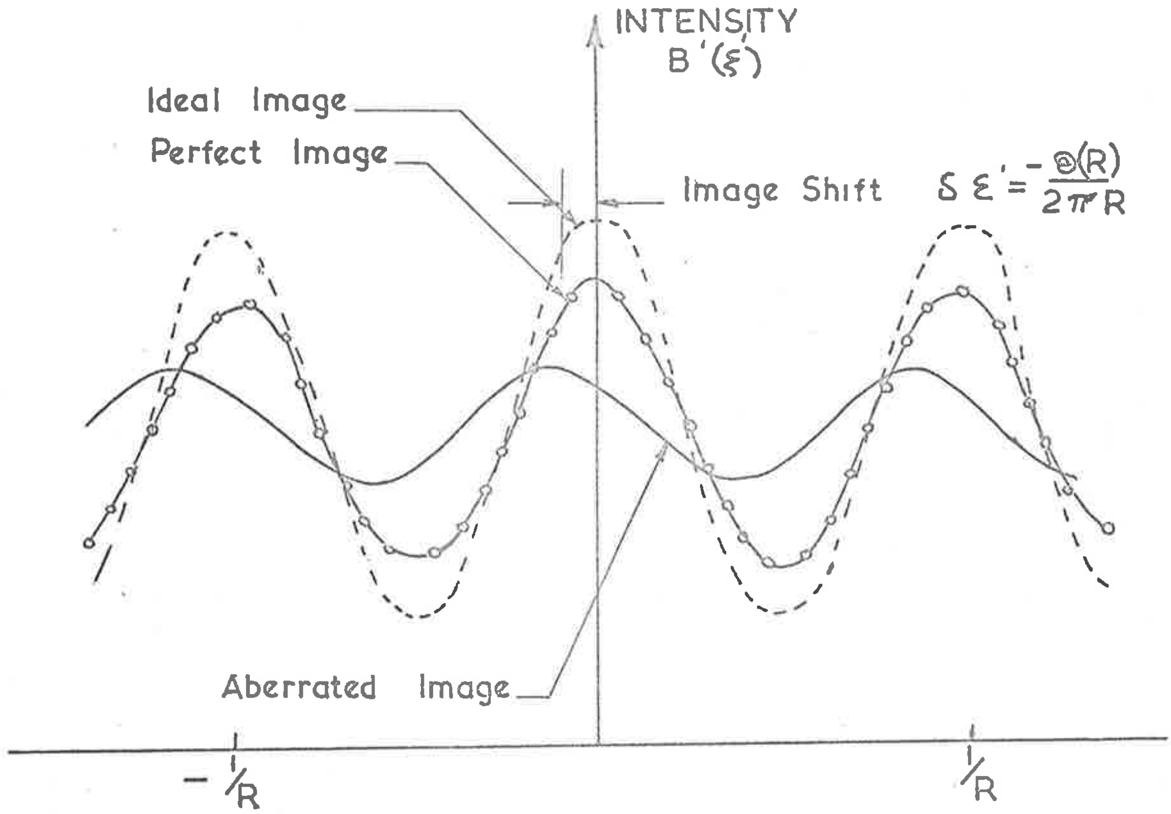

DISTANCE ACROSS IMAGE ε'

FIGURE 1.3

To overcome this difficulty Frieser(9) (1935) showed that the complete photographic process could be considered in two stages. The first consists of the actual exposure of the photographic emulsion to light, together with, in this context, the linear scattering of light in the emulsion layer. Thus the original "printed-on" exposure results in a different distribution of light in the emulsion which is called the "effective exposure". For cosine-wave test objects the variation of illumination in the effective exposure will be similar to that in the printed-on exposure but will have smaller amplitude, that is it will be of lower contrast. On development the effective exposure gives rise to a density distribution whose form depends on the development conditions. In this stage there is a non-linear relationship between the effective exposure and the resulting density. Frieser obtained the form of the effective exposure from measured density distributions in the photographic images of cosine-wave test objects using the H & D macrocharacteristic curve to relate them. That is the curve relating density and $\log_{10}$ (exposure). Provided no pronounced neighbourhood effect is present, a density distribution, which contains in fact both the fundamental of the cosine-wave test object and harmonics introduced by the non-linearity, leads to an effective exposure of cosinusoidal form (figure 1.4).

Frieser further showed that the effective exposure of a cosine-wave has the same mean value as the printed-on exposure, but that it is of reduced amplitude variation, that is of lower contrast. The ratio of the amplitude of the effective exposure to that of the printed-on exposure was shown to be a function of the spatial frequency of the test object - the relation between the two constituting the frequency response of the emulsion.

If b'' (R) denotes the Fourier spectrum of an "effective" image, the original object having a spectrum b (R) then :

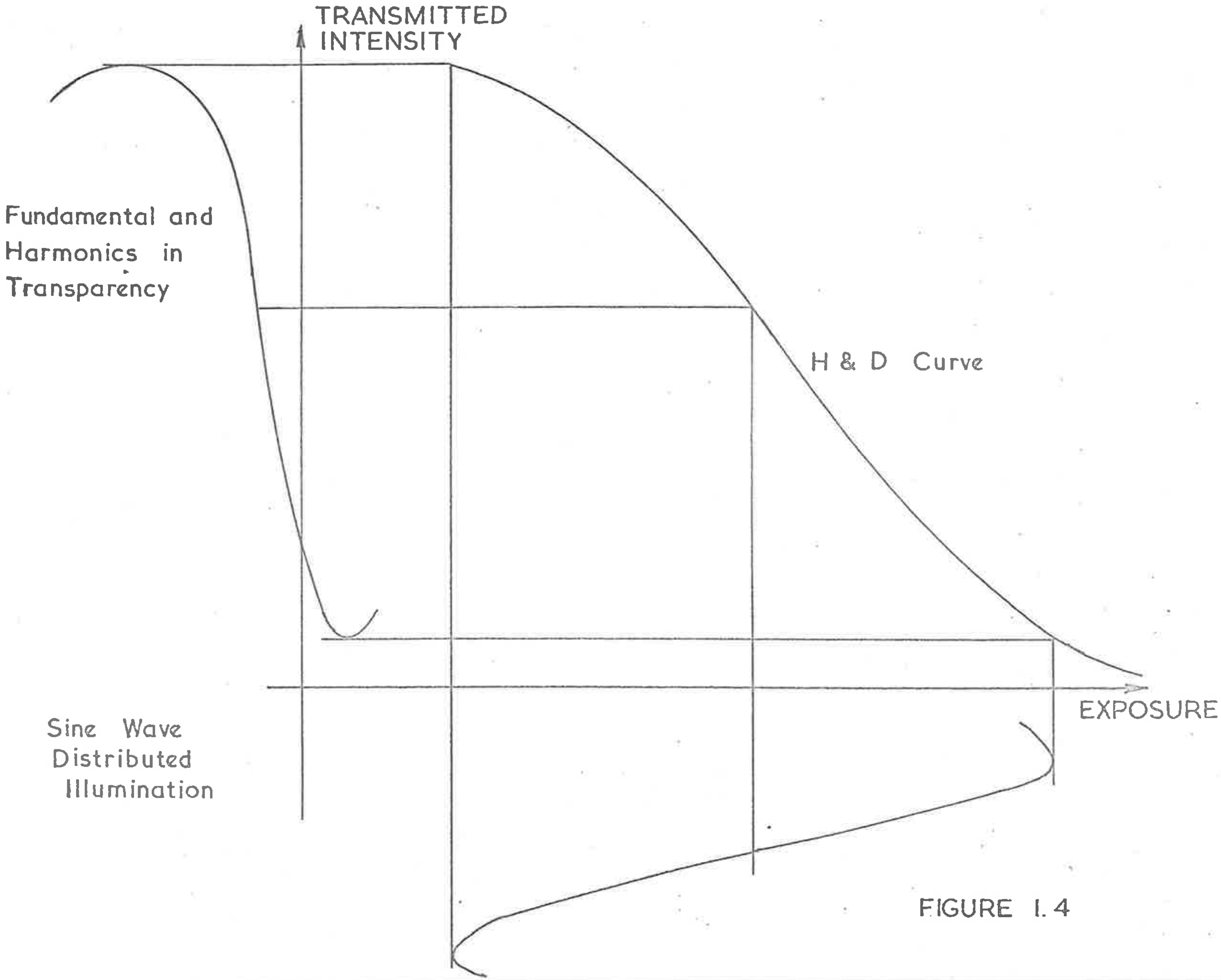
TRANSMITTED
INTENSITY
Fundamental and
Harmonics in
Transparency
H & D Curve
EXPOSURE
Sine Wave
Distributed
Illumination

FIGURE 1.4

where D (R, ψ) is the frequency response of the imaging system and E (R) the response of the emulsion.

Unfortunately the "effective image" cannot be observed and must be developed in order to be investigated. In this process linearity is lost and harmonics are detectable together with the fundamental spatial frequencies.

I.5 The non-linear part of the photographic process

As already mentioned, due to the relationship between exposure and resulting density, the photographic image is distorted. In the case of sine wave objects this distortion takes the form of an introduction of harmonics into the image.

If an objective method of evaluating photographic image quality is to be established, knowledge of the amount of harmonic distortion which is likely to occur and the factors influencing it is important.

In approaching the problem of harmonic distortion introduced in the photographic image of sine wave objects, it is useful to establish an analogy between the operation of a triode valve and the photographic process. Let us assume that a voltage signal is applied through an attenuating low pass filter to the grid of a triode valve, and let the frequency spectrum of the signal be given by equation (1.4). The relation between the grid voltage and anode volts is non-linear and therefore the anode volts will contain not merely all the components, b (R), of the input signal but also their harmonics. If one substitutes transmitted intensity for anode volts, b(R) for grid input signal, the H & D curve in linear scale for the static characteristic of a triode valve, then a comparison between the frequency response of an emulsion and the attenuation characteristics of the amplifying stage with a low pass input filter completes the analogy. Having established this analogy the same general approach as is used to analyse the performance of audio frequency amplifiers may be adopted to study the non-linearity of the photographic process, and the same numerical methods applied.

Using these techniques it should be possible to show to what approximation the photographic process may be regarded as linear.

The straightness of the H & D curve could also be investigated with the view of predicting harmonic distortion by simply measuring the slope, or γ as it is generally known, of this curve.

It should be possible to provide quantitative measurements on the influence of exposure to the quality and microstructure of the image.

The fidelity of tone reproduction may be evaluated by finding the amount of harmonic distortion present in the final photographic print.

If an image is to be transmitted by a delay recording system the method may be used not only to choose an exposure to obtain maximum modulation of the carrier frequency but to introduce a correction system to eliminate any non-linearity present.

In assessing image quality of a system a factor, which is not very well understood, is the contribution of different spatial frequencies to the final image quality. Various experiments have been conducted(10) to solve this problem mainly from the point of view of attempting to correlate image quality and the transfer function of the system. Although many of these have some qualitative merit a direct relationship between image quality and transfer function has not been established. In most of these experiments assessment of the extent to which different spatial frequencies were present in the object being photographed was not made. Thus, although the transfer function was known, the spatial frequency range of its effectiveness was not obvious and a vital link in the experiment was missing. Also the effect of the non-linearity of the photographic process was ignored although it could have a pronounced effect on the Fourier content of the final image. Both of these shortcomings could be overcome using the apparatus to be described and possibly a better understanding of the relationship between frequency content and acceptability of images could be found.

REFERENCES

1.	Duffieux, P.M. (1946)	"L'entegrale de Fourier et ses applications a l'optique". Private publication, Rennes.
2	Haase, Muller (1960)	Optik, 17, 1.
3	Linfoot, E.H. (1955)	J.O.S.A., 45, 808.
4	Hopkins, H.H. (1955)	Proc. Roy. Soc., A, 231, 91.
5	De, M. (1955)	Proc. Roy. Soc., 71, 231.
6	Goodbody, A.M. (1958)	Proc. Phys. Soc., 72, 411.
7	Birch, K.G. (1958)	Acta Electronica, 2, 271.
8	Kelsall, D. (1959)	Proc. Phys. Soc., 73, 465.
9	Frieser, H. (1935)	Kinotechnik, 17, 165.
10	Higgins, G.C., Lambert, R.L., Wolfe, R.N. (1959)	Reprints of the 5th meeting and conference of I.C.O.

CHAPTER II

THE FOURIER SPECTRA OF TRANSPARENCY FUNCTIONS

II.1 Methods of determining experimentally the Fourier transforms of transparency distributions

The determination of the Fourier spectrum of a transparency function can be made in several ways. The method which immediately comes to mind is to scan the transparency with a microphotometer and analyse the resulting trace numerically. Besides being a rather tedious method, irregularities, introduced by the grain structure of most emulsions considered, limit the accuracy with which the transform can be obtained. The numerical computation takes an appreciable time especially if a digital computer is not available. In the initial stages of the investigation when the apparatus was still being assembled, this method was employed. Fortunately the author had had need some two years ago to write a programme for the IBM 7090 digital computer to enable one to find the Fourier spectrum of optical spread functions; this was easily adjusted to suit the present needs. It is of interest to note that it is possible to do in a number of minutes on the computer calculations which take a trained operator some weeks to accomplish on a desk calculator.

A second method which has been used successfully by a number of authors makes use of the auto-correlation function. The auto-correlation function $\Phi\ (\xi_0)$, of a function $B\ (\xi)$, can be defined as the product of the function with itself displaced by a distance ξ_0, that is :

$$\Phi\ (\xi_0) = \int_{-\infty}^{\infty} B\ (\xi)\ .\ B\ (\xi - \xi_0)\ d\ \xi \qquad 2.1$$

A physical interpretation of this can be given as follows. Let two identical transparencies be uniformly illuminated. The amount of light passing through the two copies will change when one is shifted with respect to the other, and the light flux can be measured by means of a photocell. The transmission is obviously a maximum for no shift since opaque areas overlap corresponding opaque areas but will generally decrease when a shift is made causing opaque areas to overlap transparent ones.

We must return to equation 2.1 to see how this phenomenum can help us in finding the Fourier spectrum of the transparency. We have :

$$\Phi(\xi_0) = \int_{-\infty}^{\infty} B(\xi)\, B(\xi - \xi_0)\, d\xi$$

where $$B(\xi - \xi_0) = \int_{-\infty}^{\infty} b(R) \exp\left\{ i\, 2\pi R(\xi - \xi_0)\right\} dR \qquad 2.2$$

and $$b(R) = \int_{-\infty}^{\infty} B(\xi) \exp\left\{ -i\, 2\pi R\xi \right\} d\xi \qquad 2.3$$

$$b(-R) = \int_{-\infty}^{\infty} B(\xi) \exp\left\{ i\, 2\pi R\xi \right\} d\xi \qquad 2.4$$

Therefore $$\Phi(\xi_0) = \int_{-\infty}^{\infty}\int B(\xi)\, b(R) \exp(i\, 2\pi R\xi) \exp(-i\, 2\pi R\xi_0)\, d\xi\, dR \qquad 2.5$$

Changing the order of integration and using equation 2.4

$$\Phi(\xi_0) = \int_{-\infty}^{\infty} b(R)\, .\, b(-R) \exp(-i\, 2\pi R\xi_0)\, dR \qquad 2.6$$

If $B(\xi)$ is real, its Fourier transform satisfies

$$b(-R) = b^*(R) \qquad 2.7$$

Then $$\Phi(\xi_0) = \int_{-\infty}^{\infty} |b(R)|^2 \exp(-i\, 2\pi R\xi_0)\, dR \qquad 2.8$$

or $$\varphi(R) = |b(R)|^2 \qquad 2.9$$

$\varphi(R)$ being the Fourier transform of $\Phi(\xi_0)$.

This result is often referred to as the Weiner-Khintchine theorem. The spectrum of the auto-correlation function of $B\ (\xi)$ is the squared modulus of the spectrum of $B\ (\xi)$. $\varphi\ (R)$ is sometimes called the power spectrum, it relates only to the squared modulus of $b\ (R)$ the phase shift in the latter being lost. Several devices have been proposed for the measurement of $\Phi\ (\xi_o)$. Some avoid the difficulty of preparing identical transparencies, achieving the lateral displacement by the use of coner cubes or tilting mirrors e.g Fellgett (1953), Kovasznay and Arman (1957). A distinct disadvantage of this method is that again it leaves us with a function to be numerically analysed before we arrive at the square of the quantity we require. An advantage over direct scanning is that large areas can be used and noise due to grain is less significant.

A direct method, known as the interferometric method, consists of measuring the total light flux passing through an extended area of a plate, or film, already developed. The flux is simply related to the amplitudes of the components of different spatial frequency occurring in the recorded photographic image. If $B\ (\xi)$ is the integrated transparency along the ordinate at the distance ξ from the origin, the real and imaginary parts, R_e and I_m, of the spectrum $b\ (R)$ are given by :

$$\begin{matrix} R_e \\ I_m \end{matrix} \left\{ b\ (R) \right\} = \int_{-\infty}^{\infty} B\ (\xi) \begin{matrix} \text{Cos} \\ \text{Sin} \end{matrix} \left\{ 2\pi R \xi \right\} d\ \xi \qquad 2.10$$

This shows that if we illuminate a plate of transparency $B\ (\xi)$ with a cosinusoidal distribution of light $R_e \left\{ b\ (R) \right\}$ and $I_m \left\{ b\ (R) \right\}$ can be found for a given R by displacing the fringes. The complete transform is determined by varying R through the complete frequency range. This being the method employed in the instrument made, it will now be discussed in more detail.

II.2 The interferometric method

(a) Theory

Let P (ξ) be the distribution of intensity in two beam interference fringes, having frequency R lines/mm and let α be the mean intensity and β the amplitude of variation. The ratio β/α is the Michelson visibility or contrast of the fringe pattern and

$$P(\xi) = \alpha + \beta \operatorname{Cos} 2\pi R \xi \qquad 2.11$$

Provided the transparency function is taken to be zero outside the region to be analysed the total light flux transmitted through a photographic plate illuminated by the fringes is given by :

$$F(\xi_o, R) = \int_{-\infty}^{\infty} B(\xi) \left\{ \alpha + \beta \operatorname{Cos} (2\pi R (\xi - \xi_o)) \right\} d\xi \qquad 2.12$$

where B (ξ) is the integrated transparency as defined before, ξ_o being the displacement of the fringe system along the ξ axis.

If the above expression for F (ξ_o, R) is written in the form :

$$F(\xi_o, R) = \alpha \int_{-\infty}^{\infty} B(\xi) d\xi + \beta \operatorname{Cos}(2\pi R\xi_o) \int_{-\infty}^{\infty} B(\xi) \operatorname{Cos}(2\pi R\xi) d\xi$$

$$+ \beta \operatorname{Sin}(2\pi R\xi_o) \int_{-\infty}^{\infty} B(\xi) \operatorname{Sin}(2\pi R\xi) d\xi \qquad 2.13$$

it is possible to write the various integrals in terms of the Fourier transforms of the transparency function. If C (R) and S(R) are the magnitudes of the real and imaginary parts of the Fourier spectrum b (R), then

$$C(R) = \int_{-\infty}^{\infty} B(\xi) \operatorname{Cos}(2\pi R\xi) d\xi$$

$$2.14$$

$$S(R) = \int_{-\infty}^{\infty} B(\xi) \operatorname{Sin}(2\pi R\xi) d\xi$$

The spectrum b (R) whose modulus is $|b(R)|$ and whose argument is θ (R)

$$b(R) = |b(R)| \exp(i\,\theta(R)) \qquad 2.15$$

may be written as

$$b(R) = C(R) - i\,S(R) \qquad 2.16$$

and then

$$F(\xi_o, R) = \alpha\, b(o) + \beta \left\{ C(R) \operatorname{Cos} 2\pi R\xi_o + S(R) \operatorname{Sin} 2\pi R\xi_o \right\}$$

The modulus of the Fourier Spectrum is

$$|b(R)| = \left\{ |C(R)|^2 + |S(R)|^2 \right\}^{\frac{1}{2}}$$

and the phase shift

$$\theta(R) = \tan^{-1} (S(R)/C(R))$$

is the argument of b (R), with the condition that

$0 \leqslant \theta(R) \leqslant \pi$

Finally using the above definitions 2.13 may be written as :

$$F(\xi_o, R) = \alpha\, b(o) + \beta\, |b(R)| \operatorname{Cos} \left\{ 2\pi R\,\xi_o - \theta/R) \right\} \qquad 2.17$$

As ξ_o is made to vary, the total light flux transmitted has a zero frequency component, α b (o), and a component of frequency proportional to R, of amplitude β |b (R)|. If the phase of this alternating component is measured, it will give the lateral phase shift θ (R). The modulus of b (R) describes the relative strength of this frequency in the region of the photograph explored. When normalized to make |b (o)| = 1, this modulus will be denoted by T (R). T (R) is called the frequency density and then, apart from a photometric scale factor, the total flux transmitted by the transparency B (ξ) is :

$$F(\xi_o, R) = \alpha + \beta\, T(R) \operatorname{Cos} (2\pi R\,\xi_o - \theta(R)) \qquad 2.18$$

(b) General requirements

The above expressions shows that the Fourier spectrum, T (R) exp (i θ (R)), of a transparency function may be found by measuring the amplitude of the alternating component of the total light flux transmitted when it is scanned with cosinusoidal fringes of varying spatial frequency, R.

There are certain precautions which must be observed to ensure accurate measurements :

(i) All the light passing through the illuminated region must be gathered onto the photocathode of the receptor.

(ii) The contrast of the scanning fringes must remain constant as the spatial frequency is varied or the relationship between contrast and frequency known so that a correction coefficient may be introduced.

(iii) The size of the limiting mask, when small areas are being scanned, must be an integral number of periods of the scanning frequency, this is especially important for low frequencies. The theory behind this condition is discussed later in the section on measurement procedure.

II.3 A Fourier analyser based upon the interferometric method

An apparatus operating on the preceding principles was constructed by Vienot (1959) and improved by Wilezynski (1960). Combining the ideas and discoveries of both a similar apparatus has been constructed which in its final form constitutes an automatic Fourier analyser for transparency functions. A schematic diagram of the instrument can be seen in figure 2.1.

The apparatus is fully automatic and to be so certain conditions must be satisfied. It must be possible to change the spatial frequency R continuously and at the same time linearly displace the fringe position ξ_o. Only if these conditions are satisfied and the Michelson visibility, $\frac{\beta}{\alpha}$, remains constant will the mean value of the

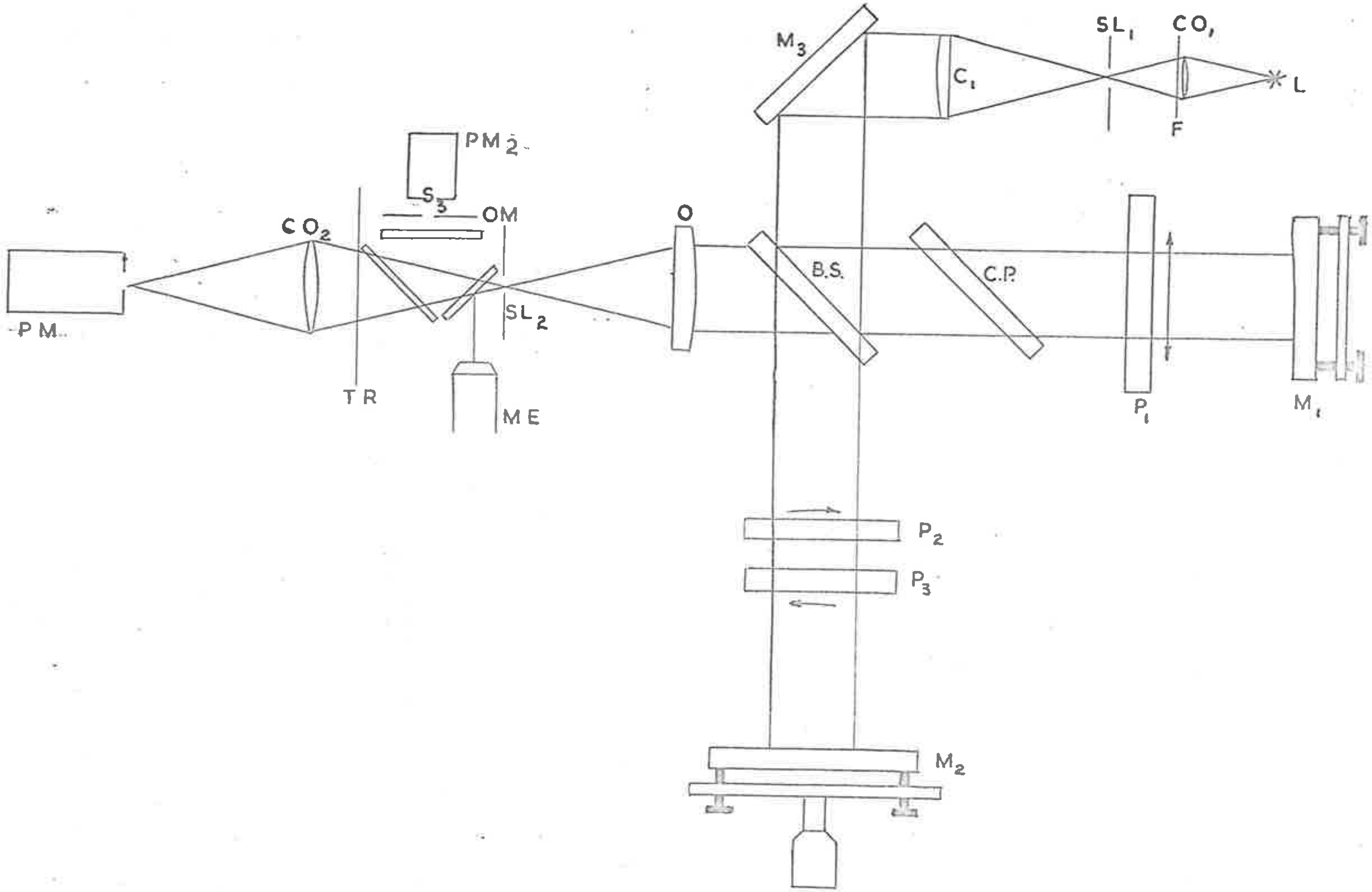

FIGURE 2.1 SCHEMATIC DIAGRAM OF APPARATUS.

apparatus consists of three main parts :

(i) A Michelson interferometer

(ii) Optical mechanical devices for changing the spatial frequency and for shifting the fringes.

(iii) Electronic and recording units.

II.3.1 The interferometer (figure 2.1)

The apparatus is located in an underground air raid shelter which serves to isolate it from vibrations which would normally be encountered within a laboratory. Stability of ambient temperature is also improved and the drift of adjustment due to temperature fluctions is minimized.

The interferometer consists of two aluminium coated mirrors M_1 M_2, a dielectric beam splitter and a bloomed compensator plate. A collimated beam of light, monochromatic at $\lambda = 5461A^{0}$, is formed by the collimator lens C_1, at the focus of which is a slit illuminated by a low pressure mercury lamp through a green filter. This beam is directed into the interferometer by mirror M_3.

To vary the spatial frequency R a pair of equal small angle prisms P_2 P_3, capable of rotating in opposite senses, are located in one arm of the interferometer. A third prism P_1, located in the other arm, is capable of being reciprocated linearly and serves to shift the fringes.

An objective O images the fringes which are located on the mirror M_1 or M_2 onto the transparency TR.

Each component will now be described in more detail.

The light source L is a WOTAN HG2 medium pressure mercury lamp supplied from a d.c. source. This lamp is designed primarily to run from an a.c. source but it has been found to run on d.c. quite satisfactorily. With this apparatus it is essential that the source be best illustrated by considering the zeros in the spectrum of a slit. At these positions the slit width is an equal number of fringe spacings and the transmitted intensity when scanning contains no alternating component. However, if the light is being flashed on and off at a frequency of 100 c/s as is the case with arc lamps run from an a.c. source there will be an alternating component at this frequency in the transmitted intensity and thus it will be impossible to obtain true zeros.

Prior to using this particular lamp several others were tried, in particular an OSRAM medium pressure lamp ML/D2.0 supplied again from a d.c. source. This lamp proved to be quite satisfactory except for the fact that its intrinsic brightness is low. This makes it difficult to adjust the instrument with the room lights on and makes exposure times very long when photographing fringes. Also if it is necessary to scan with fringes of high contrast the collimator slit has to be very narrow with a consequent reduction in the mean light level. This results in a poor signal to noise ratio which is an undesirable feature. These disadvantages are all overcome by using the HG2 lamp but the ML/D2.0 does provide a readily available alternative lamp for most scanning purposes.

Initially to overcome the light level problem a high pressure MAZDA 200/250 V, 250 W d.c. ME/D lamp was used but unfortunately the half width of its spectral green line proved to be too great. Even when the fringe spacing is kept constant the sinusoidally varying component of the light flux passing through the transparency varies slightly with a frequency equal to twice that of the cam rotation which moves prism P_1. This is because the fringes vary in contrast with the position of P_1, this being more appreciable when the half width of the spectral line is large and the contrast more critically influenced

Hopkins (1957) has given a relationship between the optical path difference of the two arms $(L_1 - L_2)$ and the half width $(\delta\lambda)$ of the spectral line. The chromatic coherence factor remains ≥ 0.90 if the conditions satisfy :-

$$(L_1 - L_2) \leq \frac{\lambda^2}{4\delta\lambda} \qquad 2.19$$

If initially the two arms are made equal in optical path length with the prism P_1 at its centre position, then the path difference introduced by moving it to either of its extreme positions is of the order of 0.04 mm. Now the half width of the spectral green line (λ = 5461A^{o}) of a medium pressure mercury lamp is about 2.2A^{o} which means that the tolerance on the optical path difference is of the order of 0.4 mm. With the prism P_1 we are well within this tolerance and as expected there is no appreciable change in fringe contrast with prism position when a medium pressure lamp is used. However with the MAZDA lamp the contrast varied by as much as 0.55, being 0.90 with the prism at its centre position and falling to 0.35 at its extreme positions. Clearly its spectral half width is too great and for this reason it was discarded.

The slit SL_1, situated at the focus of the collimator C_1, is a Hilger Spectrometer slit capable of adjustment in microns. It is illuminated by the light source through a condenser CO_1 and a Wratten 77A filter, thus providing a monochromatic slit source.

The dielectric beam splitter, compensator, and two end mirrors are in mounts rigidly attached to a cast iron surface table. The mounts have adjustments so that the components **can rotate about** two perpendicular **axes** . The mirror M_2 is also on a kinematic slide and can be moved backwards or forwards by means of a micrometer screw. This facility is required in order to be able to make the two arms of the interferometer equal in optical path length, the condition for maximum contrast of the fringes. The contrast can be varied by moving this mirror and introducing a path difference between the two arms.

The spatial frequency is changed by means of a pair of identical rotating prisms P_2, P_3 placed in one arm of the interferometer. They are rotated in opposite directions and together are equivalent to a variable angle prism. The resulting frequency of the fringes obtained is given by the formula :

$$R = \frac{4\ (n - 1)\ \text{Sin}\ \alpha\ \text{Sin}\ \varphi}{\lambda} \qquad 2.20$$

where α is the angle of each prism, φ the angle of rotation of the prisms from the position in which $R = 0$, λ the wavelength of the light used, and n the refractive index of the glass.

Equation 2.20 indicates that if one desires to change the frequency R linearly, the angle of rotation must be varied such that its sine varies linearly with time. This is achieved in the following manner. With reference to figure 2.2 the arm A is reciprocated linearly with time by the archimedean cam C which is driven by a synchronous motor. Connected and perpendicular to this arm is a bearing slot in which runs a pin connected to the gear wheel G_1. The motion imparted to this gear wheel by the arm is such that the sine of the angle of rotation varies linearly. This motion is transferred to two other gears G_2 and G_3 which hold the prisms P_2 and P_3. G_2 is driven directly by G_1 and G_3 is driven through an idler, thus G_2 and G_3 rotate in opposite directions and in the required manner. The result is that any records on a pen recorder are easier to interpret. The whole unit can be seen in figure 2.3. Great care has to be taken in mounting the prisms and aligning the bearings in which they run so that the fringe pattern remains vertical when the prisms are rotated. Firstly the axes of the two bearings are made parallel, this is achieved by placing an optical flat on their surfaces and adjusting

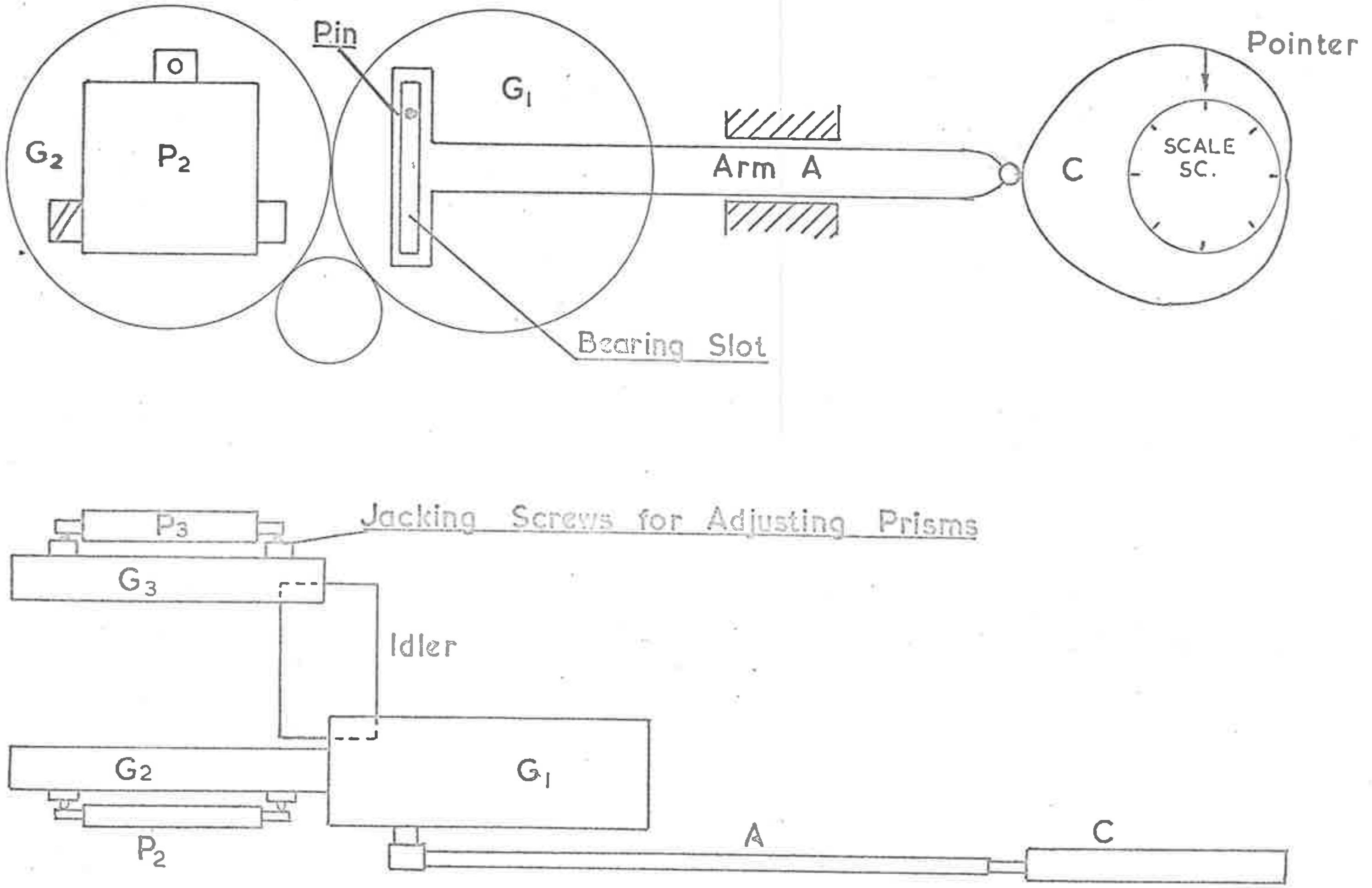

FIGURE 2.2. SCHEMATIC DIAGRAM OF FREQUENCY CHANGING UNIT.

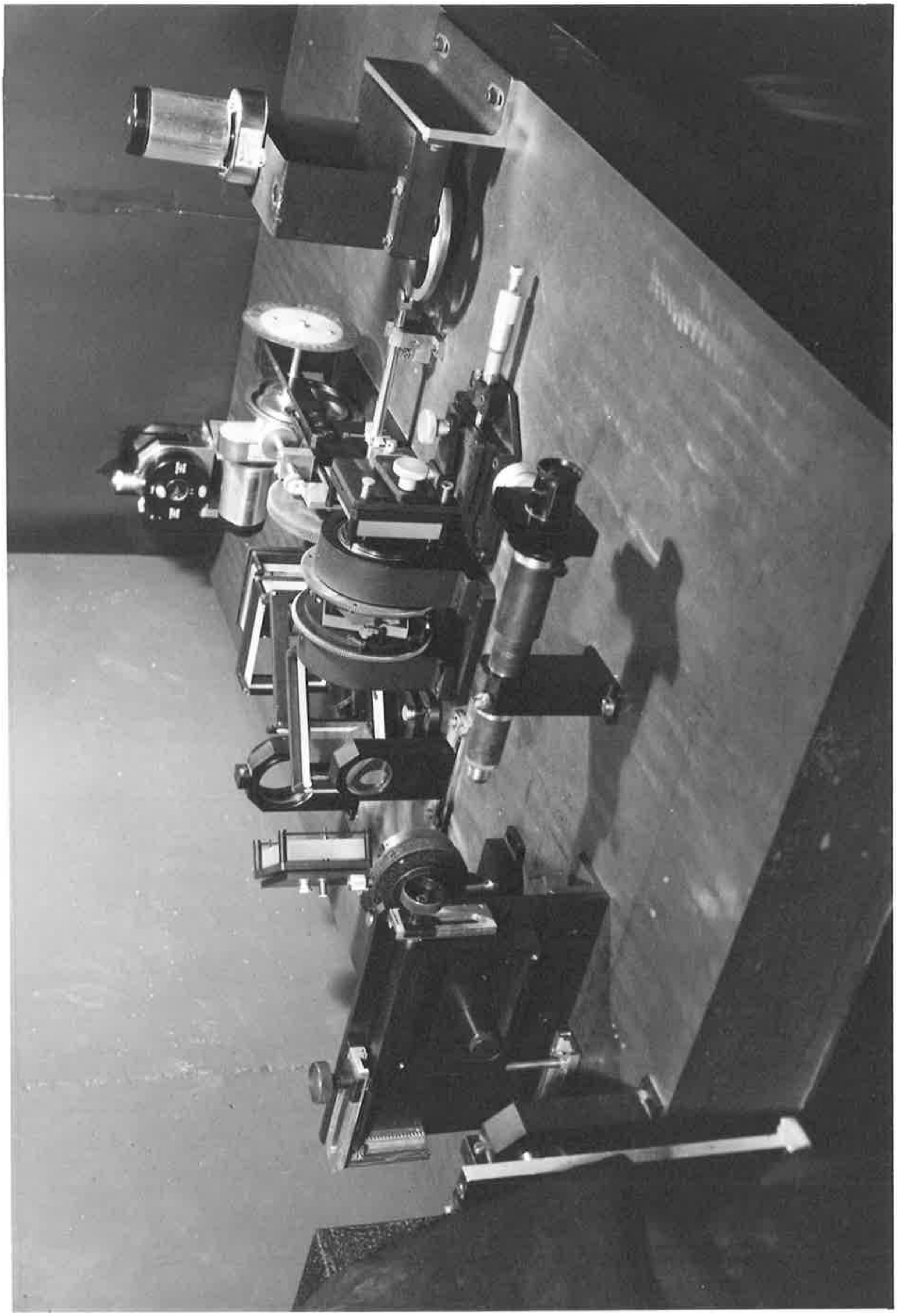

FIGURE 2.3.

them by suitable packing and twisting until the return beams from an auto-collimator coincide and remain stationary on rotation of the bearings. The prisms are then placed in their mounts and adjusted on three small jacking screws until **those** surfaces which are perpendicular to all four edges are parallel to one another and perpendicular to the axis of rotation. This is again achieved with the aid of an auto-collimator. The whole assembly is then placed in front of the beam emerging from the collimator C_1 and the transmitted beam viewed again with an auto-collimator. One of the cross wires in the auto-collimator is made to be parallel with the object slit and the prisms are adjusted by rotation in their mounts until only a horizontal shift of the object slit image is observed when contra rotating them as a pair. This is best achieved by closing down the object slit in length until only a small point of light is viewed and adjusting the prisms until this small point of light travels along the other cross wire in the auto-collimator. By doing this we have achieved two things, we have checked whether the prisms are firmly held in their mounts and whether we can expect any tilt of the fringes, and we have insured that the fringes will be formed parallel to the entrance slit which is one condition which must be observed to keep the maximum contrast available high, that is in the region of 0.9.

The spatial frequency can be measured with the microscope ME which has a micrometer eyepiece, this is focussed on a plane conjugate with the transparency plane and a small mirror is inserted to deviate the light beam in order to make the measurement. The scale SC gives a quick indication of the spatial frequency, it is attached to the axis of the archimedean cam which moves the prisms, and rotation of this, as discussed above, bears a linear relationship to the spatial frequency. Thus by measuring the angle of rotation of the cam we can estimate the frequency reasonably accurately. This is achieved by attaching a protractor to one end of the axle of the cam, this moves past a pointer and the angle of rotation is read off directly. The protractor and pointer constitute the scale and can be calibrated with the microscope; it is then possible to select any pre-desired frequency approximately which is an advantage when scanning transparencies known to contain only certain frequencies, a complete scan through the whole range not being required.

With the apparatus built there are three sets of prisms which can be used, the first have angles of 0.5° and give a range of frequencies from zero to 33 lines/mm, the second pair have 1° angles and give zero to 66 lines/mm, and the third are 2° prisms giving a range of zero to 132 lines/mm. The motor driving the Archimedean cam is a Philips small synchronous motor type AU5100 with a basic speed of 250 rev/min. It drives the cam through a reduction gear box of ratio 1:6250, this results in a scanning speed with the 1° prisms of approximately 11 lines/mm/min. This can be readily altered by changing the gear box or using another pair of prisms.

The prism P_1 is used to shift the fringes across the photographic plate. When this prism is reciprocated linearly with time along a direction perpendicular to the light passing through it, a linearly varying thickness of glass is introduced into the beam, so that a similar linear variation in path difference is introduced.

The movement of the prism is provided by an Archimedean cam, and results in the great advantage of a frequency of variation of the total light flux to be measured which is independent of the spatial frequency of the fringe pattern. This enables a frequency selective amplifier to be used in the following electrical circuitry with consequent increase in signal to noise ratio. The frequency of the

$$f = \frac{4\,(n-1)\,l\,\alpha\,m}{\lambda} \qquad 2.21$$

where l is the stroke length, α the prism angle, m the number of cam revolutions per second, and λ the wavelength of light used (5461 A°). For $l = 1.5$ in., $\alpha = 7$ min, $m = 0.25\,\mathrm{sec}^{-1}$, the frequency f is equivalent to 67.5 c/s.

The mean thickness of the prisms P_2, P_3 is chosen to compensate the path difference introduced by the prism P_1 otherwise a considerable loss of fringe visibility is experienced.

The focal length of the objective O, which images the fringes onto the transparency at a magnification of approximately unity, should be as short as possible since this limits the pupil diameter and the useful transparency size or the maximum spatial frequency R which may be examined. In the apparatus described a doublet of 5 in. focal length and $1\frac{3}{4}$ in. diameter is used.

The slit SL_2, situated at the focus of the objective acts as a limiting stop and prevents most of the stray and ghost image light from reaching the transparency, with a consequent improvement in the fringe visibility.

The transparency TR is mounted in a small plate camera especially made for the apparatus. It takes plates $2\frac{1}{2}$ in. by $3\frac{1}{2}$ in. which are a standard size. The plate holder may be adjusted in two perpendicular directions and two scales are used to determine the coordinates on the plate which coincide with the exit pupil of the instrument. When scanning a transparency, the back of the camera is removed, the plate remaining held in position. Details of the camera can be found in technical drawing figure 2.4.

The photomultiplier cathode is illuminated by the condenser CO_2 which acts purely as a flux lens. The diameter has to be large

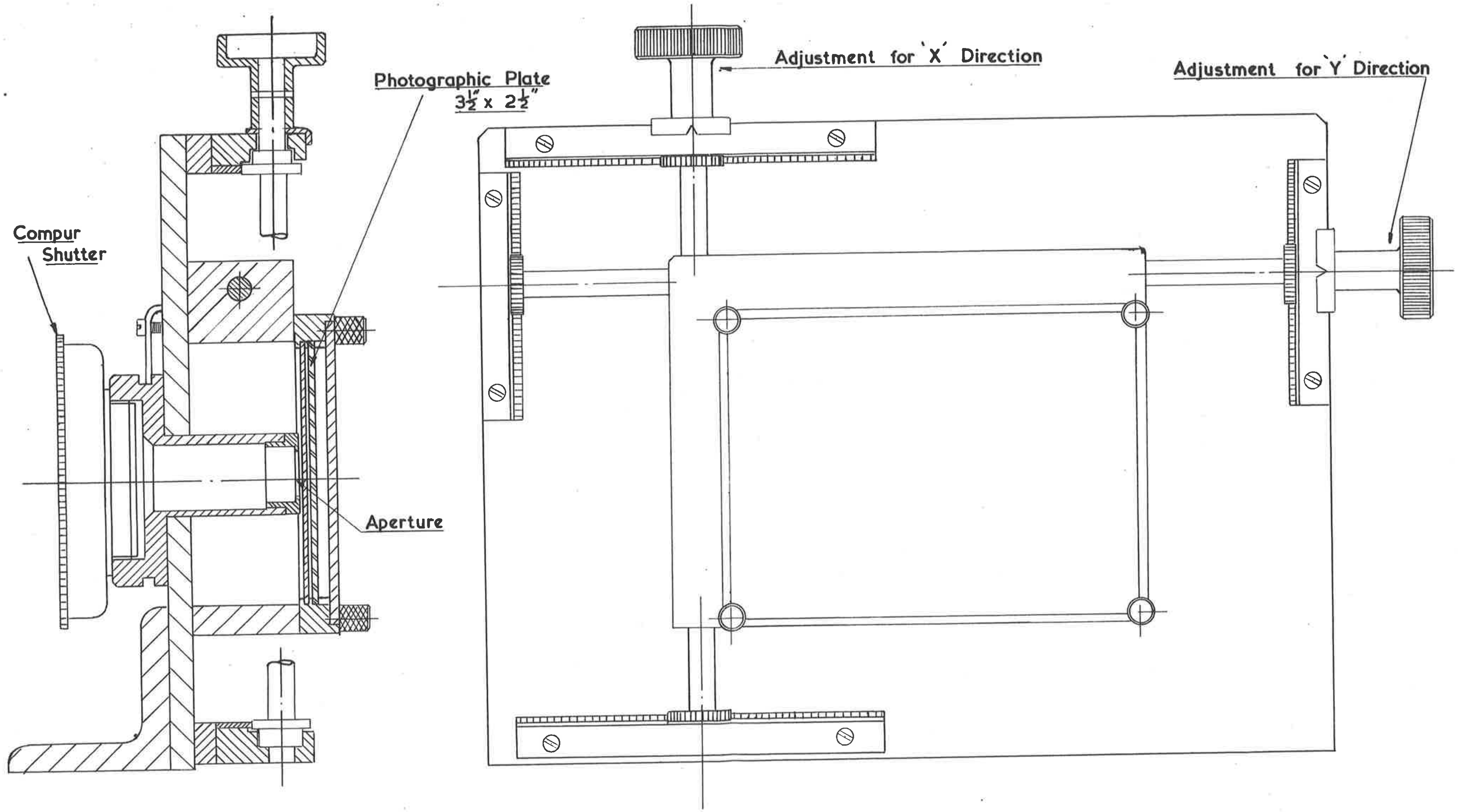

FIGURE 2.4 CAMERA

enough to gather all the light passing through the transparency assuming that this latter acts as a grating of spatial frequency R_{max}. In front of the transparency is a beam splitter which deviates part of the light beam onto a reference slit S_3. This is used to determine the phase distribution of the frequency components in the transparency. An optical micrometer OM serves to position the fringe pattern accurately onto this slit. The light flux passing through the slit is collected by a photomultiplier PM2.

The width of the slit S_3 is adjusted so that the first zero in its Fourier spectrum occurs at a spatial frequency well above the maximum frequency to be investigated. When a transparency function is to be analysed and the phase distribution of the various frequency components is required the following procedure is followed. A very low frequency is chosen say 0.2 lines/mm and the slit S_3 is positioned so that the signals from the two photomultipliers are in phase. Now as the frequency is increased we know that the phase of the components from S_3 will not change so that any phase difference measured between the signals from the two photomultipliers is due to a phase shift of that particular frequency in the transparency function being analysed.

That this procedure works can easily by verified by observing the phase changes of π which occur when passing through the zeros of the spectrum of a fairly wide slit. In the test case the reference slit was about 10μ wide with its first zero occurring at 100 lines/mm and the test slit was about 0.3 mm wide.

II.3.2 Electronic and Recording Apparatus

The photomultiplier which integrates the light flux is an 11 stage E.M.I. 6094B with an antimony caesium photocathode. The voltage to the cathode and dynodes is supplied by an Isotope Developments power pack which can supply up to 2000 V. The output of the photomultiplier passes to a frequency selective pre-amplifier and from this to a high fidelity 10 W audio frequency amplifier. The output of this amplifier is rectified and the rectified signal further smoothed by a Hewlett Packard d.c. voltmeter. This voltmeter also acts as an amplifier giving an output of 1 V for full scale deflection on any range. A Honeywell d.c. pen recorder is used to record the output of the d.c. voltmeter in permanent form.

With the circuitry briefly described here, the pen recorder readings are directly proportional to the amplitude of the light flux variations of frequency 67.5 c/s and hence to the spatial frequency density in the analysed transparency.

Similar circuitry is used to measure the signal from the phase slit except that the rectifying stage is omitted. The phase is determined by comparing the signals from the frequency selective amplifiers on a C.R.O.

II.3.3 The selective amplifier

The main purpose of the pre-amplifier is to convert the current from the photomultiplier into a voltage signal, then to amplify it and finally to select the desired frequency, so improving the signal/noise ratio. The conversion of current into voltage is made by the grid resistor R_1 figure 2.5 of the cathode follower input stage. The value of this resistor depends on the amount of light available. The output of this stage is amplified by the voltage amplifier constructed on the EF 86 valve. This amplifier has a negative voltage feedback loop through the condenser C_3 and resistor R_7 to stabilise the gain. The output to the next stage is fed through a potentiometer R_{10}, which acts as a gain control for the whole amplifier.

The requirement of the tuned amplifier is to accept the frequency band 67.5 c/s ± 7 c/s. This bandwidth is necessary to avoid serious

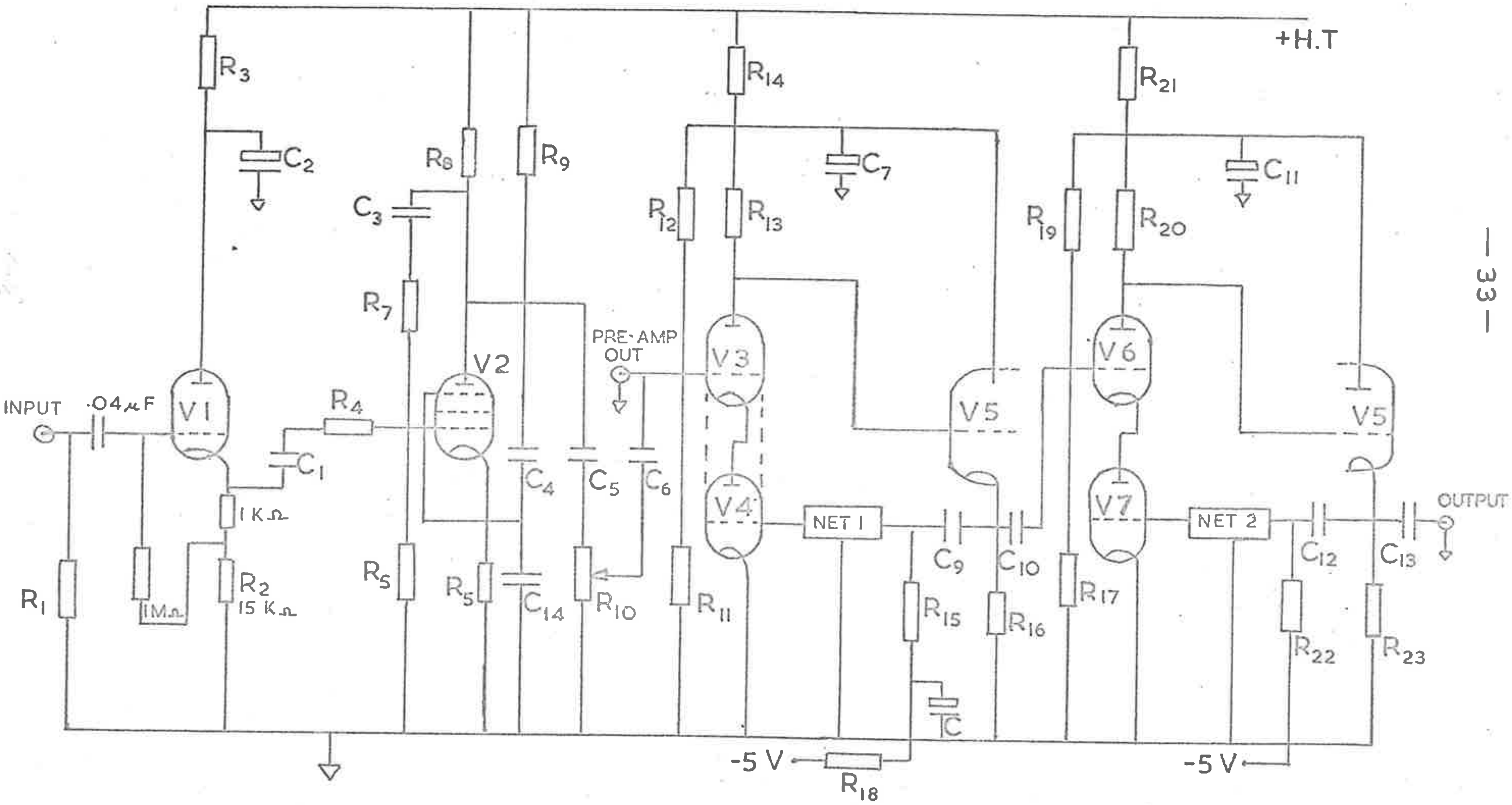

FIGURE 2.5 FREQUENCY SELECTIVE AMPLIFIER

the output frequency of the instrument. The frequency variation arises since the velocity of the prism P_1 is not strictly constant especially at the end of its stroke.

Basically the amplifier circuit described by Fleisher (1948) is used. To obtain the required bandwidth the frequency selective section of the amplifier consists of two stagger tuned stages using identical twin T-units. One such stage is constructed on valves 3 and 4 in conjunction with network 1. The input signal to the stage as applied to the grid of valve 3 is amplified and the output applied to the cathode follower valve 5. The feedback from the cathode of this stage is via the network, which is illustrated in figure 2.6. This is tuned to have maximum impedance at 67.5 c/s and then signals at other frequencies give destructive feedback and are not amplified.

The two stages constructed may be stagger-tuned and a bandpass characteristic may be obtained to accommodate any small spread of the output frequency of the instrument. The method of tuning the amplifier is briefly as follows. Each network is individually fed with a signal at 67.5 c/s and the output observed on an oscilloscope or a.c. valve voltmeter, all valves having been removed from the amplifier. The variable resistors are then adjusted for minimum output signal which corresponds to maximum impedance. The valves are replaced in the amplifier, the amplifier warmed up and a signal of 67.5 c/s applied to the input. The variable resistors are adjusted to give maximum amplification at 67.5 c/s. If the twin T-networks worked under the same conditions no such retuning would be required. The next step is to tune network 1 to pass its maximum signal at 62.5 c/s and network 2 to pass 72.5 c/s and then the anode load in both stages is selected to give a flat transmission characteristic between these two frequencies. The bandwidth characteristic of the amplifier is shown in figure 2.7.

TUNING NETWORK

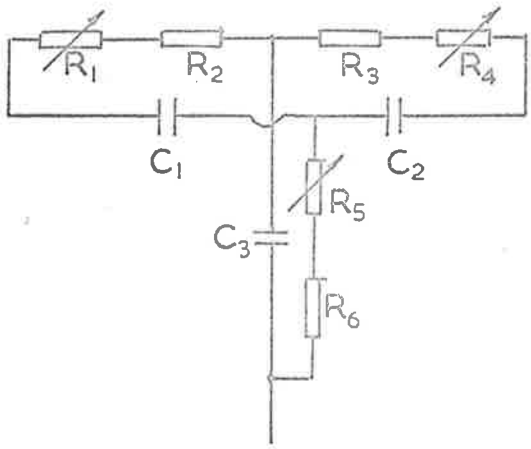

R_1	100 KΩ
R_2	27 KΩ
R_3	27 KΩ
R_4	100 KΩ
R_5	50 KΩ
R_6	15 KΩ
C_1	0·05 μF
C_2	0·05 μF
C_3	0·10 μF

FIGURE 2·6

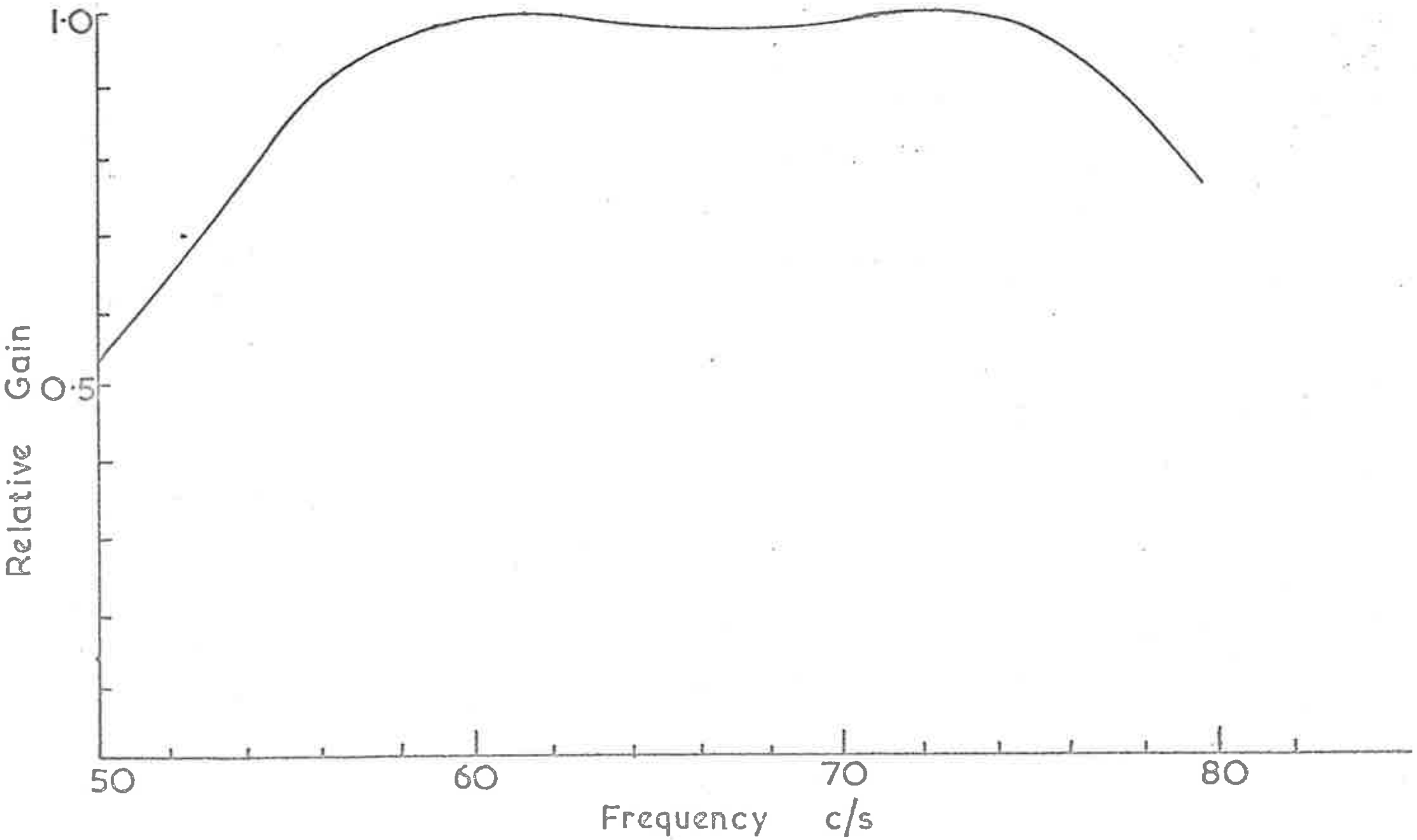

FIGURE 2.7 BANDWIDTH CHARACTERISTIC OF FREQUENCY SELECTIVE AMPLIFIER.

II.3.4 The power amplifier

The output of the selective amplifier is fed to a Mullard 5-10 amplifier. This amplifier satisfies the strictest conditions placed on its linearity, is very stable and has good response to pulse signals and is therefore ideally suitable for this purpose. The output from this amplifier can simply be read by a voltmeter or rectified, smoothed, and recorded by the Honeywell Potentiometric Pen Recorder.

II.4 Adjustment of the apparatus

First of all the collimating lens is adjusted to give a parallel beam of light; this is done by illuminating the object slit and adjusting the separation of slit and lens until the image as seen in an auto-collimator is in focus. Again using a Taylor, Taylor and Hobson auto-collimator the mirror M_1 is set perpendicular to the axis of the collimator. Then with the aid of matrix blocks set to give an angle of 45° the compensator and beam splitter are set at 45° to the mirror M_1 and parallel to each other. Finally mirror M_2 is set so that the return beams from both arms coincide, and M_3 is placed in position to direct the collimated beam into the interferometer.
The mirror M_2 is now adjusted on its slide until, using white light, we obtain fringes in the centre of the field. The interferometer is now in the condition that the two arms have the same optical path length. The prisms P_1 and P_2 P_3 are now introduced into the interferometer and any adjustment in the position of M_2, to keep the path length equal, is made.

For the E.M.I. 6094 photomultiplier used as a detector, good signal/noise ratio is obtained for 90 V/stage between the dynodes. For small amounts of light the photomultiplier voltage may be increased but usually it is kept between 900 to 1 300 V and under no circumstances exceeds 1 400 V. The cathode follower input resistance can also be increased to increase **sensitivity** but usually is kept at about 1 MΩ.

II.5 Checking the apparatus

The light source was checked for stability by blocking off one beam of the interferometer and using the photomultiplier purely as a photometer recording the intensity of one beam. The output of the photomultiplier was fed directly to a Hewlett Packard d.c. voltmeter which is also a d.c. amplifier the output of which can be recorded. Over a period of about half an hour the d.c. medium pressure mercury lamp was found to be stable to better than 1%.

Mechanical stability was found to be good and the apparatus would stay in good adjustment for a number of hours. This was verified by setting up the interferometer to give zero fringes and leaving it running, that is the reciprocating prism P_1, for an hour or so. On stopping the prism after this period the fringe pattern was viewed to see if the apparatus had gone out of adjustment. Instability can be due to a number of factors but the main ones, temperature fluctuations and mechanical vibrations, are overcome to a large extent by the situation of the apparatus, in a tunnel some fifteen feet underground.

The contrast of the fringes is measured by setting up a slit of about 5μ width in the transparency plane. The prisms P_2 P_3 are rotated to give the desired frequency and the fringes are scanned across the slit by rotating the axis of the motor driving prism P_1 slowly by hand or through a gear box of ratio 1:1250. The output of the photomultiplier is again read directly by the d.c. voltmeter or its output recorded. For each frequency the dark, minimum and maximum voltages are measured and the contrast computed from the relationship :

$$\frac{\beta}{\alpha} = \frac{V_{max} - V_{min}}{V_{max} + V_{min}} \qquad 2.22$$

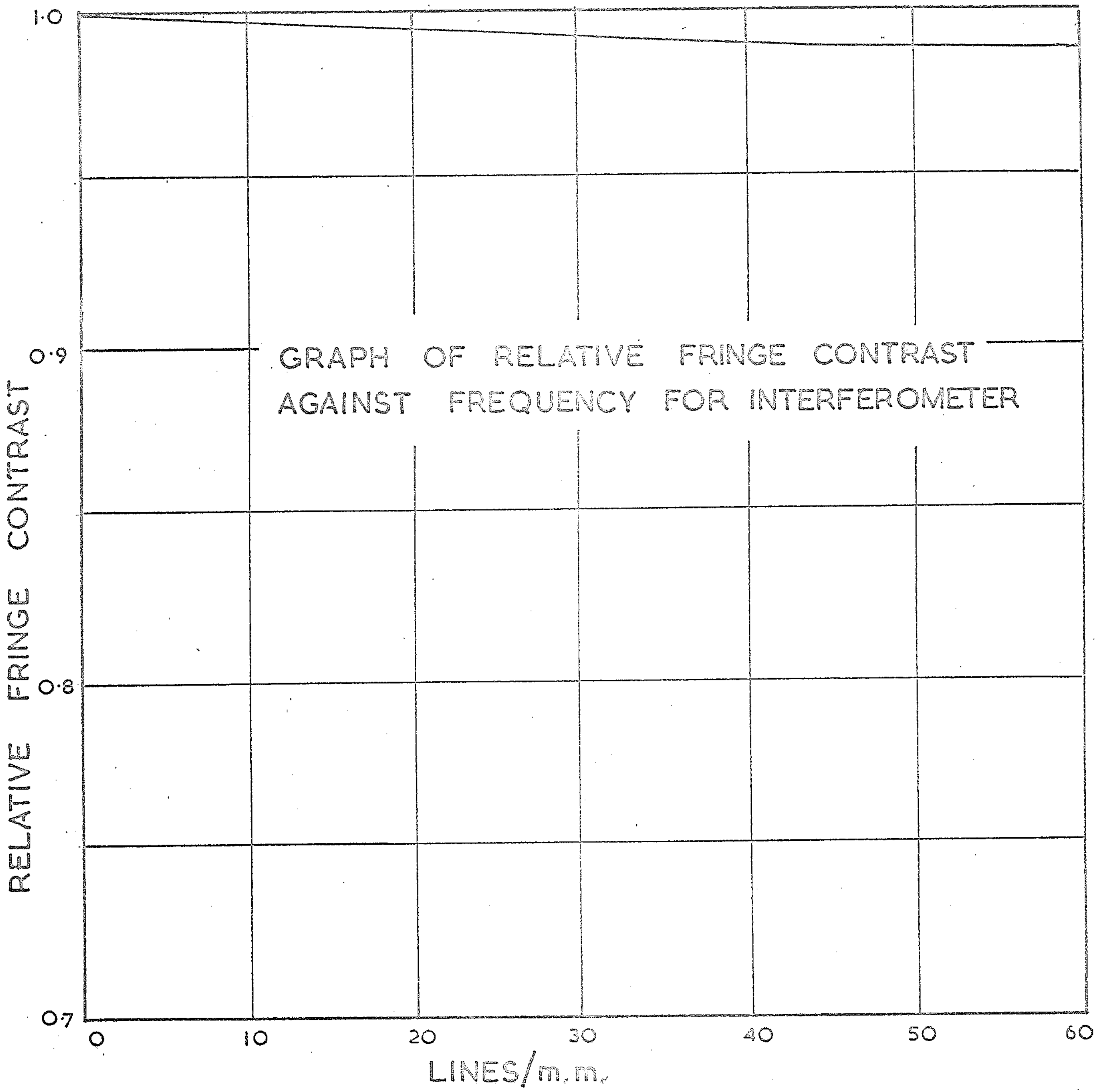
GRAPH OF RELATIVE FRINGE CONTRAST AGAINST FREQUENCY FOR INTERFEROMETER
RELATIVE FRINGE CONTRAST
1·0
0·9
0·8
0·7
0
10
20
30
40
50
60
LINES/m.m.

FIGURE 2.8.

FOURIER TRANSFORM OF SLIT

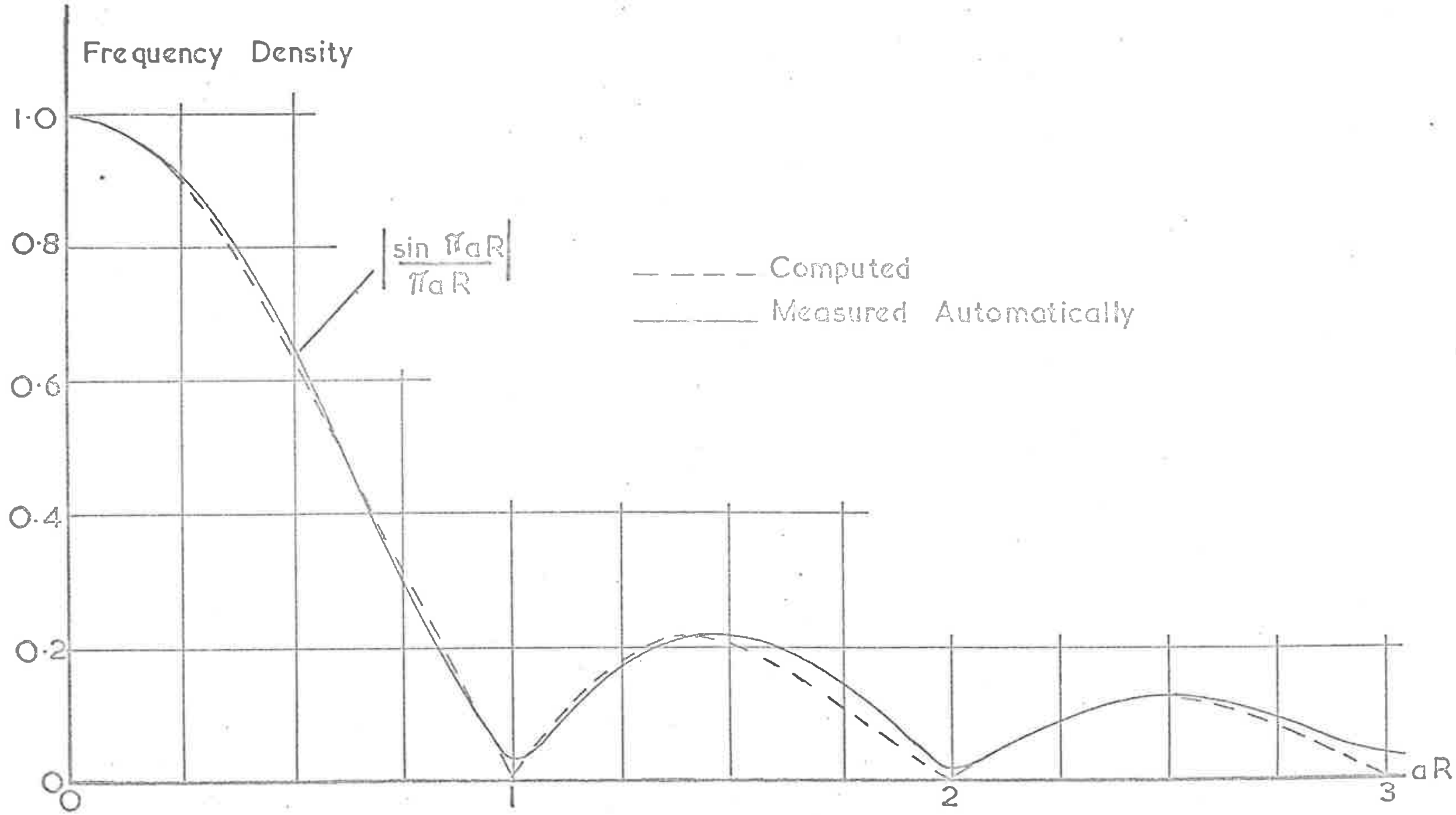

FIGURE 2.9.

The record of contrast against frequency can be seen in figure 2.8. There is no significant change in contrast up to a frequency of 50 lines/mm, this being the limiting frequency at which it was measured.

The next check was to measure automatically the Fourier transform of a slit. The record of this experiment is shown in figure 2.9. Good agreement is found with the theoretical values and an overall accuracy of about 2% can be attributed to the apparatus for the measurement of the frequency density of transparency functions.

REFERENCES

Fellgett, P. (1953)	J.O.S.A., 43, 271.
Fleisher, H. (1948)	Radiation Laboratory Services, Vol. 18, Vacuum Tube Amplifiers; (New York: McGraw Hill Co.)
Kovasznay, L.S.G., Arman, A. (1957)	Rev. Sc. Instr. 28, 783.
Vienot, J. Ch. (1958)	Proc. Phys. Soc., 72, 661.
Vienot, J. Ch. (1958)	Thesis. University of London
Wilezynski, J. (1960)	Thesis. University of London

CHAPTER III

HARMONIC DISTORTION APPLIED TO THE PHOTOGRAPHIC RECORDING OF SINE WAVE OBJECTS

THEORETICAL AND EXPERIMENTAL RESULTS

III.1 Introduction

The results of the following theoretical calculations and experiments are all given in terms of transmitted intensity, this being the quantity which is measured directly by the previously described instrument. Previous authors, in describing similar investigations, have used various other quantities namely opacity or density but, as the magnitude of these is not readily appreciated by visual examination, it was decided to use transmitted intensity throughout this treatment of the subject.

As indicated by the heading the investigations are restricted to the images of sine wave objects. This facilitates the theoretical considerations and also the establishment of a method for measuring the frequency response function of emulsions.

III.2 Harmonic distortion of sine wave images recorded on the straight portion of the H & D curve

Due to the relationship between transmission and exposure the photographic process is non linear and thus the image of a sine wave will contain harmonics in addition to the original fundamental frequency. In many cases measurements are made on negatives and thus some knowledge of the magnitude of this distortion and the factors influencing it is necessary. Exposures are generally restricted to the straight part of the H & D curve, and these cases will be considered first.

If the H & D curve were truly straight, it could be defined by the equation:-

$$I_T = \text{Const. } (E)^{-\gamma} \qquad 3.1$$

where I_T is the intensity transmitted by the negative, E is the exposure, and γ the slope of the H & D curve when plotted in terms of density and

$\log_{10}$ (exposure). Using equation 3.1 the form of the images of sine waves of various contrasts developed to various gammas can be deduced. These deduced waveforms can be numerically analysed and the contrasts and ratios of the harmonics found.

By adapting a programme, written previously by the author for the analysis of optical spread functions, sine waves of contrasts 0.2, 0.4, 0.6, and 0.8 developed in turn to gammas of 0.5, 1.0, and 2.0, were analysed using the IBM 7090 electronic digital computer. The results of these calculations are presented in graphical form in two sets figures (3.1 - 3.6). In one set the ratio of the harmonics and the contrast of the transmitted fundamental are plotted as a function of effective exposure contrast for a particular γ; in the second set the same variables are plotted as a function of γ for a particular effective exposure contrast.

From the graphs it is clear that harmonic distortion increases both with contrast and γ and that in some cases it can reach very high levels, for high contrast exposures 50% second harmonic would not be uncommon. It is interesting to note that if we confine our attention to the fundamental frequency no gain in contrast is achieved until the gamma exceeds 2.0 (figure 3.6).

III.3 The five point method for assessing the harmonic distortion in sine wave images over the complete H & D curve

The previous analysis was confined to theoretical straight H & D curves, a situation which is experienced in practice over a limited exposure range. In order to be able to assess the amount of harmonic distortion taking place over the complete H & D curve, we make use of a method developed by Espley in the field of electronics. If we plot the H & D curve in terms of transmitted intensity and exposure, the five point method can be used to deduce the harmonic distortion present in the image of a sine wave of known contrast centred about a known

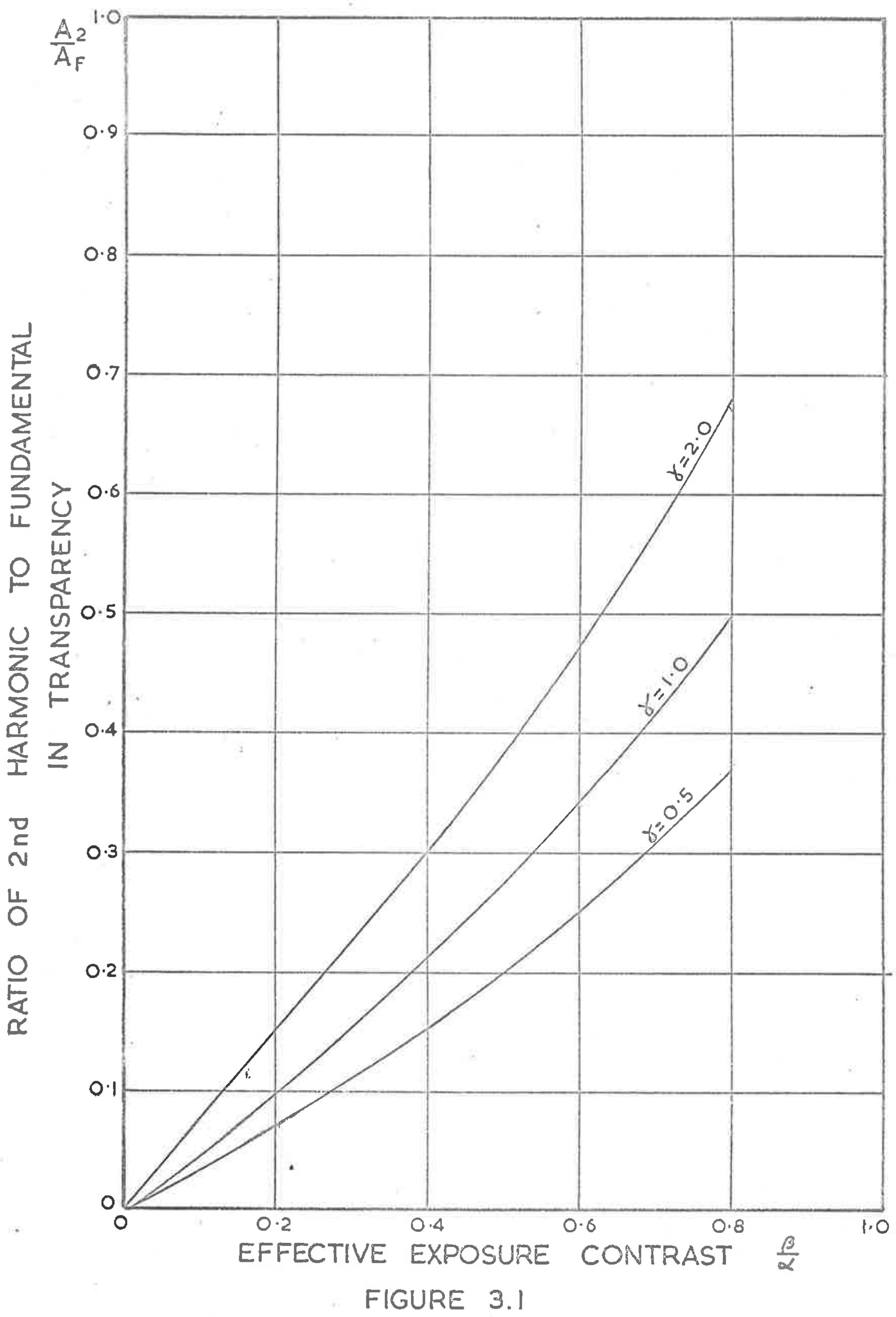

$\frac{A_2}{A_F}$
1·0
0·9
0·8
0·7
0·6
0·5
0·4
0·3
0·2
0·1
0
RATIO OF 2nd HARMONIC TO FUNDAMENTAL IN TRANSPARENCY
$\gamma = 2·0$
$\gamma = 1·0$
$\gamma = 0·5$
0
0·2
0·4
0·6
0·8
1·0
EFFECTIVE EXPOSURE CONTRAST $\frac{\beta}{\alpha}$

FIGURE 3.1

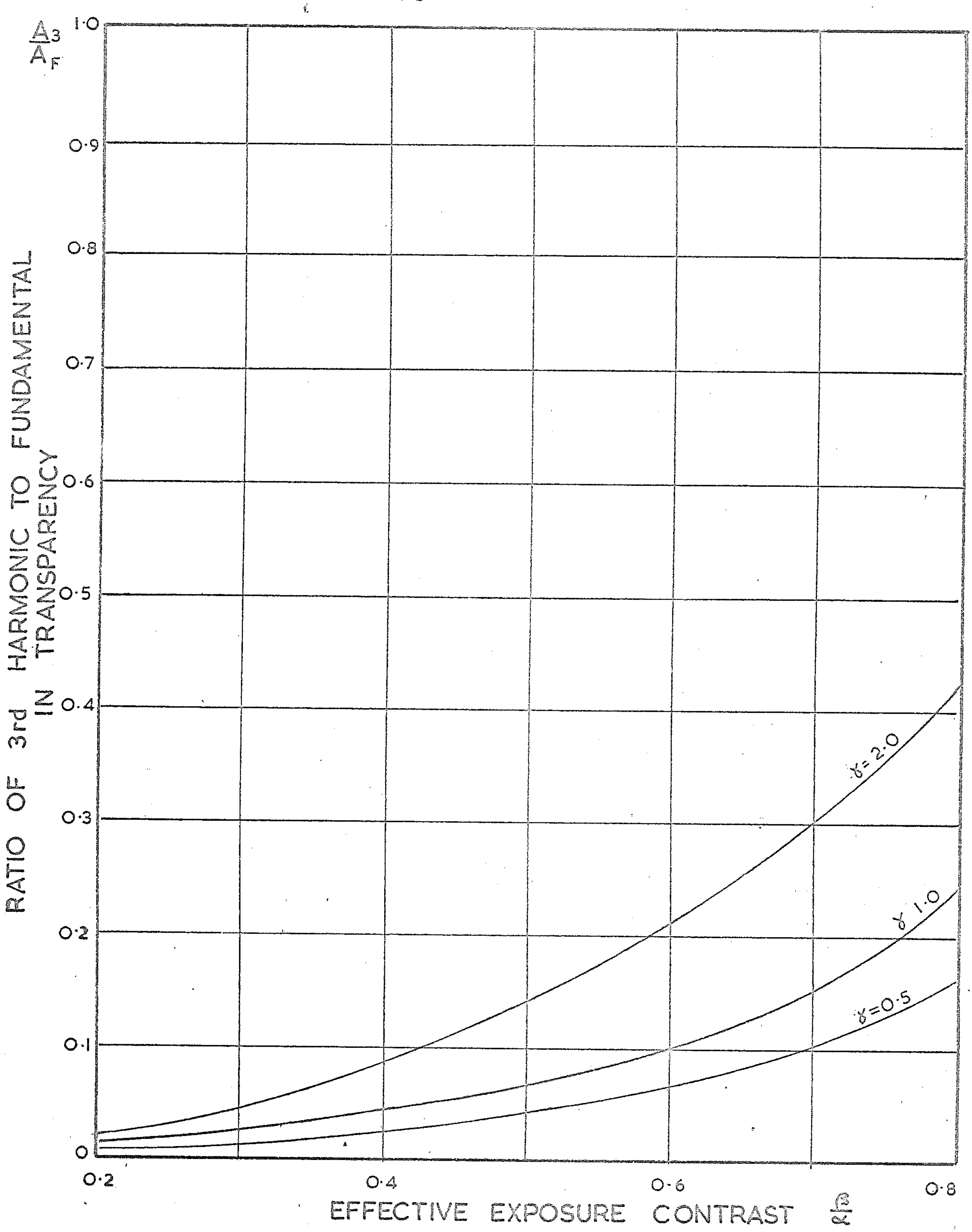

$\frac{A_3}{A_F}$
RATIO OF 3rd HARMONIC TO FUNDAMENTAL IN TRANSPARENCY
1·0
0·9
0·8
0·7
0·6
0·5
0·4
0·3
0·2
0·1
0
0·2
0·4
0·6
0·8
EFFECTIVE EXPOSURE CONTRAST $\frac{\alpha}{\beta}$
γ= 2·0
γ 1·0
γ=0·5

FIGURE 3.2

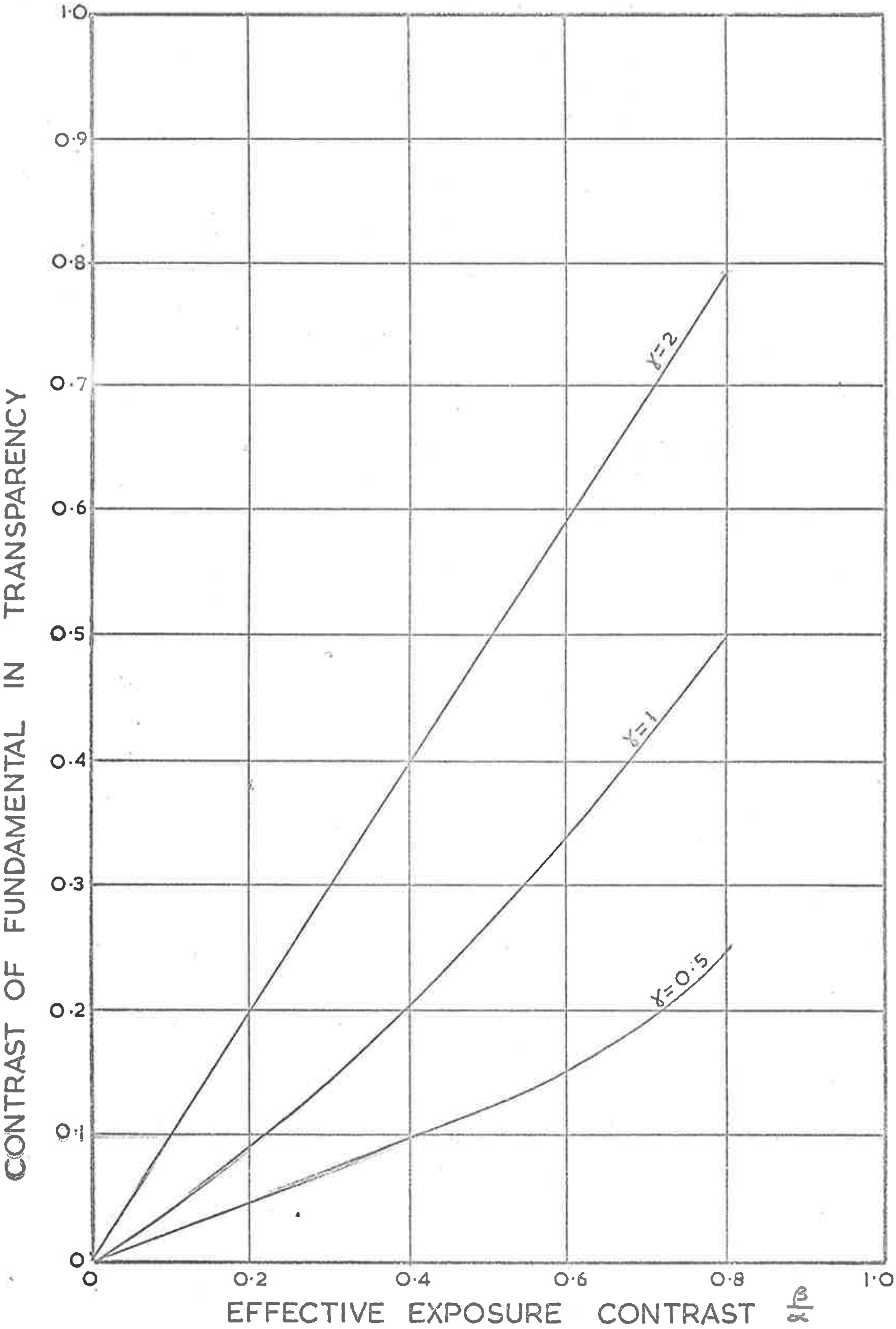

1·0
0·9
0·8
0·7
0·6
0·5
0·4
0·3
0·2
0·1
0
CONTRAST OF FUNDAMENTAL IN TRANSPARENCY
γ=2
γ=1
γ=0·5
0
0·2
0·4
0·6
0·8
1·0
EFFECTIVE EXPOSURE CONTRAST β/α

FIGURE 3.3.

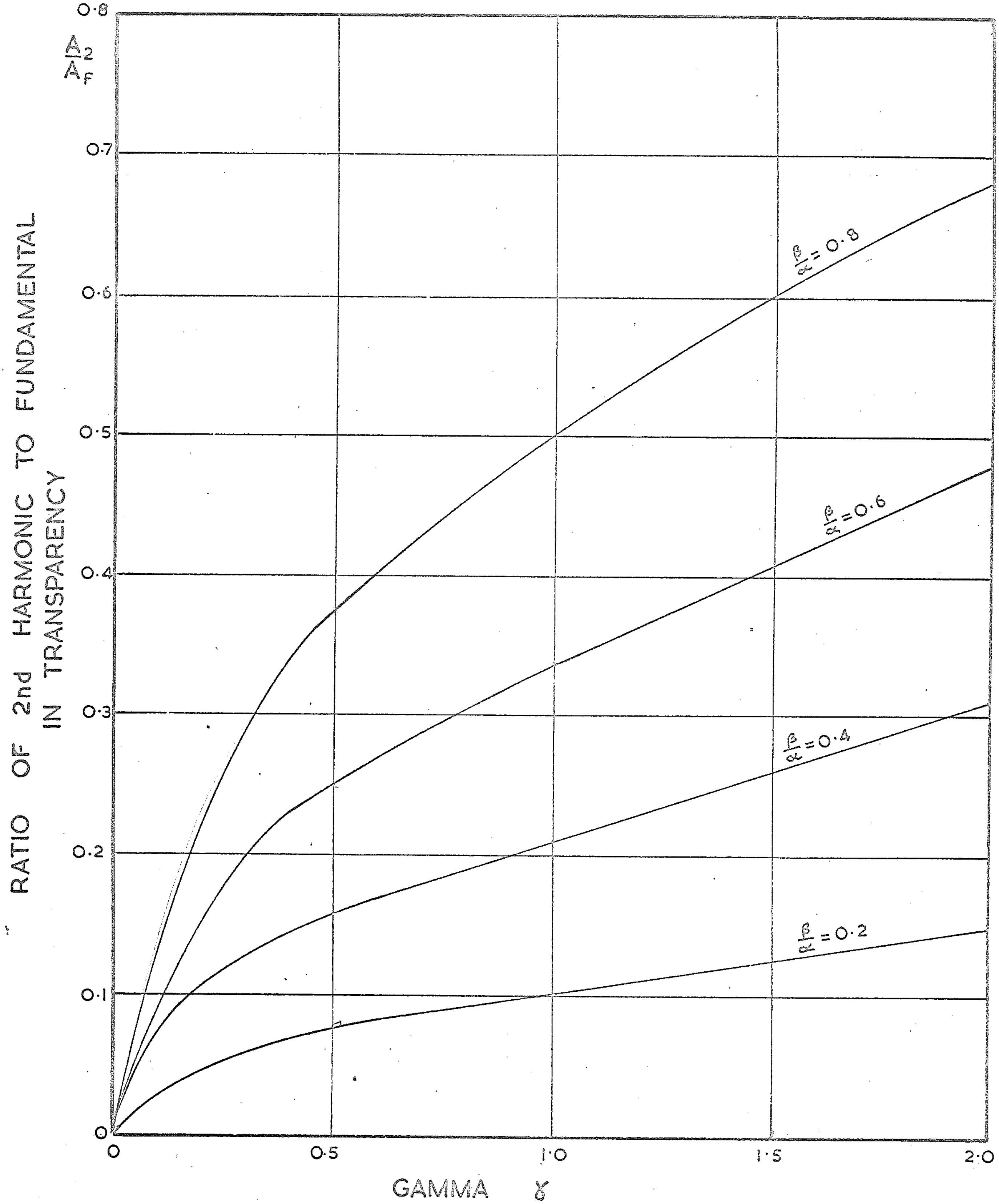
$\frac{A_2}{A_F}$
RATIO OF 2nd HARMONIC TO FUNDAMENTAL IN TRANSPARENCY
0.8
0.7
0.6
0.5
0.4
0.3
0.2
0.1
0
$\frac{\beta}{\alpha} = 0.8$
$\frac{\beta}{\alpha} = 0.6$
$\frac{\beta}{\alpha} = 0.4$
$\frac{\beta}{\alpha} = 0.2$
0
0.5
1.0
1.5
2.0
GAMMA γ

FIGURE 3.4.

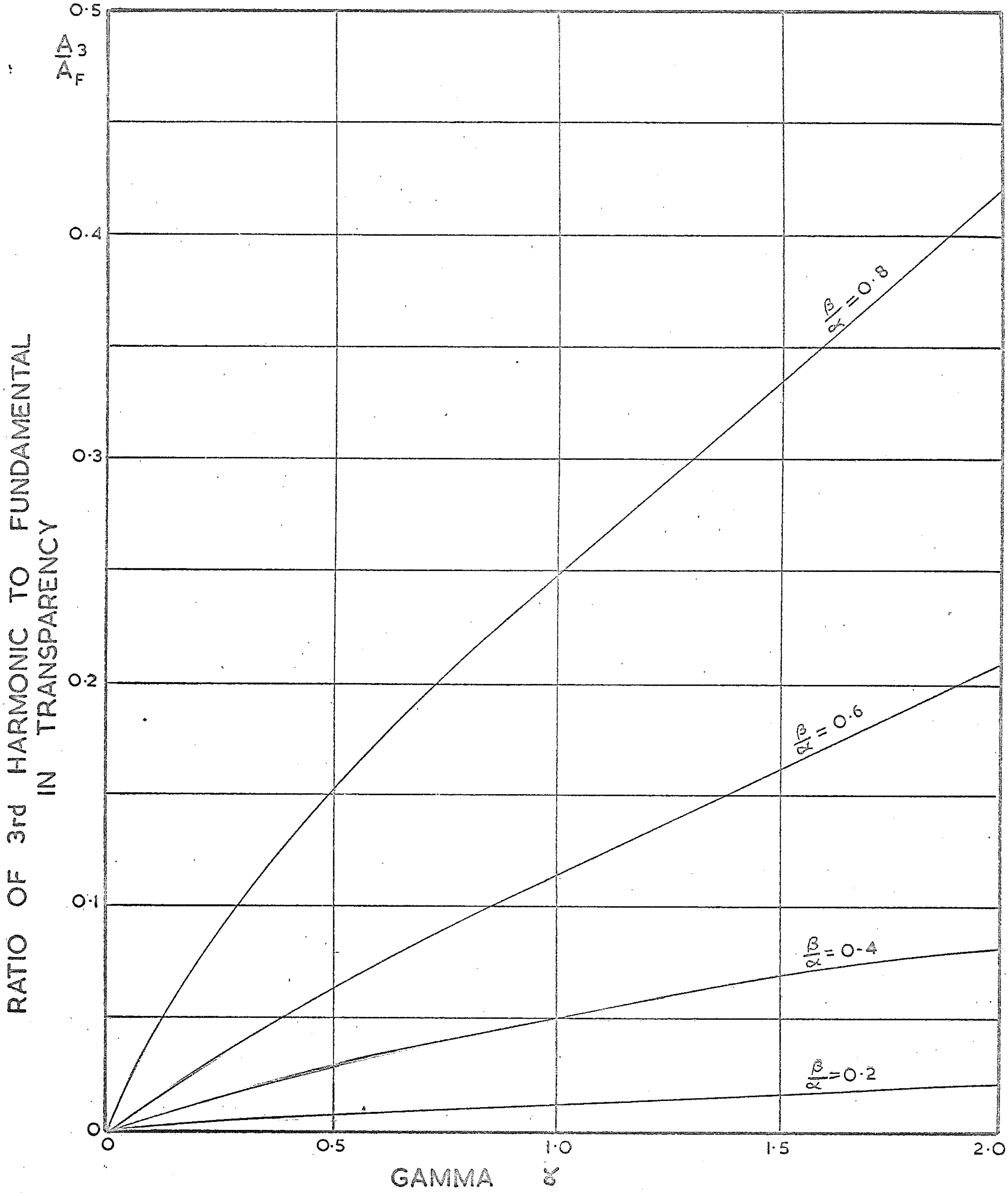

0·5
$\frac{A_3}{A_F}$
0·4
0·3
0·2
0·1
0
RATIO OF 3rd HARMONIC TO FUNDAMENTAL IN TRANSPARENCY
$\frac{\beta}{\alpha} = 0{\cdot}8$
$\frac{\beta}{\alpha} = 0{\cdot}6$
$\frac{\beta}{\alpha} = 0{\cdot}4$
$\frac{\beta}{\alpha} = 0{\cdot}2$
0
0·5
1·0
1·5
2·0
GAMMA γ

FIGURE 3.5

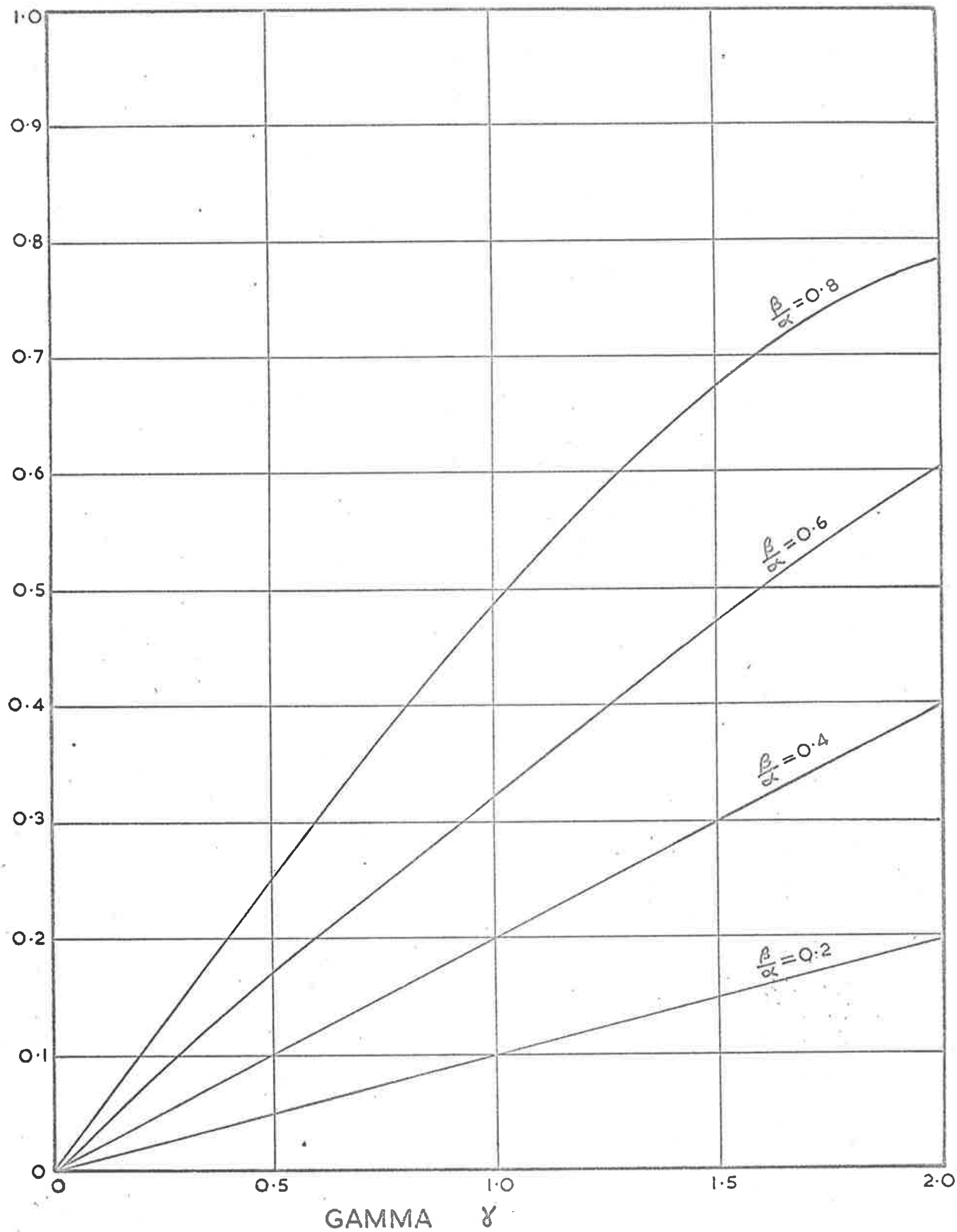
1·0
0·9
0·8
0·7
0·6
0·5
0·4
0·3
0·2
0·1
0
0
0·5
1·0
1·5
2·0
β/α = 0·8
β/α = 0·6
β/α = 0·4
β/α = 0·2
GAMMA γ

FIGURE 3.6

We assume that the equation of the H & D curve, using transmitted intensity I_T and exposure E as the variables, may be represented by the power series:-

$$I_T = f(E) = f(\alpha) + a_1 (E-\alpha) + a_2 (E-\alpha)^2 + a_3 (E-\alpha)^3 + a_4 (E-\alpha)^4 + a_5 (E-\alpha)^5 + a_6 (E-\alpha)^6 \qquad 3.2$$

where α is the mean exposure and higher terms are neglected. If the effective exposure as defined previously varies sinusoidally according to the equation:-

$$E = \alpha + \beta \operatorname{Sin} 2\pi R x \qquad 3.3$$

then equation 3.2 may be re-written in the form:-

$$\begin{aligned} I_T = f(\alpha) &+ a_1 \beta \operatorname{Sin} \Omega \\ &+ a_2 \beta^2 (\tfrac{1}{2} - \tfrac{1}{2} \operatorname{Cos} 2\Omega) \\ &+ a_3 \beta^3 (\tfrac{3}{4} \operatorname{Sin} \Omega - \tfrac{1}{4} \operatorname{Sin} 3\Omega) \\ &+ a_4 \beta^4 (\tfrac{3}{8} - \tfrac{1}{2} \operatorname{Cos} 2\Omega + \tfrac{1}{8} \operatorname{Cos} 4\Omega) \\ &+ a_5 \beta^5 (\tfrac{5}{8} \operatorname{Sin} \Omega - 5/16 \operatorname{Sin} 3\Omega + 1/16 \operatorname{Sin} 5\Omega) \\ &+ a_6 \beta^6 (5/16 - 15/32 \operatorname{Cos} 2\Omega + 3/16 \operatorname{Cos} 4\Omega - 1/32 \operatorname{Cos} 6\Omega) \end{aligned} \qquad 3.4$$

where for convenience $2\pi R x$ is put equal to Ω.

Collecting coefficients of different harmonics and assuming the absence of harmonics above the fourth i.e. a_5 and a_6 equal to zero, we get:-

$$\begin{aligned} I_T = f(\alpha) &+ \tfrac{1}{2} a_2 \beta^2 + \tfrac{3}{8} a_4 \beta^4 \\ &+ (a_1 \beta + \tfrac{3}{4} a_3 \beta^3) \operatorname{Sin} \Omega \\ &- (\tfrac{1}{2} a_2 \beta^2 + \tfrac{1}{2} a_4 \beta^4) \operatorname{Cos} 2\Omega \\ &- (\tfrac{1}{4} a_3 \beta^3) \operatorname{Sin} 3\Omega \\ &+ (\tfrac{1}{8} a_4 \beta^4) \operatorname{Cos} 4\Omega \end{aligned} \qquad 3.5$$

Equation 3.5 may be regarded as describing the output signal of the photographic emulsion for a sine wave illumination within the approximation implied by equation 3.2.

If five points having equally spaced values of E, as shown in figure 3.7, are selected on the sine wave, five values of I_T denoted by I_{max}, I_2, I_0, I_1, I_{min} are obtained.

The five equations resulting from inserting these values in 3.5 are:-

$$I_{max} = f(\alpha) - a_1 \beta + a_2 \beta^2 - a_3 \beta^3 + a_4 \beta^4$$

$$I_2 = f(\alpha) - \frac{a_1 \beta}{2} + \frac{a_2 \beta^2}{4} - 1/8\, a_3 \beta^3 + 1/16\, a_4 \beta^4$$

$$I_0 = f(\alpha)$$

$$I_1 = f(\alpha) + \frac{a_1 \beta}{2} + 1/4\, a_2 \beta^2 + 1/8\, a_3 \beta^3 + 1/16\, a_4 \beta^4$$

$$I_{min} = f(\alpha) + a_1 \beta + a_2 \beta^2 + a_3 \beta^3 + a_4 \beta^4 \qquad 3.6$$

These five equations may be inverted to give:-

$$a_1 = \frac{1}{6\beta} (I_{max} - 8 I_2 + 8 I_1 - I_{min})$$

$$a_2 = -\frac{1}{6\beta^2} (I_{max} - 16 I_2 + 30 I_0 - 16 I_1 + I_{min})$$

$$a_3 = -\frac{2}{3\beta^3} (I_{max} - 2 I_2 + 2 I_1 - I_{min})$$

$$a_4 = \frac{2}{3\beta^4} (I_{max} - 4 I_2 + 6 I_0 - 4 I_1 + I_{min}) \qquad 3.7$$

Given a knowledge of these coefficients the equation of the H & D curve may be obtained in terms of the power series 3.2.

The coefficients in 3.5 give the mean intensity transmitted and the amplitudes of the fundamental and harmonic terms. The following notation may be introduced:-

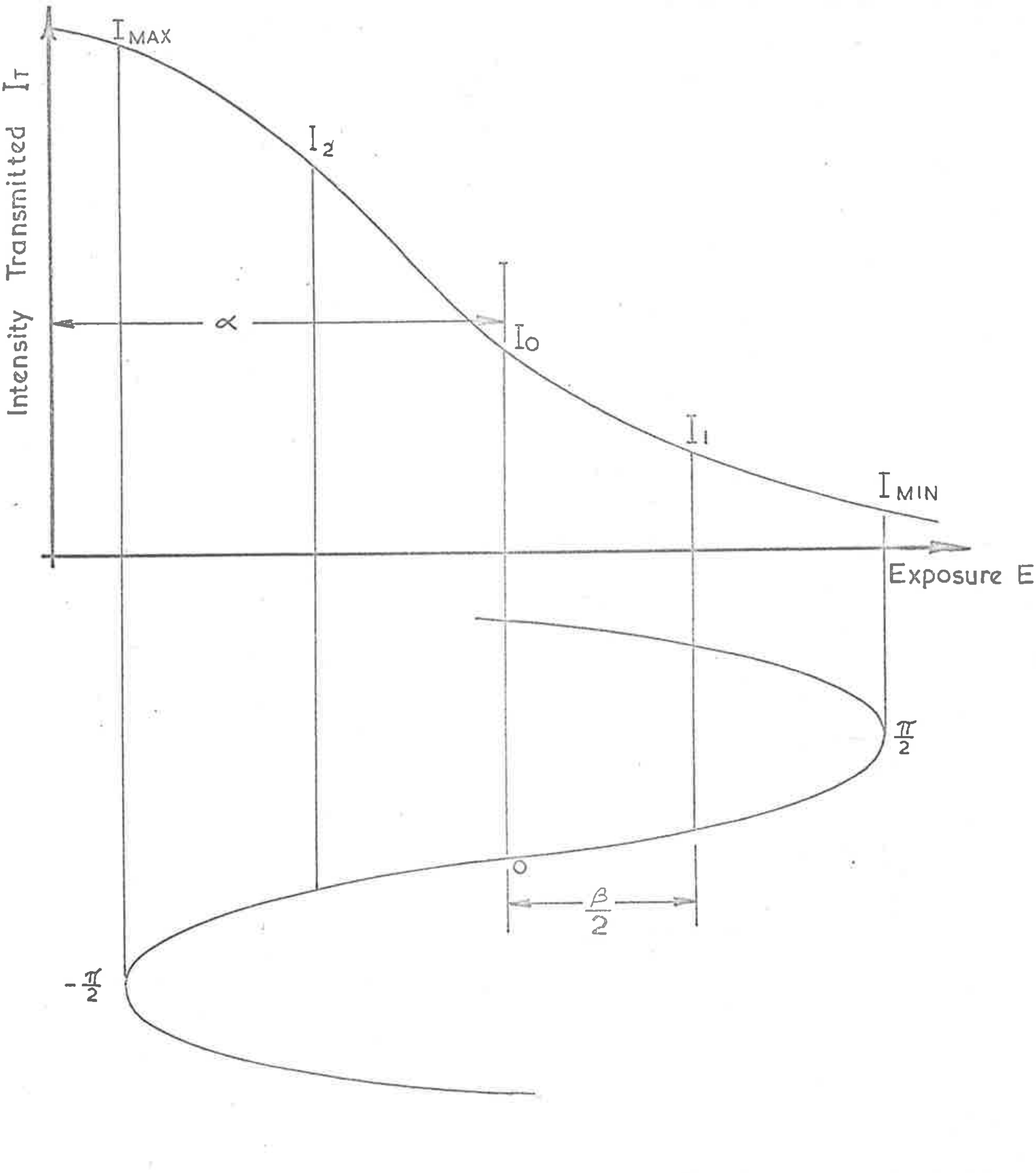

Intensity Transmitted I_T
I_{MAX}
I_2
α
I_0
I_1
I_{MIN}
Exposure E
$\frac{\pi}{2}$
0
$\frac{\beta}{2}$
$-\frac{\pi}{2}$

FIGURE 3.7

Mean intensity	$T_0 = f(\alpha) + 1/2\, a_2\, \beta^2 + 3/8\, a_4\, \beta^4$
Fundamental Amplitude	$A_F = a_1\, \beta + \frac{3}{4}\, a_3\, \beta^3$
2nd Harmonic Amp.	$A_2 = 1/2\, a_2\, \beta^2 + 1/2\, a_4\, \beta^4$
3rd Harmonic Amp.	$A_3 = 1/4\, a_3\, \beta^3$
4th Harmonic Amp.	$A_4 = 1/8\, a_4\, \beta^4$ 3.8

Substituting the values of the coefficients from 3.7 to 3.8 gives:-

$$T_0 = \frac{1}{6}\left[I_{max} + 2\, I_2 + 2\, I_1 + I_{min}\right]$$

$$A_F = \frac{1}{3}\left[I_{max} + I_2 - I_1 - I_{min}\right]$$

$$A_2 = -\frac{1}{4}\left[I_{max} - 2\, I_0 + I_{min}\right]$$

$$A_3 = -\frac{1}{6}\left[I_{max} - 2\, I_2 + 2\, I_1 - I_{min}\right]$$

$$A_4 = \frac{1}{12}\left[I_{max} - 4\, I_2 + 6\, I_0 - 4\, I_1 + I_{min}\right] \qquad 3.9$$

By inversion of these equations we can also write:-

$$I_{max} = T_0 + A_F + A_2 + A_3 + A_4$$

$$I_2 = T_0 + 1/2\, A_F - 1/2\, A_2 - A_3 - 1/2\, A_4$$

$$I_0 = T_0 - A_2 + A_4$$

$$I_1 = T_0 - 1/2\, A_F - 1/2\, A_2 + A_3 - 1/2\, A_4$$

$$I_{min} = T_0 - A_1 + A_2 - A_3 + A_4 \qquad 3.10$$

From the set of equations 3.9 we see that, by choosing five suitable points on a sine wave of known contrast centred about a known exposure we can, from the five corresponding values of I_m, calculate the harmonic amplitudes in the resulting image. Conversly from the set of equations 3.10 by measuring the mean intensity transmitted and the harmonic amplitudes, it is possible to deduce the five values of I_T and subsequently the five original exposure values.

For greater accuracy and to cover the cases where harmonics up to the sixth exist one can use a seven point method which yields the following results for the mean transmitted intensity and harmonic amplitudes:-

$$T_0 = \frac{1}{1280}\Big[167\,I_7 + 378\,I_6 - 135\,I_5 + 460\,I_4 - 135\,I_3 + 378\,I_2 + 167\,I_1\Big]$$

$$A_F = \frac{1}{640}\Big[167\,I_7 + 252\,I_6 - 45\,I_5 + 45\,I_3 - 252\,I_2 - 167\,I_1\Big]$$

$$A_2 = -\frac{1}{2560}\Big[559\,I_7 + 486\,I_6 - 1215\,I_5 + 340\,I_4 - 1215\,I_3 + 486\,I_2 + 559\,I_1\Big]$$

$$A_3 = -\frac{1}{256}\Big[45\,I_7 - 36\,I_6 - 63\,I_5 + 63\,I_3 + 36\,I_2 - 45\,I_1\Big]$$

$$A_4 = \frac{9}{1280}\Big[17\,I_7 - 42\,I_6 + 15\,I_5 + 20\,I_4 + 15\,I_3 - 42\,I_2 + 17\,I_1\Big]$$

$$A_5 = \frac{81}{1280}\Big[I_7 - 4\,I_6 + 5\,I_5 - 5\,I_3 + 4\,I_2 - I_1\Big]$$

$$A_6 = -\frac{81}{2560}\Big[I_7 - 6\,I_6 + 15\,I_5 - 20\,I_4 + 15\,I_3 - 6\,I_2 + I_1\Big] \qquad 3.11$$

Because of the unweidly nature of these equations, consideration has been restricted to the five point method in this investigation.

Having established this method of predicting the harmonic amplitudes it was decided to test it on straight H & D curves where it should give the same results as predicted by the approach used in III.2. The comparison may be seen in table 3.8.

It can be seen that in most cases the agreement is very good but the two sets tend to disagree when the gamma and contrast become large. In these cases it is felt that the results calculated by harmonic analysis of the waveform are more realiable because the profile is sampled at many more points i.e., twenty one points are used compared with only five in the five point method. Thus it seems reasonable to state that the five point method is expected to give reasonable results provided that the gamma or the contrast does not become large.

β/α	γ	5PT. METHOD			WAVE ANALYSIS		
		A_2/A_F	A_3/A_F	A_4/A_F	A_2/A_F	A_3/A_F	A_4/A_F
0.2	0.5	0.077	0.007	0.000	0.076	0.006	0.001
	1.0	0.101	0.010	0.001	0.101	0.011	0.001
	2.0	0.151	0.020	0.003	0.150	0.020	0.003
0.4	0.5	0.157	0.027	0.005	0.157	0.027	0.005
	1.0	0.209	0.044	0.009	0.209	0.043	0.009
	2.0	0.308	0.085	0.021	0.308	0.085	0.022
0.6	0.5	0.251	0.070	0.019	0.251	0.070	0.020
	1.0	0.333	0.110	0.033	0.333	0.111	0.036
	2.0	0.476	0.203	0.072	0.481	0.208	0.082
0.8	0.5	0.380	0.155	0.056	0.379	0.157	0.065
	1.0	0.494	0.235	0.094	0.498	0.245	0.115
	2.0	0.648	0.374	0.168	0.682	0.423	0.237

Table 3.8

It has the advantage over the previous method in that it can be extended into the regions of the H & D curve where it is no longer straight.

III.4 Experiments to test the validity of the five point method of predicting harmonic distortion

Test objects of low spatial frequency were selected for these experiments because the frequency response of the emulsion is then high and has negligible influence on the developed image. Consequently the H & D curve should be the primary factor influencing the final image and controlling the amount of harmonic distortion. The aim of the first experiment was to photograph sine wave objects of various content of the images, using both the five point technique and the treatment of III.2, with the measured values using the apparatus described. In anticipation of gamma being a contributing factor, three plates were exposed and developed for different times.

The emulsion used was Ilford H.P.3 which was dish developed in Microphen, using the brush technique. Microphen was chosen because it is known to introduce very little neighbourhood effect, this also being the reason for using brush development.

III.4.1 Experimental procedure

The interferometer was adjusted to give fringes of spatial frequency 3 lines/mm and the contrast of the fringes was set by moving the back mirror on the micrometer screw. A fine slit, situated in the focal plane, was used to measure the contrast of the fringes which were made to scan across it slowly using the scanning prism P_1.

Having adjusted the fringes to a suitable contrast, they were photographed using the small plate camera. A constant exposure time of ten seconds was used and the exposure was varied through a range of three logarithmic units by inserting neutral density filters in front of the collimator slit. On each plate there were also eleven exposures used to determine the H & D curve. These were obtained by blocking one of the beams of the interferometer thus leaving an evenly illuminated field in the plane of the emulsion. The intensity of this field was varied as before with neutral density filters.

Fringes of contrast 0.45, 0.59 and 0.67 were exposed on each plate making a total number of exposures in each case of forty four. The three plates were developed for 3, 5 and 7 minutes giving gammas of 1.27, 1.60 and 1.99.

It was important to be able to locate accurately the sine wave exposures on the H & D curve. This was achieved by using the instrument as a photometer with a fine slit ($10\,\mu$ wide) set up in the transparency plane. First of all one beam was blocked as for the gamma curve exposures and a suitable filter inserted before the collimator slit. The amount of light passing through the fine slit was recorded by the d.c. voltmeter connected directly to the photomultiplier. Fringes of the contrast to be photographed were now set up and slowly scanned across the slit. The mean level of illumination was noted and when compared with the previous level enabled its location on the H & D curve to be established.

III.4.2 Measurement of H & D curve

The developed plate was returned to the apparatus and a rectangular aperture (5 m.m. x 3 m.m.) set up before it. The exposures for determining the characteristic curve were moved in turn behind the aperture and the amount of light passing through the plate measured with the voltmeter again directly coupled to the photomultiplier. For these measurements only one beam was used and its intensity was adjusted so that the incident level i.e., the level measured when the plate was removed, gave a reading of approximately one volt. This insured that the photomultiplier, with a cathode voltage of 1 000 volts, was not being overloaded. The stray light level was also measured and subtracted from all other measurements. The density was calculated for each exposure using the relationship, density is equal to $\log_{10}\ (I_0/I_T)$, where I_0 is the incident level and I_T the transmitted. The measured density was plotted against the logarithm of the exposure to obtain the characteristic curve.

III.4.3 Measurement of the contrast of frequencies present in the transparencies

The same aperture was used in the contrast measurements but this time assuming a more significant role. Its length, 5 m.m. was carefully chosen to obtain inside the scanning mask an integral number of sine wave periods, 15 in this case. This was necessary to eliminate the influence of the aperture size on the results of measurements.

If the transparency function of the sine wave structure is:-

$$B(\xi) = \alpha_0 + \beta_0 \operatorname{Cos} 2\pi R_0 \xi \qquad 3.12$$

then the real part of its Fourier transform as measured by the instrument with the length of the limiting domain a will be

$$B(R) = \int_{-a/2}^{a/2} (\alpha_0 + \beta_0 \operatorname{Cos} 2\pi R_0 \xi) \operatorname{Cos}(2\pi R \xi) d\xi \qquad 3.13$$

After the simple integration this leads to

$$b(R) = \alpha_0 \frac{\operatorname{Sin} \pi R a}{\pi R} + \beta_0 \left[\frac{\operatorname{Sin} \pi (R_0 - R)a}{2\pi (R_0 - R)} + \frac{\operatorname{Sin} \pi (R_0 + R)a}{2\pi (R_0 + R)} \right] \qquad 3.14$$

If we normalise α_0 a = 1 then

$$b(R) = \frac{\operatorname{Sin} \pi R a}{\pi R a} + \frac{\beta_0}{2\alpha_0} \left[\frac{\operatorname{Sin} \pi (R_0 - R)a}{\pi (R_0 - R)a} + \frac{\operatorname{Sin} \pi (R_0 + R) a}{\pi (R_0 + R) a} \right] \qquad 3.15$$

The first term, Sin π R a /π R a, is the Fourier transform of the aperture, and has no influence on the peak value b(R) measured as long as R_0 = n/a, where n is an integer; for these particular values of R_0 the Fourier transform of the aperture is zero. If R_0 = R and n is equal to the number of sine waves in the aperture 3.15 takes the form

$$b(R) = \beta_o / 2\alpha_o \qquad 3.16$$

Thus the output signal is directly proportional to the contrast in the sine wave transparency.

The procedure of measurement was as follows; initially the interferometer was set to give zero fringes and the transparency was scanned. The output was recorded on a pen recorder and denoted d.c. level. The frequency was now set at 3 lines/mm and again the output was recorded. By dividing this level by the d.c. level the contrast of the component of 3 lines/mm in the transparency was obtained. The procedure was repeated for harmonics up to the third and the contrast of the harmonics calculated. It was important in these measurements to have the scanning fringes parallel to the fringes in the transparency especially as the frequency increased. This was achieved by adjusting one of the back mirrors of the interferometer until the output maximised, this occurring when the two sets of fringes were parallel.

III.4.4 The evaluation of theoretical results

The H & D curve was plotted in terms of density and relative $\log_{10}$ (exposure) and this curve was used to estimate the harmonic distortion present in sine wave images distributed along the exposure axis. Using a logarithmic scale for exposure has the advantage that an indicator scale may be prepared for any given contrast and the middle of it made coincident with the exposure for which the output signal is desired. Five density values were read off and converted to values of transmitted intensity by assuming a suitable value for incident intensity. The values calculated from these five points and presented in the following graphs are fundamental contrast, ratio of second harmonic to fundamental A_2/A_F, and ratio of third harmonic to fundamental A_3/A_F. For each plate these values were calculated for effective exposure contrasts of 0.45, 0.59 and 0.67 at log (exposure) intervals of 0.3 along the exposure axis. These calculated values are represented in the graphs (figures 3.9 - 3.35) by the dotted lines and are compared with the measured values which are represented by the full line. Included on each graph is the value predicted from the treatment given in III.2 using the gamma value measured over the straight part of the H & D curve which is also included.

III.4.5 Discussion of results

For short development time the agreement between the theoretical and practical values is good in nearly all cases. As the contrast of the effective exposure increases the agreement is not so good, with the five point method having a tendency to over estimate the distortion. Similar conclusions can be drawn from the curves pertaining to the 5 and 7 minute development times.

In all cases the agreement seems to fall off at the higher densities, this probably being due to inaccuracies in reading the five density values with the five point method. Some difficulty was found in measuring the contrast of the harmonics, which are often quite small, especially in the toe and shoulder regions of the H & D curve. Thus some of the measured curves for the harmonic ratios extend over a relatively short range, but never less than two logarithmic units.

It is interesting to note that the values predicted from the straight gamma curve calculations of III.2 agree well with the measured values over a range of about one logarithmic units of exposure in nearly all cases. In the cases where the five point method values and the practical values differ, the straight gamma curve predictions tend to be more accurate. This indicates that the difference is due to limitations of the five point method rather than errors introduced in

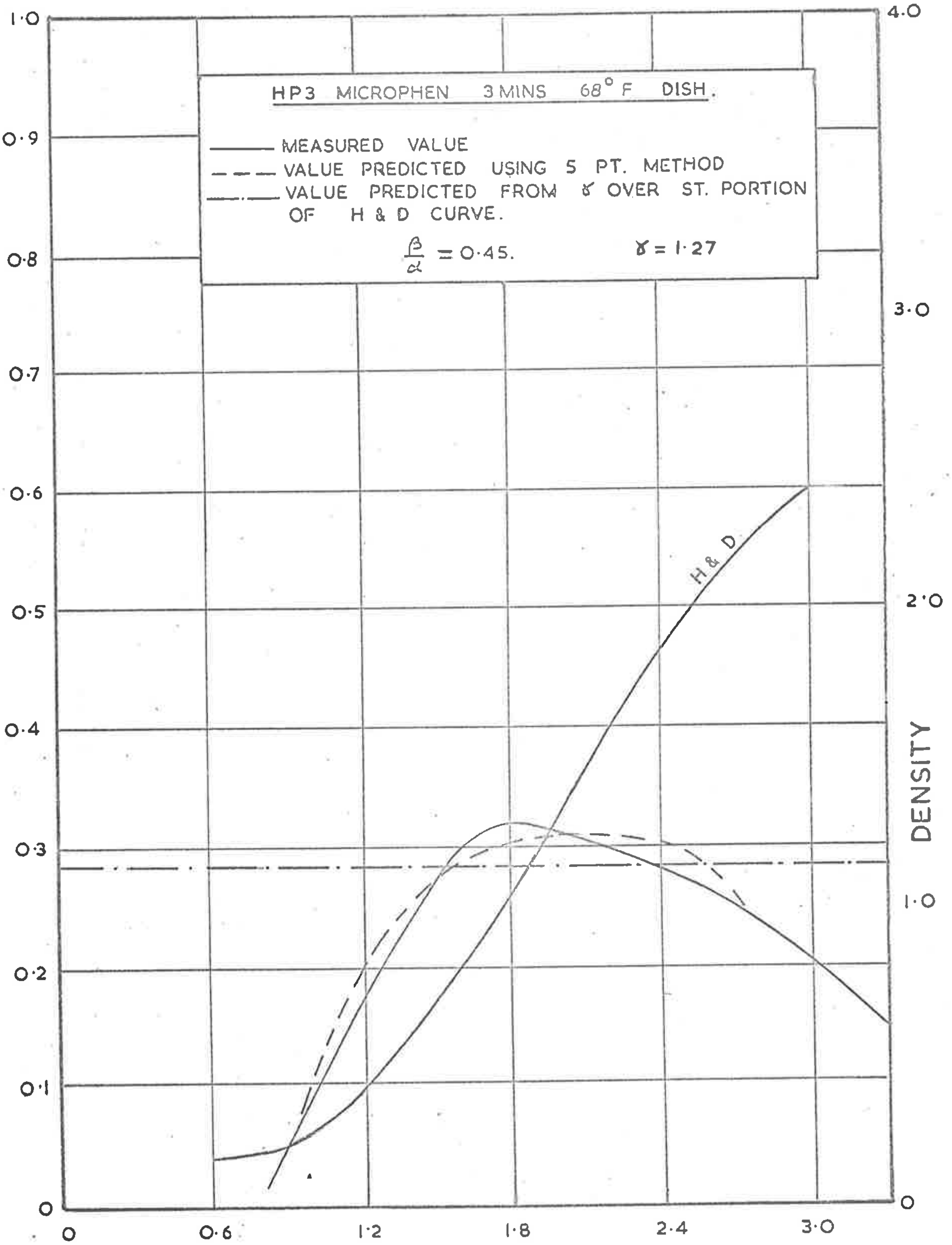
HP3 MICROPHEN 3 MINS 68° F DISH.
MEASURED VALUE
VALUE PREDICTED USING 5 PT. METHOD
VALUE PREDICTED FROM γ OVER ST. PORTION OF H & D CURVE.
β/α = 0·45.
γ = 1·27
H & D
1·0
0·9
0·8
0·7
0·6
0·5
0·4
0·3
0·2
0·1
0
4.0
3·0
2·0
1·0
0
DENSITY
0
0·6
1·2
1·8
2·4
3·0
REL. LOG. E

FIGURE 3. 9. ..

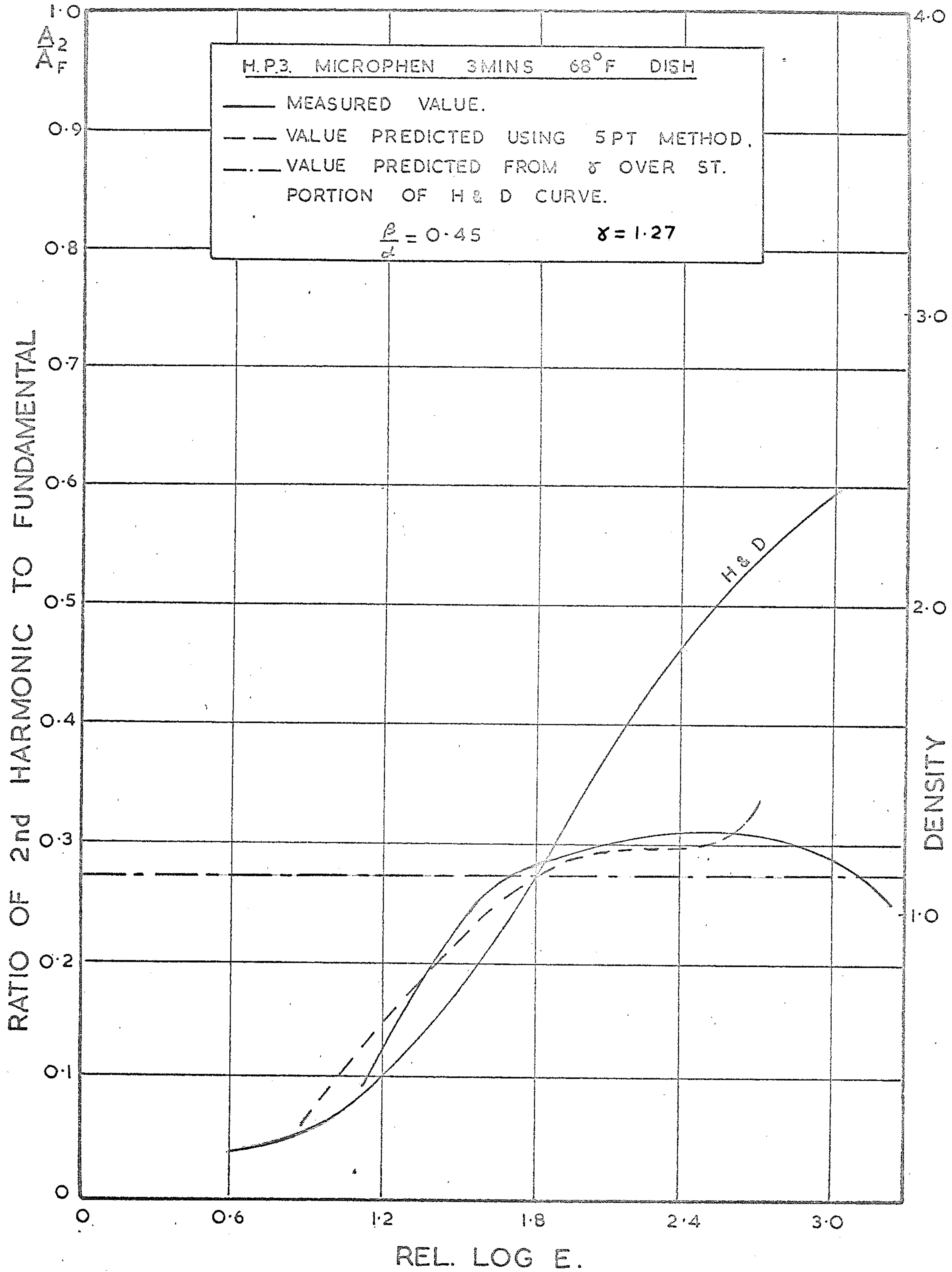
H.P.3. MICROPHEN 3MINS 68°F DISH
MEASURED VALUE.
VALUE PREDICTED USING 5PT METHOD.
VALUE PREDICTED FROM γ OVER ST. PORTION OF H & D CURVE.
β/α = 0·45
γ = 1·27
H & D
A2/AF
RATIO OF 2nd HARMONIC TO FUNDAMENTAL
DENSITY
REL. LOG E.
0
0·1
0·2
0·3
0·4
0·5
0·6
0·7
0·8
0·9
1·0
1·0
2·0
3·0
4·0
0·6
1·2
1·8
2·4
3·0

FIGURE 3. 10.

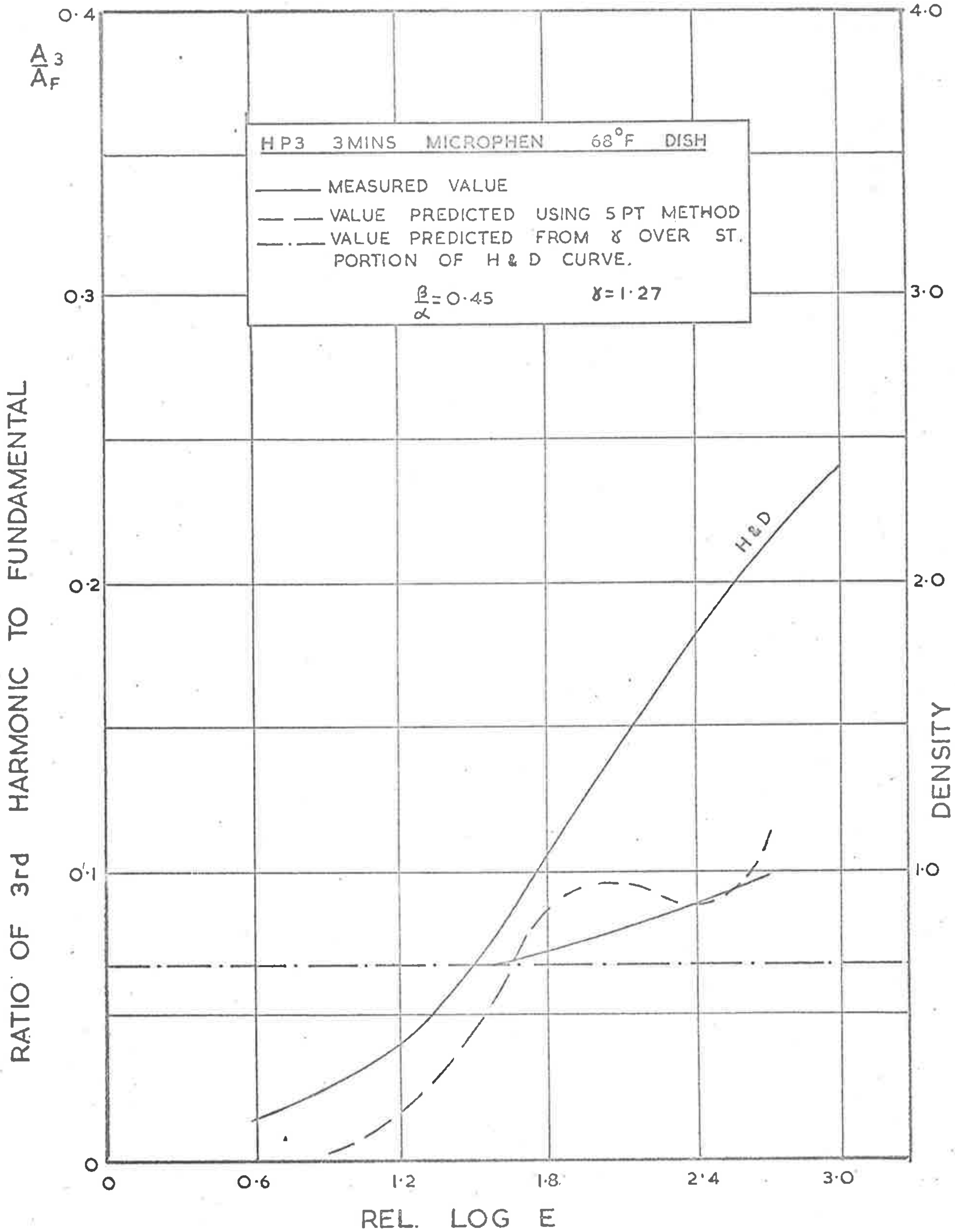
0·4
0·3
0·2
0·1
0
$\frac{A_3}{A_F}$
RATIO OF 3rd HARMONIC TO FUNDAMENTAL
4·0
3·0
2·0
1·0
DENSITY
0
0·6
1·2
1·8
2·4
3·0
H P3 3 MINS MICROPHEN 68°F DISH
MEASURED VALUE
VALUE PREDICTED USING 5 PT METHOD
VALUE PREDICTED FROM γ OVER ST. PORTION OF H & D CURVE.
$\frac{\beta}{\alpha}$ = 0·45
γ = 1·27
H & D
REL. LOG E

FIGURE 3.11.

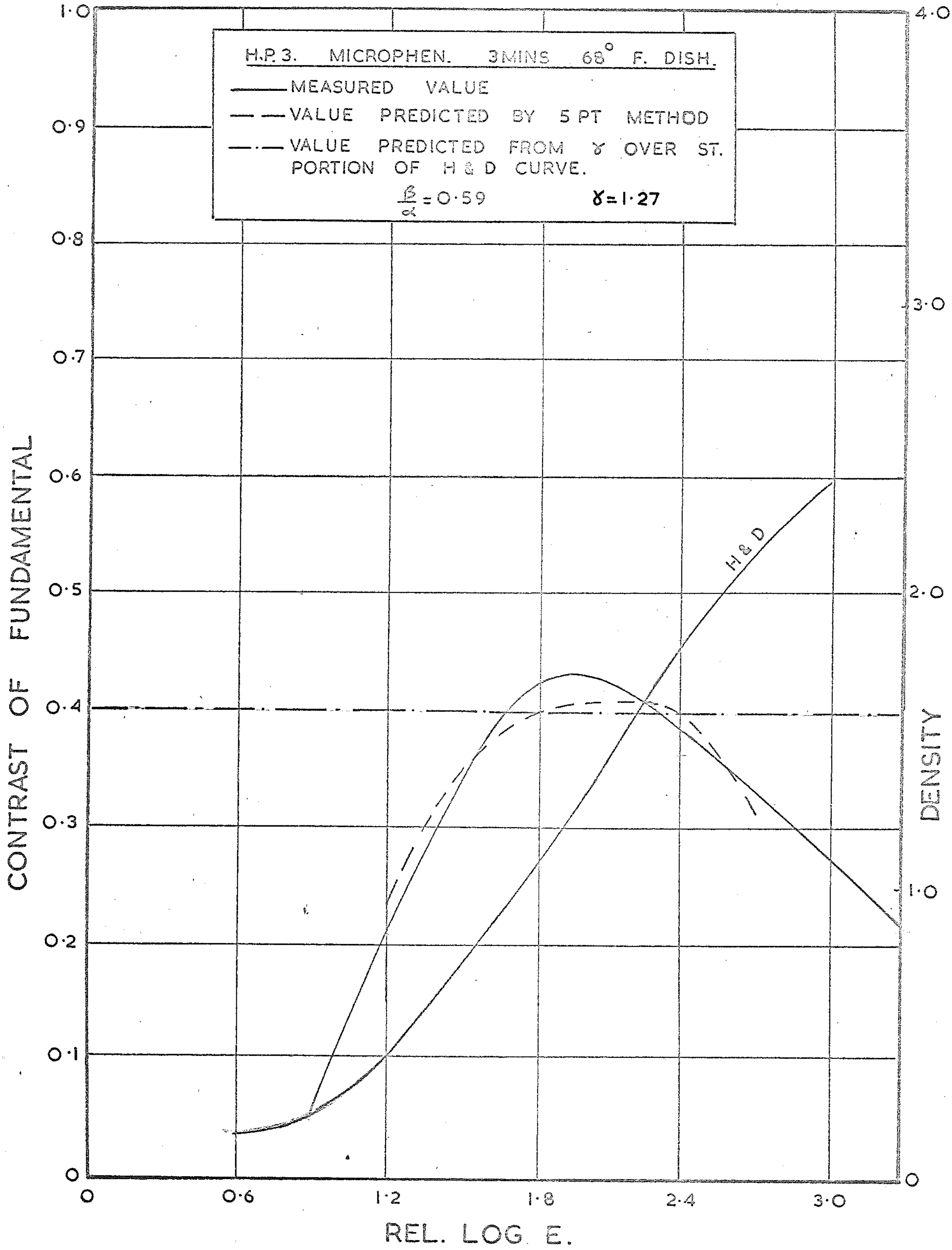
H.P. 3. MICROPHEN. 3 MINS 68° F. DISH.
MEASURED VALUE
VALUE PREDICTED BY 5 PT METHOD
VALUE PREDICTED FROM γ OVER ST. PORTION OF H & D CURVE.
β/α = 0·59
γ = 1·27
H & D
CONTRAST OF FUNDAMENTAL
DENSITY
1·0
0·9
0·8
0·7
0·6
0·5
0·4
0·3
0·2
0·1
0
4·0
3·0
2·0
1·0
0
0·6
1·2
1·8
2·4
3·0
REL. LOG E.

FIGURE 3.12

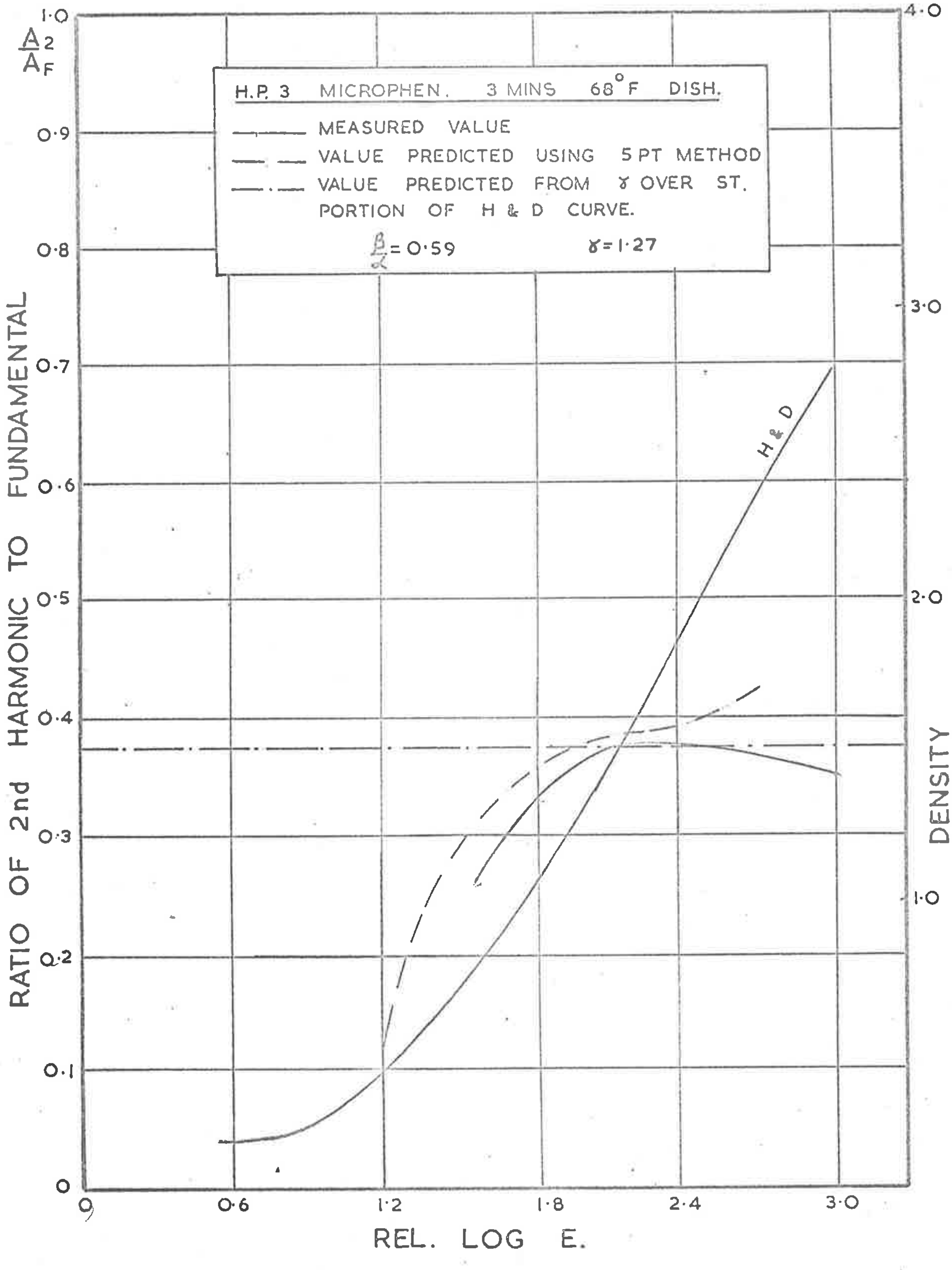
H.P. 3 MICROPHEN. 3 MINS 68°F DISH.
MEASURED VALUE
VALUE PREDICTED USING 5 PT METHOD
VALUE PREDICTED FROM γ OVER ST. PORTION OF H & D CURVE.
β/α = 0·59
γ = 1·27
H & D
$\frac{A_2}{A_F}$
RATIO OF 2nd HARMONIC TO FUNDAMENTAL
DENSITY
REL. LOG E.
0
0·1
0·2
0·3
0·4
0·5
0·6
0·7
0·8
0·9
1·0
1·0
2·0
3·0
4·0
0·6
1·2
1·8
2·4
3·0

FIGURE 3.13

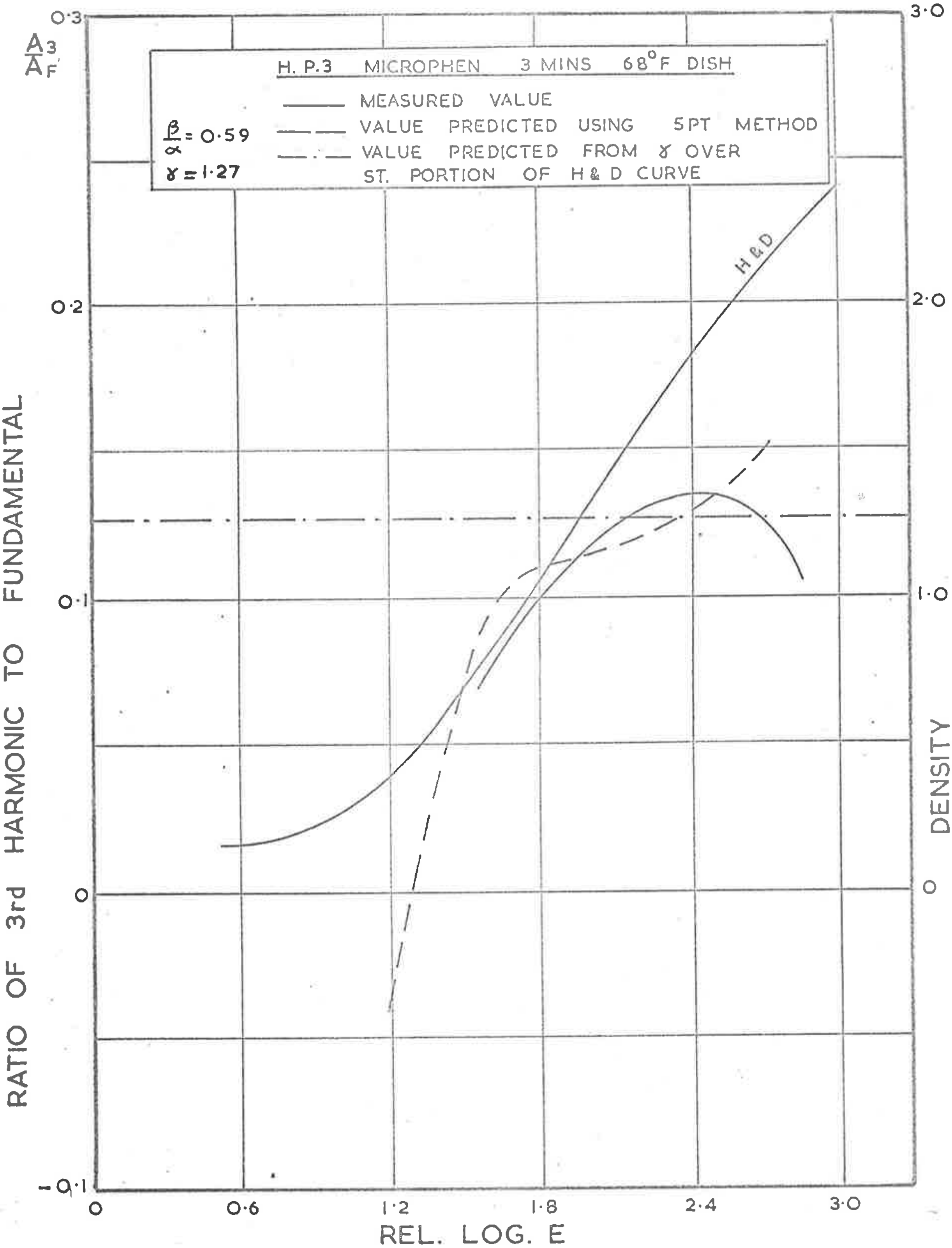
H. P.3 MICROPHEN 3 MINS 68°F DISH
MEASURED VALUE
VALUE PREDICTED USING 5PT METHOD
VALUE PREDICTED FROM γ OVER ST. PORTION OF H & D CURVE
β/α = 0·59
γ = 1·27
H & D
0·3
0·2
0·1
0
-0·1
$\frac{A_3}{A_F}$
RATIO OF 3rd HARMONIC TO FUNDAMENTAL
3·0
2·0
1·0
0
DENSITY
0
0·6
1·2
1·8
2·4
3·0
REL. LOG. E

FIGURE 3.14.

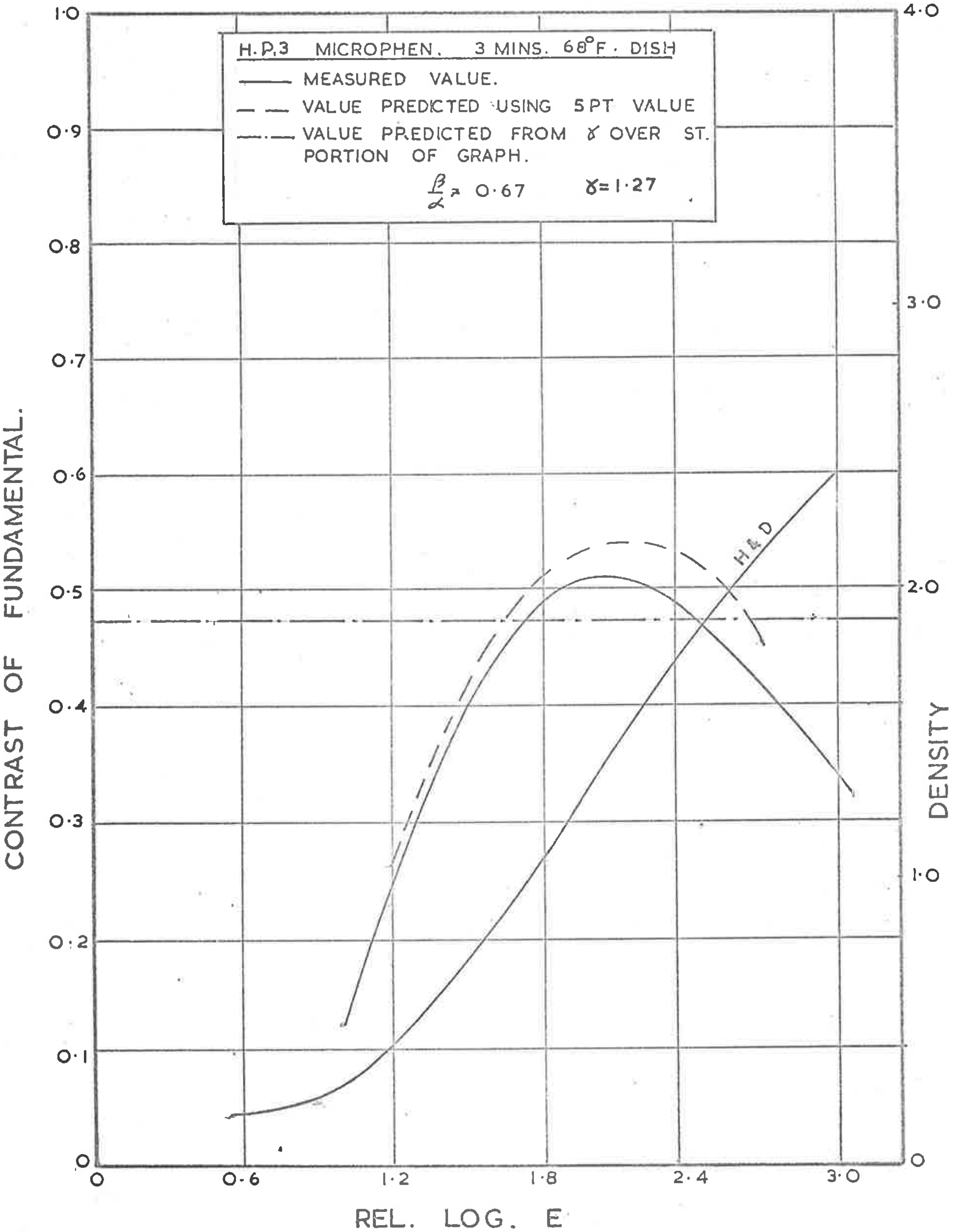

H.D.3 MICROPHEN. 3 MINS. 68°F. DISH
MEASURED VALUE.
VALUE PREDICTED USING 5PT VALUE
VALUE PREDICTED FROM γ OVER ST. PORTION OF GRAPH.
β/α = 0·67
γ = 1·27
H & D
CONTRAST OF FUNDAMENTAL.
DENSITY
REL. LOG. E
1·0
0·9
0·8
0·7
0·6
0·5
0·4
0·3
0·2
0·1
0
4·0
3·0
2·0
1·0
0
0
0·6
1·2
1·8
2·4
3·0

FIGURE 3.15.

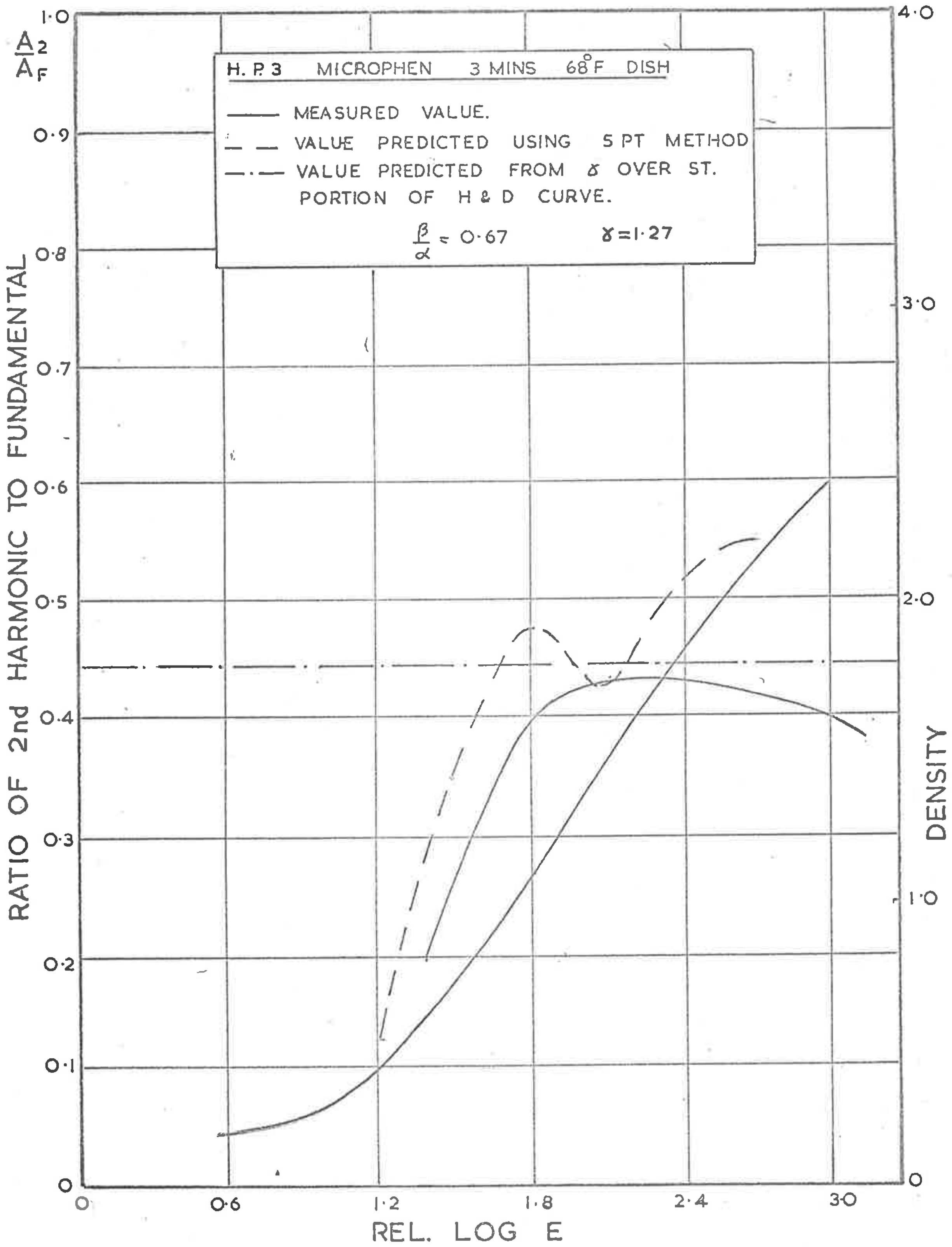

H. P. 3 MICROPHEN 3 MINS 68°F DISH
MEASURED VALUE.
VALUE PREDICTED USING 5 PT METHOD
VALUE PREDICTED FROM γ OVER ST. PORTION OF H & D CURVE.
β/α = 0·67
γ = 1·27
A2/AF
RATIO OF 2nd HARMONIC TO FUNDAMENTAL
DENSITY
REL. LOG E

FIGURE 3. 16.

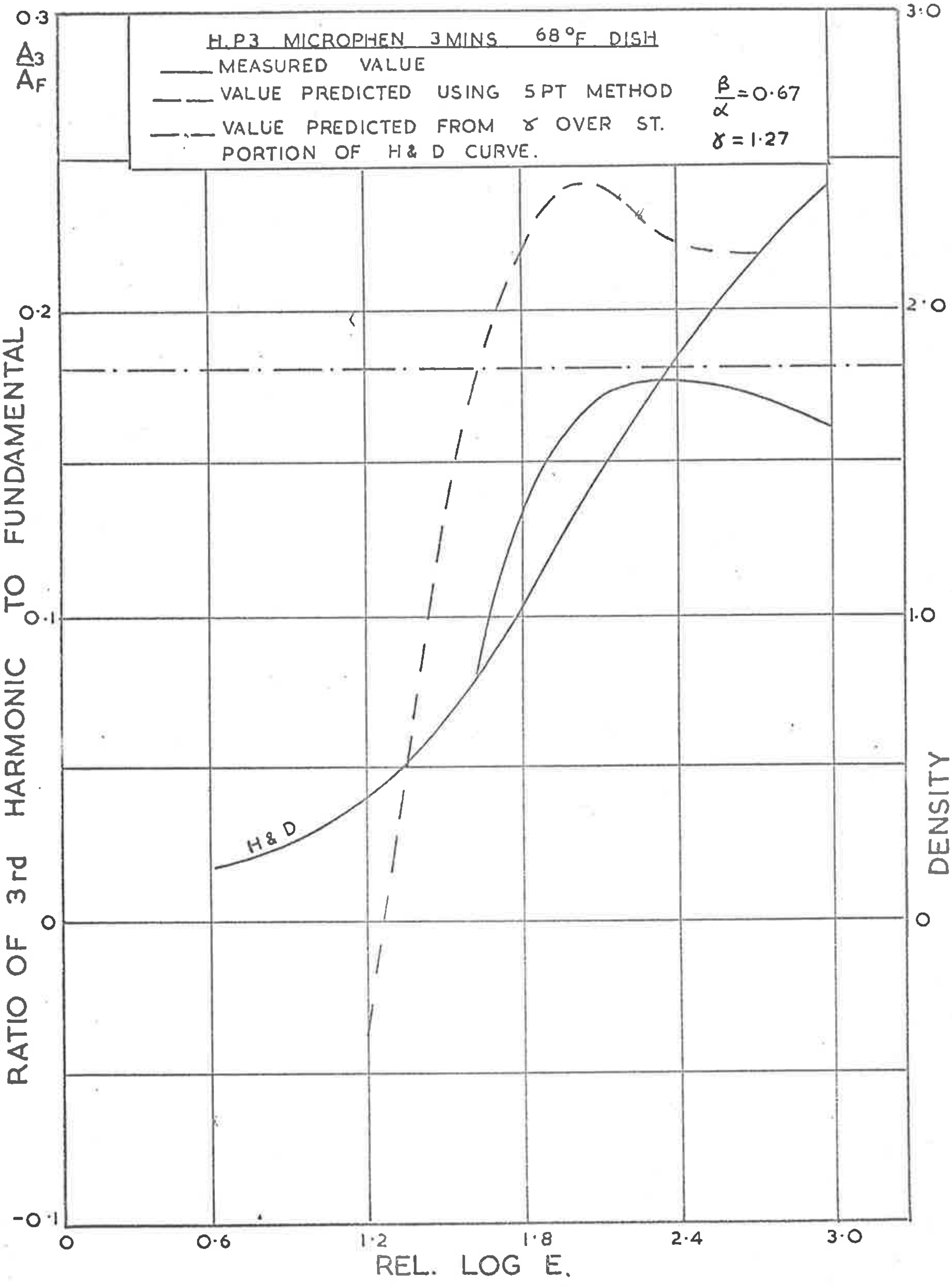
H.P3 MICROPHEN 3MINS 68°F DISH
MEASURED VALUE
VALUE PREDICTED USING 5PT METHOD
VALUE PREDICTED FROM γ OVER ST. PORTION OF H & D CURVE.
β/α = 0·67
γ = 1·27
A3/AF
RATIO OF 3rd HARMONIC TO FUNDAMENTAL
DENSITY
REL. LOG E.
H & D
0·3
0·2
0·1
0
-0·1
3·0
2·0
1·0
0
0·6
1·2
1·8
2·4
3·0

FIGURE 3.17

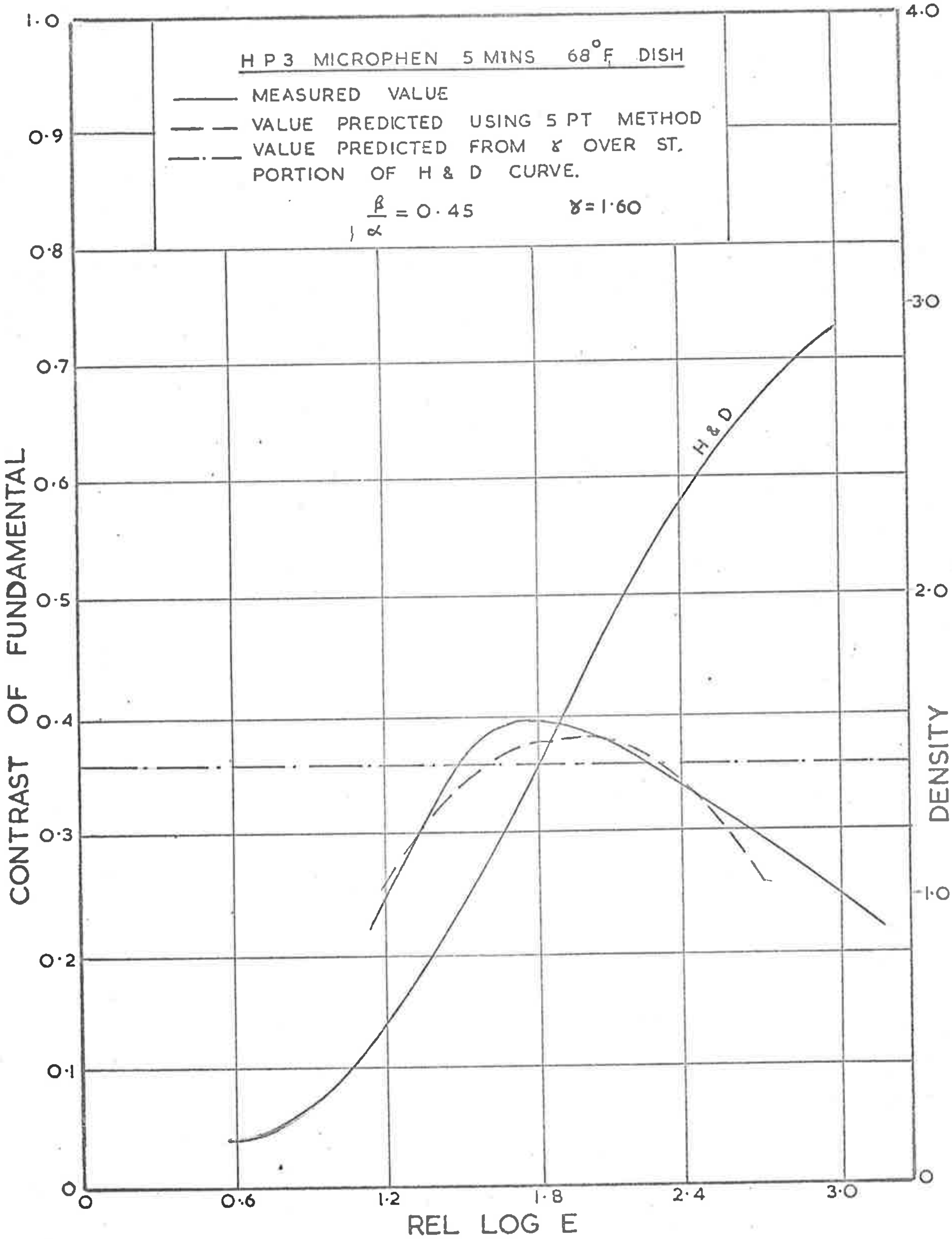
H P 3 MICROPHEN 5 MINS 68°F DISH
MEASURED VALUE
VALUE PREDICTED USING 5 PT METHOD
VALUE PREDICTED FROM γ OVER ST. PORTION OF H & D CURVE.
β/α = 0·45
γ = 1·60
H & D
CONTRAST OF FUNDAMENTAL
DENSITY
REL LOG E
1·0
0·9
0·8
0·7
0·6
0·5
0·4
0·3
0·2
0·1
0
4·0
3·0
2·0
1·0
0
0·6
1·2
1·8
2·4
3·0

FIGURE 3. 18.

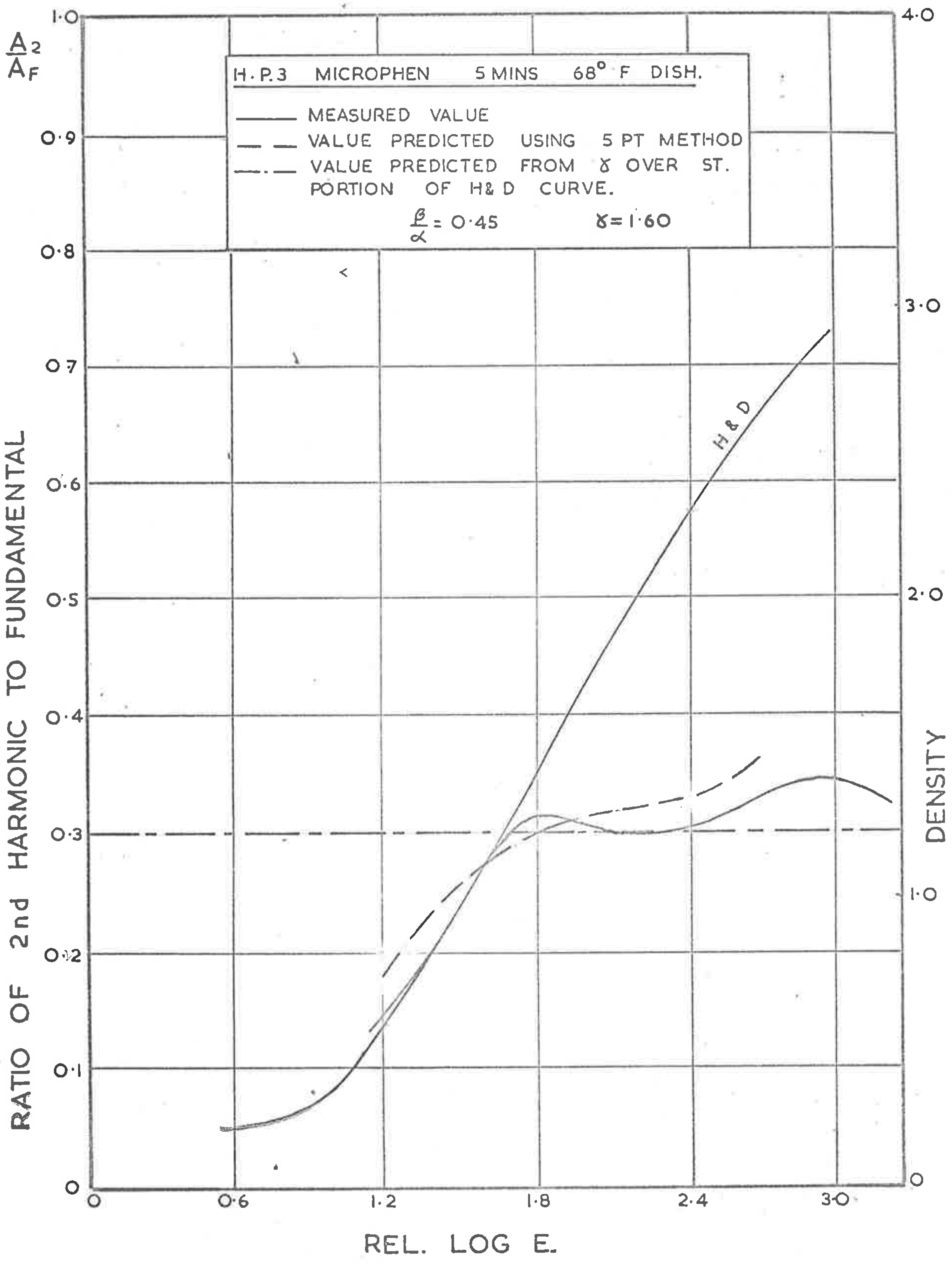
H. P. 3 MICROPHEN 5 MINS 68° F DISH.
MEASURED VALUE
VALUE PREDICTED USING 5 PT METHOD
VALUE PREDICTED FROM γ OVER ST. PORTION OF H& D CURVE.
β/α = 0·45
γ = 1·60
H & D
A_2/A_F
RATIO OF 2nd HARMONIC TO FUNDAMENTAL
DENSITY
0
0·1
0·2
0·3
0·4
0·5
0·6
0·7
0·8
0·9
1·0
1·0
2·0
3·0
4·0
0·6
1·2
1·8
2·4
3·0
REL. LOG E.

FIGURE 3. 19

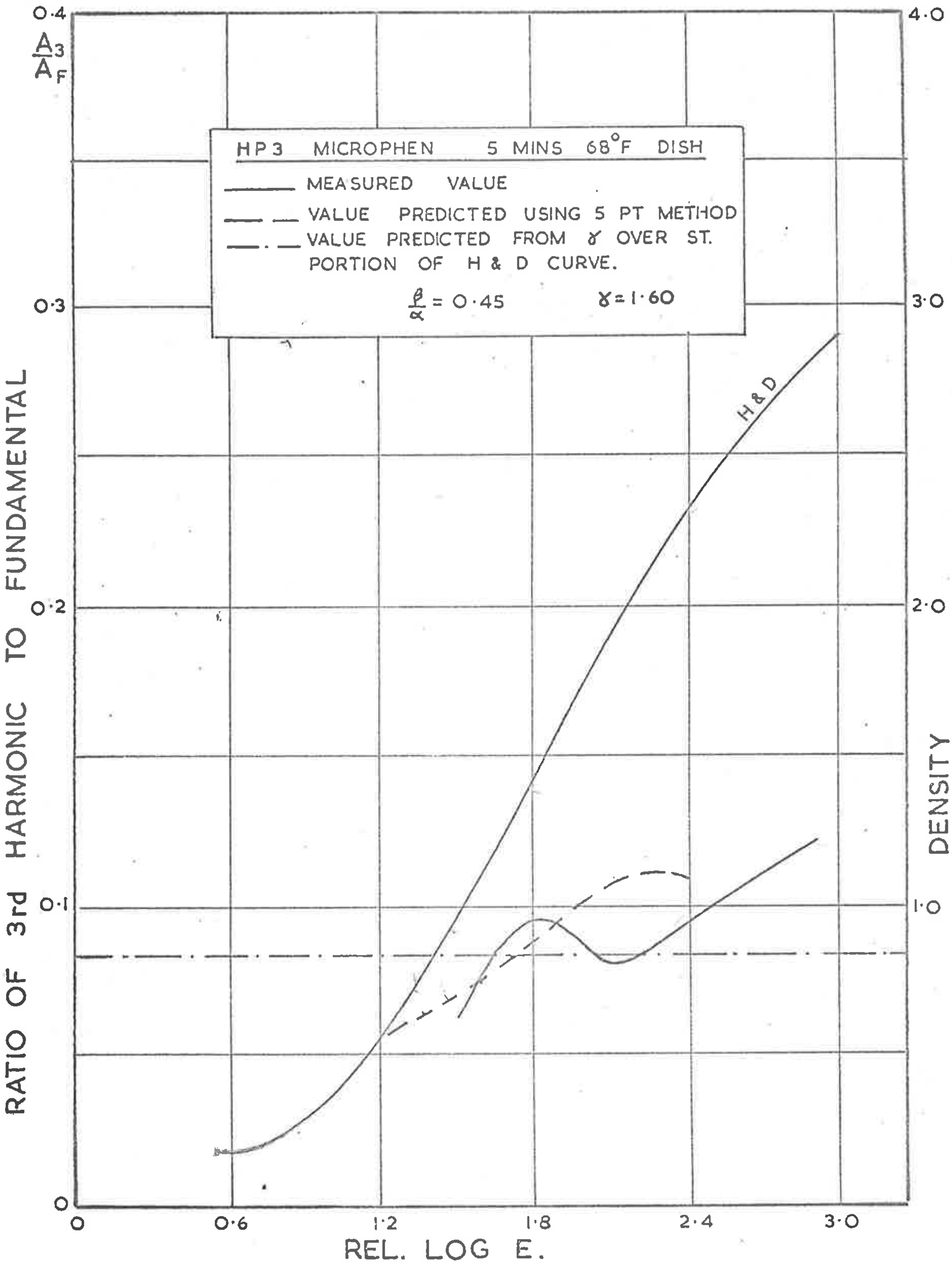

0·4
$\frac{A_3}{A_F}$
HP3 MICROPHEN 5 MINS 68°F DISH
MEASURED VALUE
VALUE PREDICTED USING 5 PT METHOD
VALUE PREDICTED FROM γ OVER ST. PORTION OF H & D CURVE.
$\frac{\beta}{\alpha}$ = 0·45
γ = 1·60
0·3
0·2
0·1
0
RATIO OF 3rd HARMONIC TO FUNDAMENTAL
4·0
3·0
2·0
1·0
DENSITY
H & D
0
0·6
1·2
1·8
2·4
3·0
REL. LOG E.

FIGURE 3. 20.

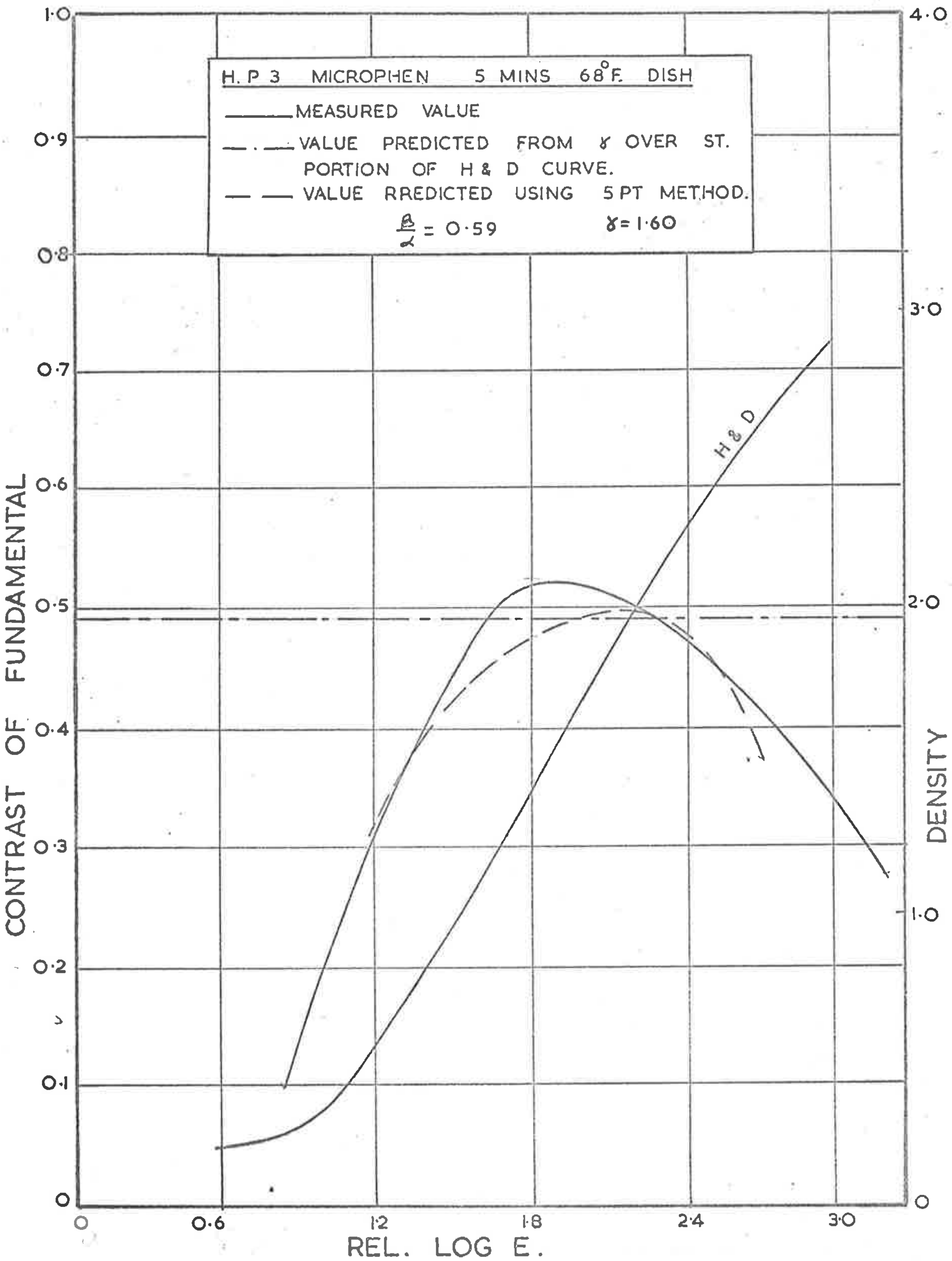

H. P 3 MICROPHEN 5 MINS 68°F DISH
MEASURED VALUE
VALUE PREDICTED FROM γ OVER ST. PORTION OF H & D CURVE.
VALUE RREDICTED USING 5 PT METHOD.
β/α = 0·59
γ = 1·60
H & D
CONTRAST OF FUNDAMENTAL
DENSITY
REL. LOG E.
0
0·1
0·2
0·3
0·4
0·5
0·6
0·7
0·8
0·9
1·0
0·6
1·2
1·8
2·4
3·0
1·0
2·0
3·0
4·0

FIGURE 3. 21.

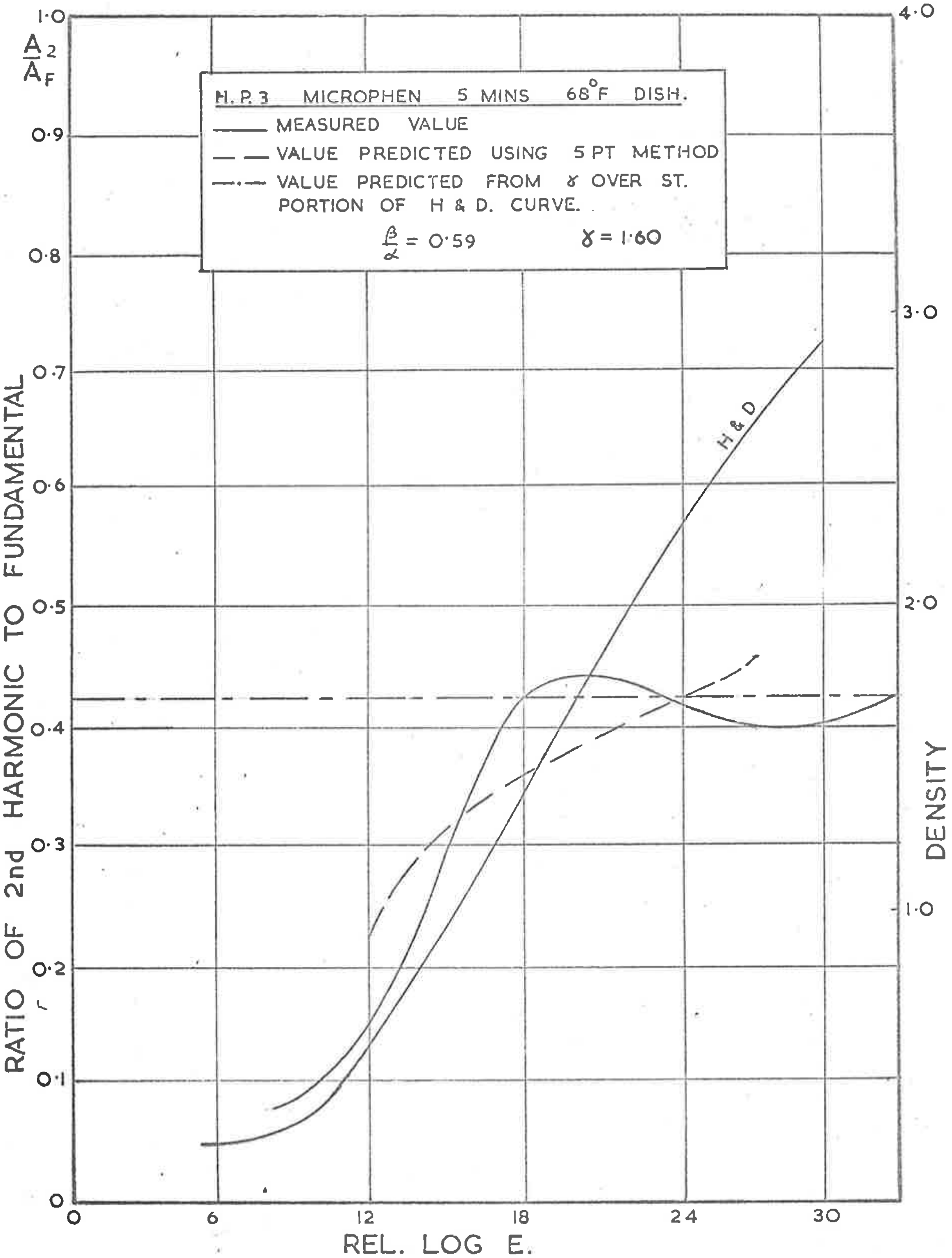
H. P. 3 MICROPHEN 5 MINS 68°F DISH.
MEASURED VALUE
VALUE PREDICTED USING 5 PT METHOD
VALUE PREDICTED FROM γ OVER ST. PORTION OF H & D. CURVE.
β/α = 0·59
γ = 1·60
H & D
RATIO OF 2nd HARMONIC TO FUNDAMENTAL
A2/AF
DENSITY
REL. LOG E.
1·0
0·9
0·8
0·7
0·6
0·5
0·4
0·3
0·2
0·1
0
4·0
3·0
2·0
1·0
0
6
12
18
24
30

FIGURE 3.22.

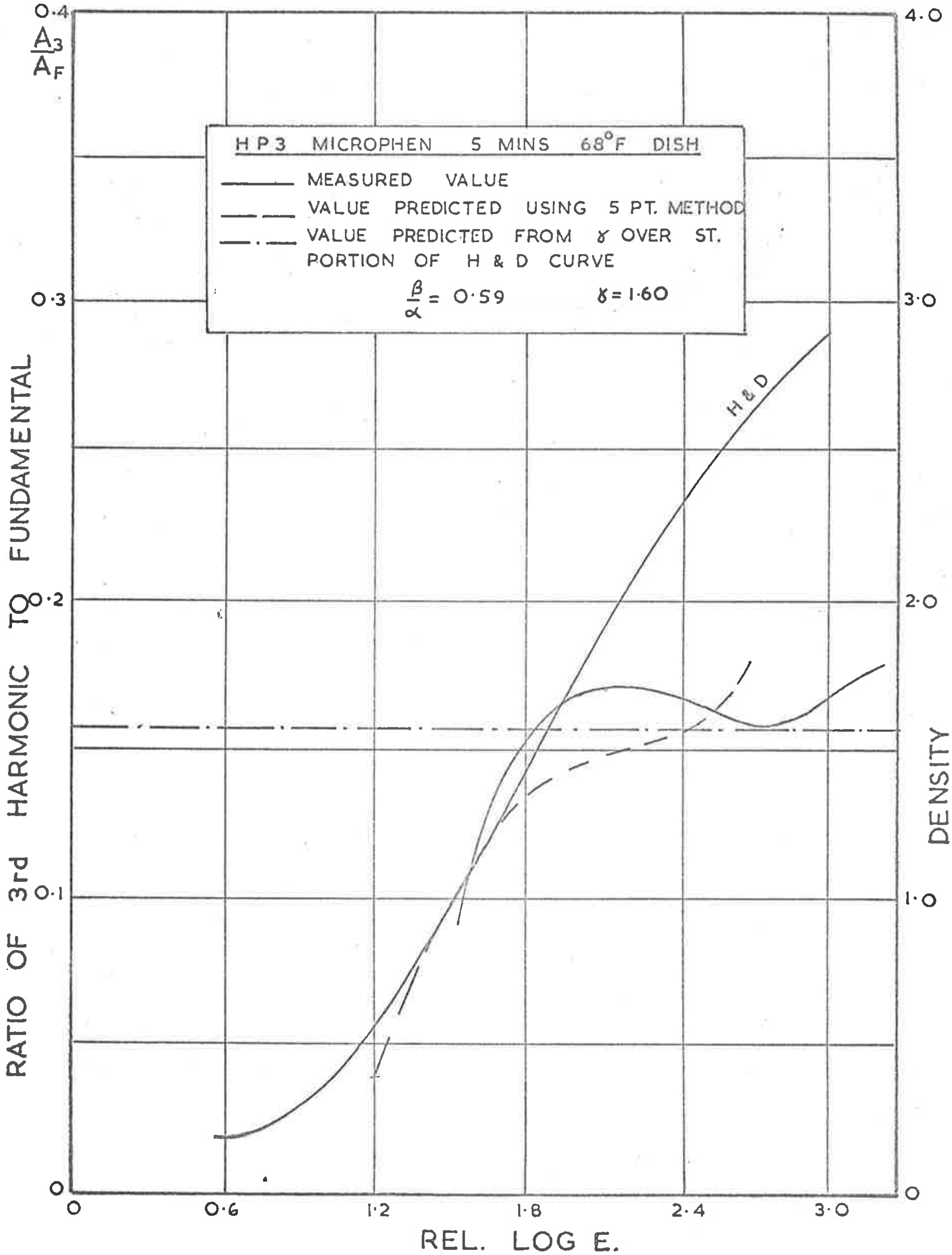

0.4
$\frac{A_3}{A_F}$
4.0
HP3 MICROPHEN 5 MINS 68°F DISH
MEASURED VALUE
VALUE PREDICTED USING 5 PT. METHOD
VALUE PREDICTED FROM γ OVER ST. PORTION OF H & D CURVE
$\frac{\beta}{\alpha}$ = 0·59
γ = 1·60
0·3
3·0
H & D
0·2
2·0
0·1
1·0
0
0
RATIO OF 3rd HARMONIC TO FUNDAMENTAL
DENSITY
0
0·6
1·2
1·8
2·4
3·0
REL. LOG E.

FIGURE 3. 23.

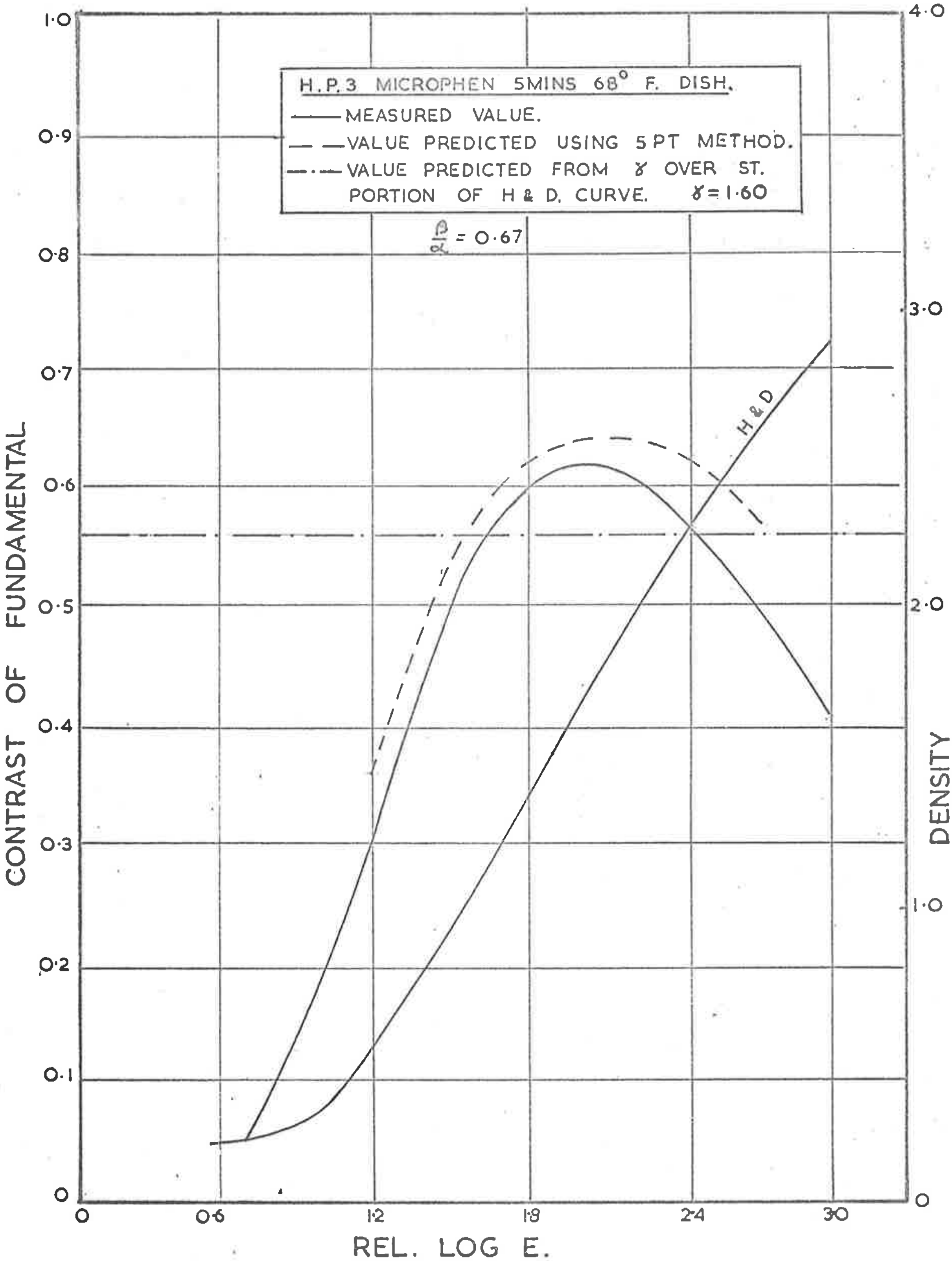
H.P.3 MICROPHEN 5MINS 68° F. DISH.
MEASURED VALUE.
VALUE PREDICTED USING 5 PT METHOD.
VALUE PREDICTED FROM γ OVER ST. PORTION OF H & D. CURVE. γ = 1·60
β/α = 0·67
H & D
CONTRAST OF FUNDAMENTAL
DENSITY
REL. LOG E.
1·0
0·9
0·8
0·7
0·6
0·5
0·4
0·3
0·2
0·1
0
0·6
1·2
1·8
2·4
3·0
4·0
3·0
2·0
1·0

FIGURE 3. 24.

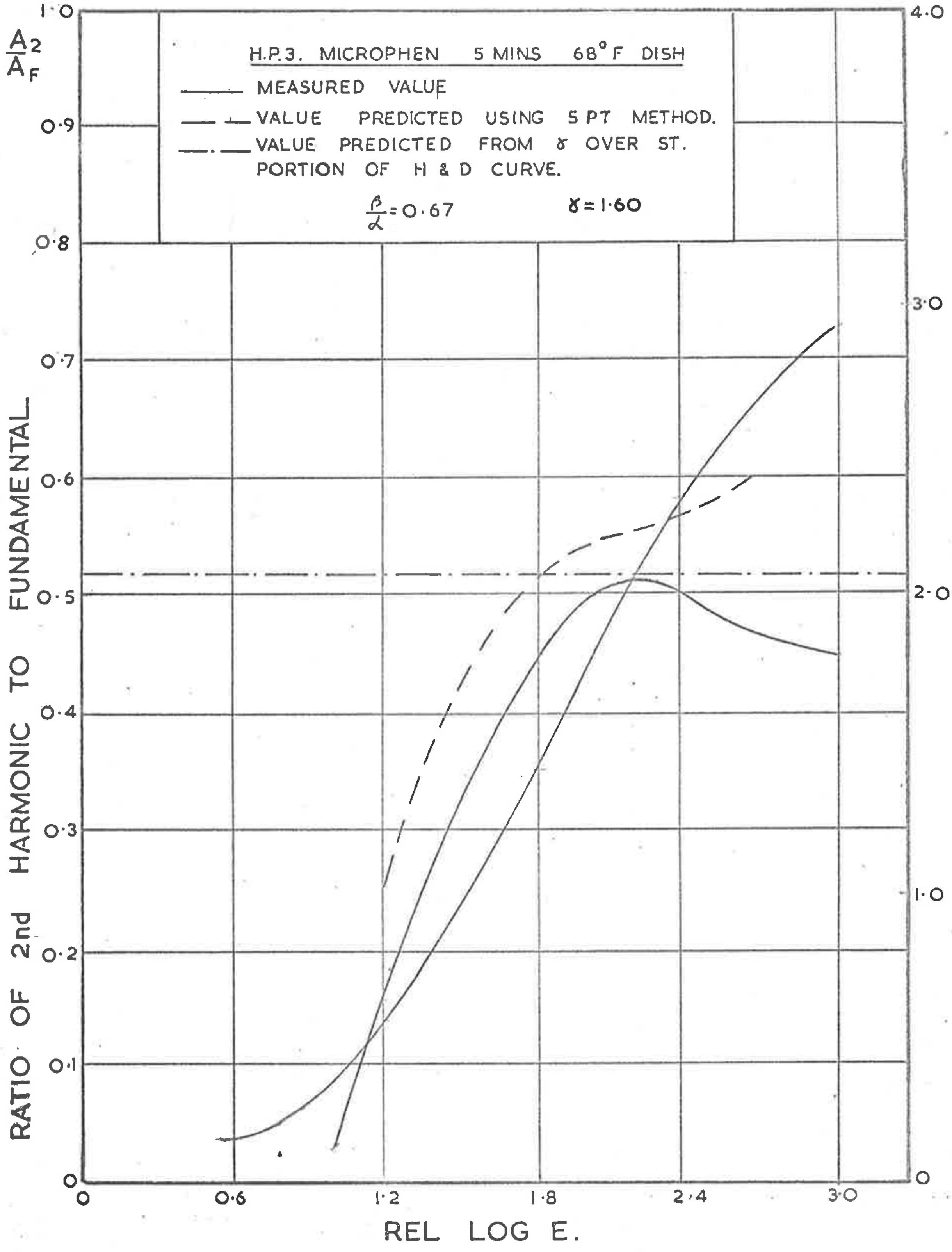
H.P.3. MICROPHEN 5 MINS 68°F DISH
MEASURED VALUE
VALUE PREDICTED USING 5 PT METHOD.
VALUE PREDICTED FROM γ OVER ST. PORTION OF H & D CURVE.
β/α = 0.67
γ = 1.60
A2/AF
RATIO OF 2nd HARMONIC TO FUNDAMENTAL
1.0
0.9
0.8
0.7
0.6
0.5
0.4
0.3
0.2
0.1
0
4.0
3.0
2.0
1.0
0
0.6
1.2
1.8
2.4
3.0
REL LOG E.

FIGURE 3.25.

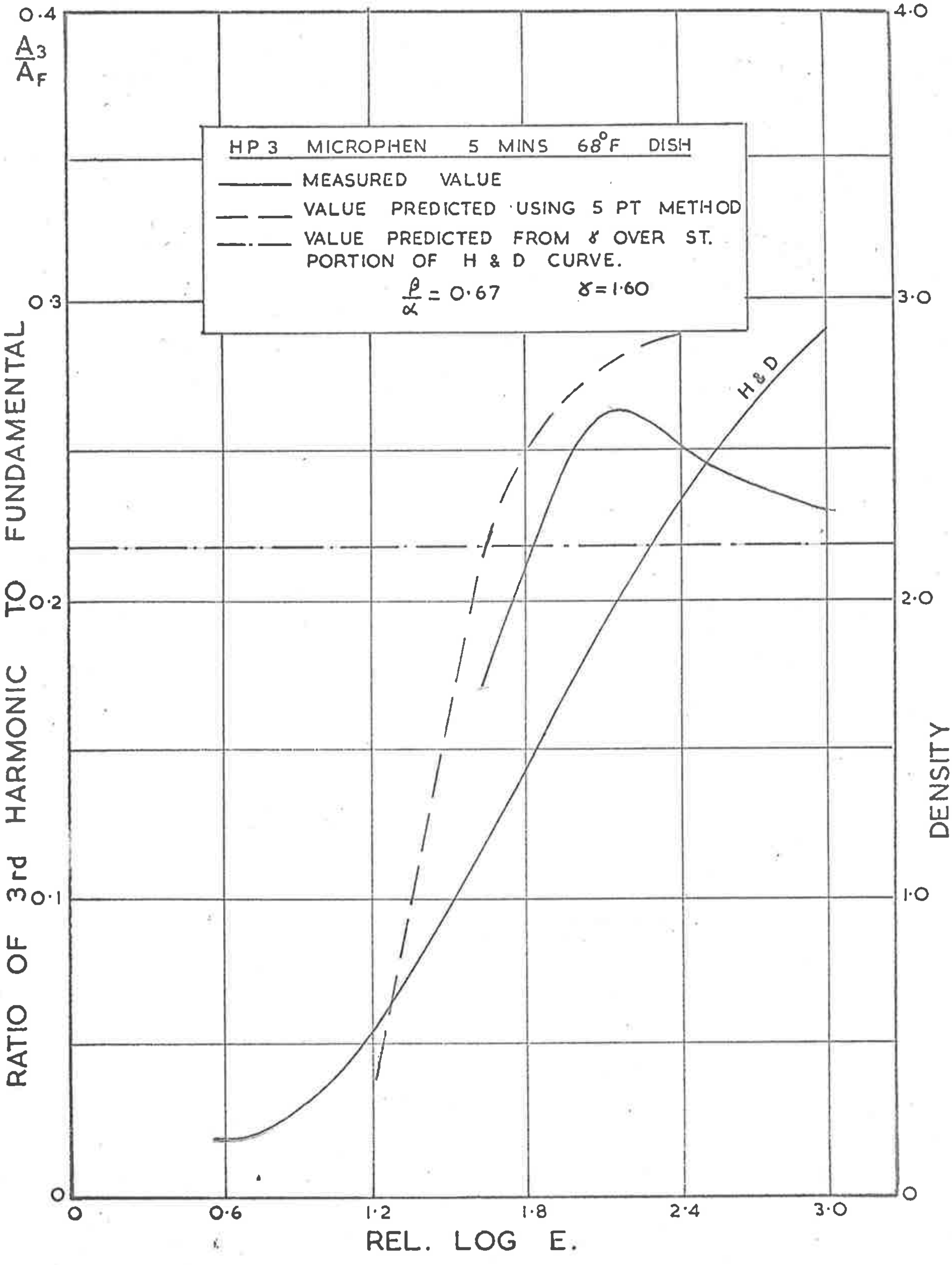
HP 3 MICROPHEN 5 MINS 68°F DISH
MEASURED VALUE
VALUE PREDICTED USING 5 PT METHOD
VALUE PREDICTED FROM γ OVER ST. PORTION OF H & D CURVE.
β/α = 0·67
γ = 1·60
H & D
A3/AF
RATIO OF 3rd HARMONIC TO FUNDAMENTAL
DENSITY
REL. LOG E.
0·4
0·3
0·2
0·1
0
0·6
1·2
1·8
2·4
3·0
4·0
3·0
2·0
1·0
0

FIGURE 3.26.

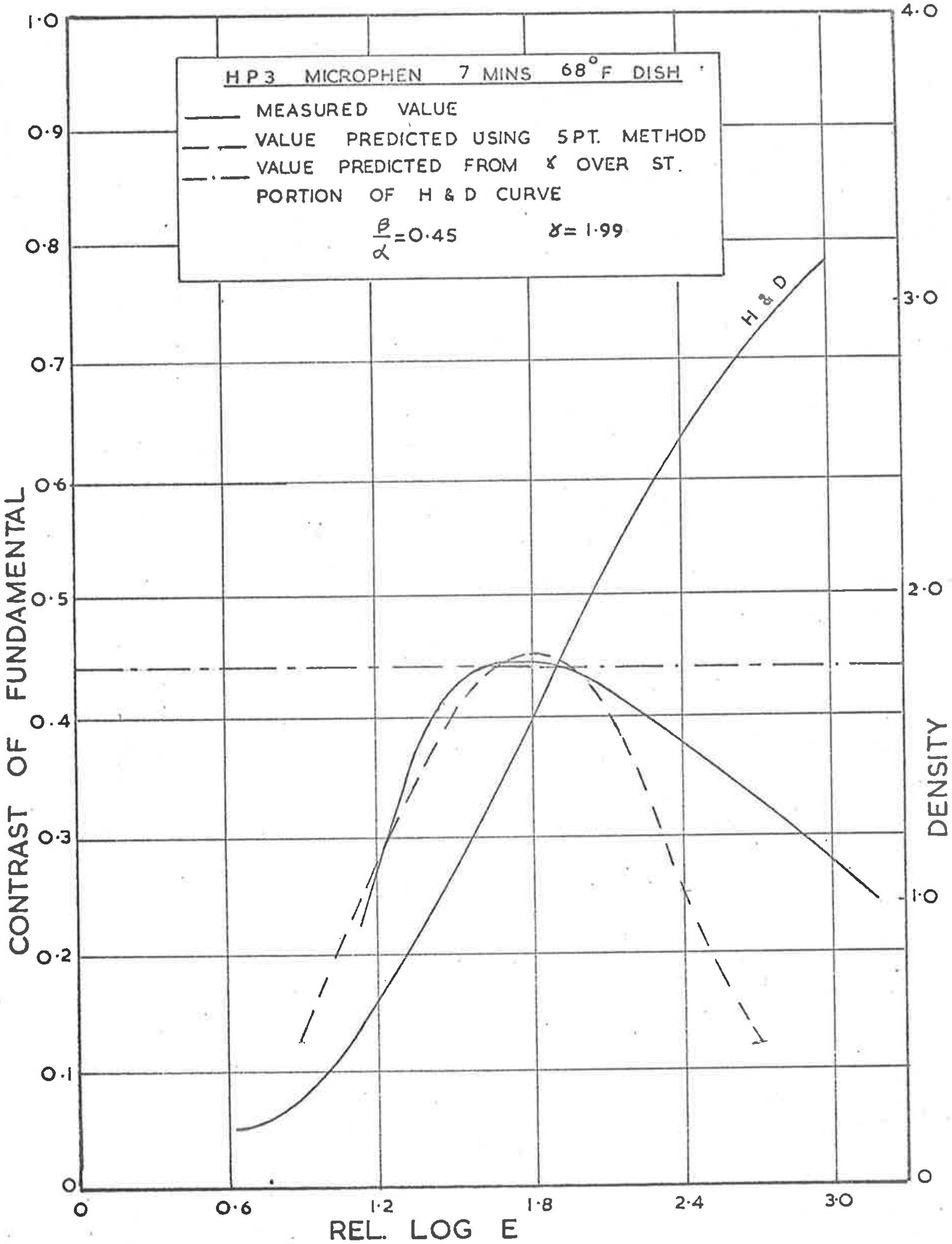

HP3 MICROPHEN 7 MINS 68°F DISH
MEASURED VALUE
VALUE PREDICTED USING 5 PT. METHOD
VALUE PREDICTED FROM γ OVER ST. PORTION OF H & D CURVE
β/α = 0·45
γ = 1·99
H & D
CONTRAST OF FUNDAMENTAL
DENSITY
REL. LOG E
1·0
0·9
0·8
0·7
0·6
0·5
0·4
0·3
0·2
0·1
0
0·6
1·2
1·8
2·4
3·0
4·0
3·0
2·0
1·0

FIGURE 3. 27.

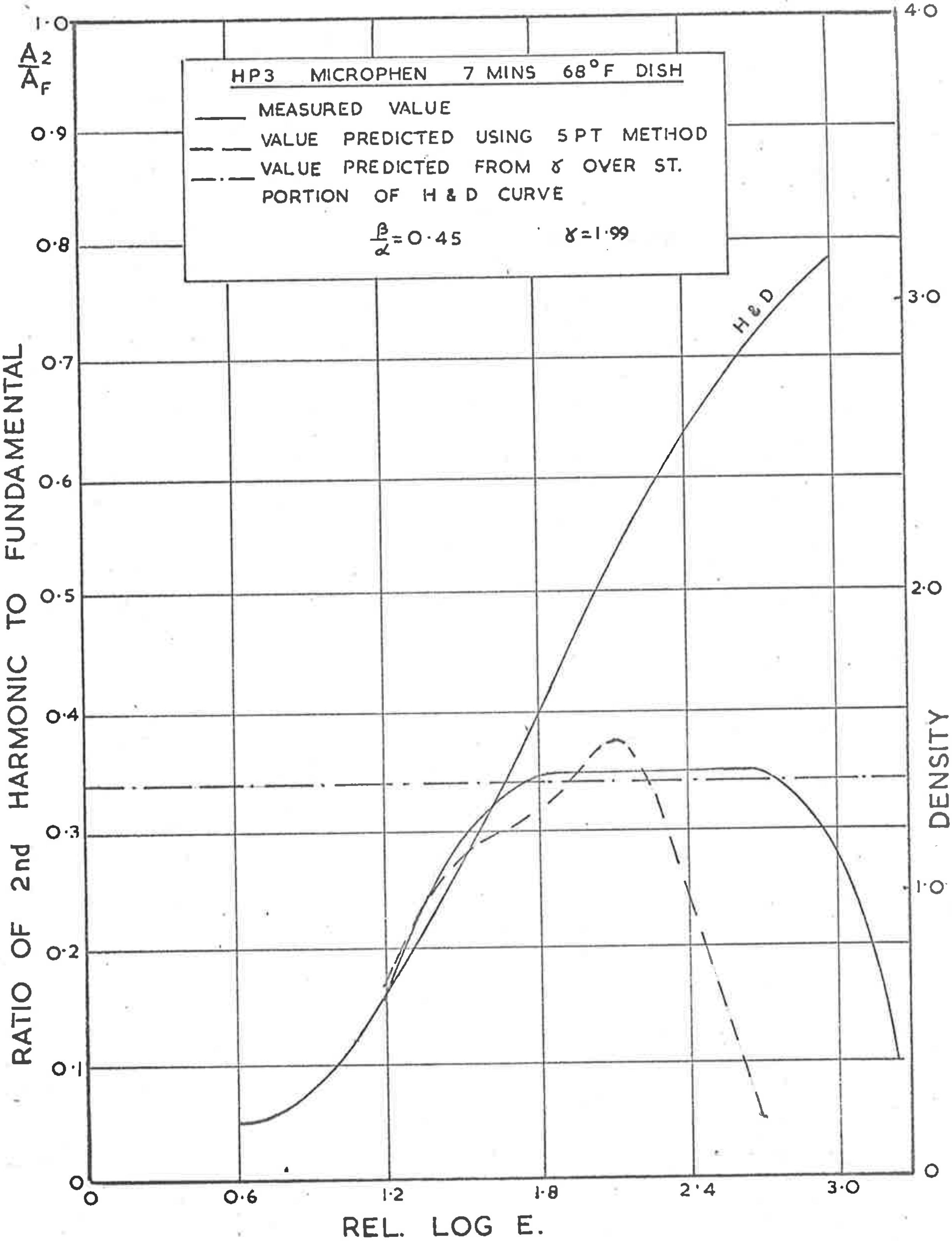

1·0
$\frac{A_2}{A_F}$
0·9
0·8
0·7
0·6
0·5
0·4
0·3
0·2
0·1
0
RATIO OF 2nd HARMONIC TO FUNDAMENTAL
HP3 MICROPHEN 7 MINS 68°F DISH
MEASURED VALUE
VALUE PREDICTED USING 5PT METHOD
VALUE PREDICTED FROM γ OVER ST. PORTION OF H & D CURVE
$\frac{\beta}{\alpha} = 0{\cdot}45$
$\gamma = 1{\cdot}99$
H & D
4·0
3·0
2·0
1·0
0
DENSITY
0
0·6
1·2
1·8
2·4
3·0
REL. LOG E.

FIGURE 3.28.

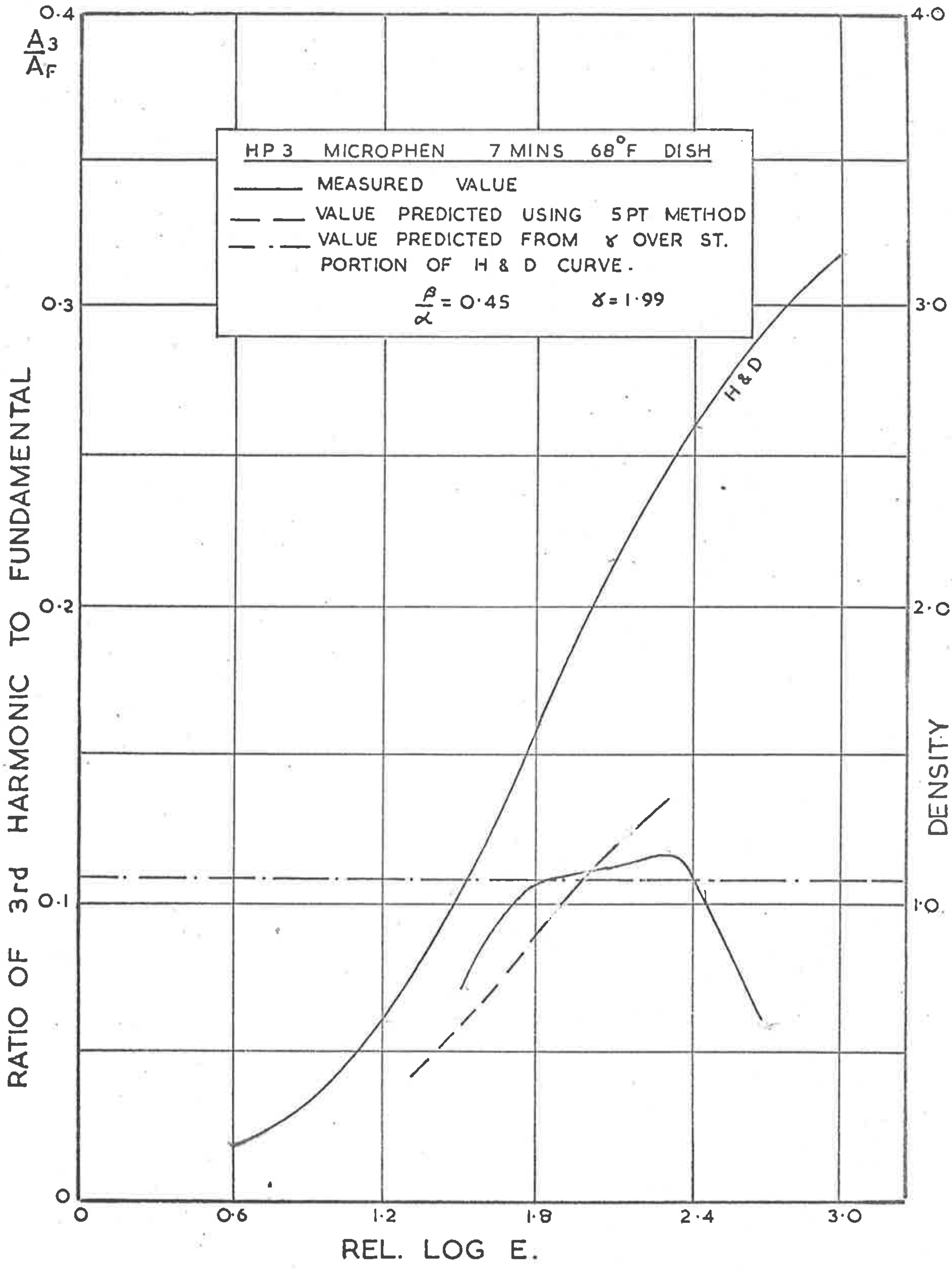
0.4
$\frac{A_3}{A_F}$
HP3 MICROPHEN 7 MINS 68°F DISH
MEASURED VALUE
VALUE PREDICTED USING 5PT METHOD
VALUE PREDICTED FROM γ OVER ST. PORTION OF H & D CURVE.
$\frac{\beta}{\alpha} = 0.45$
$\gamma = 1.99$
4.0
0.3
3.0
H & D
RATIO OF 3rd HARMONIC TO FUNDAMENTAL
0.2
2.0
DENSITY
0.1
1.0
0
0
0.6
1.2
1.8
2.4
3.0
REL. LOG E.

FIGURE 3. 29.

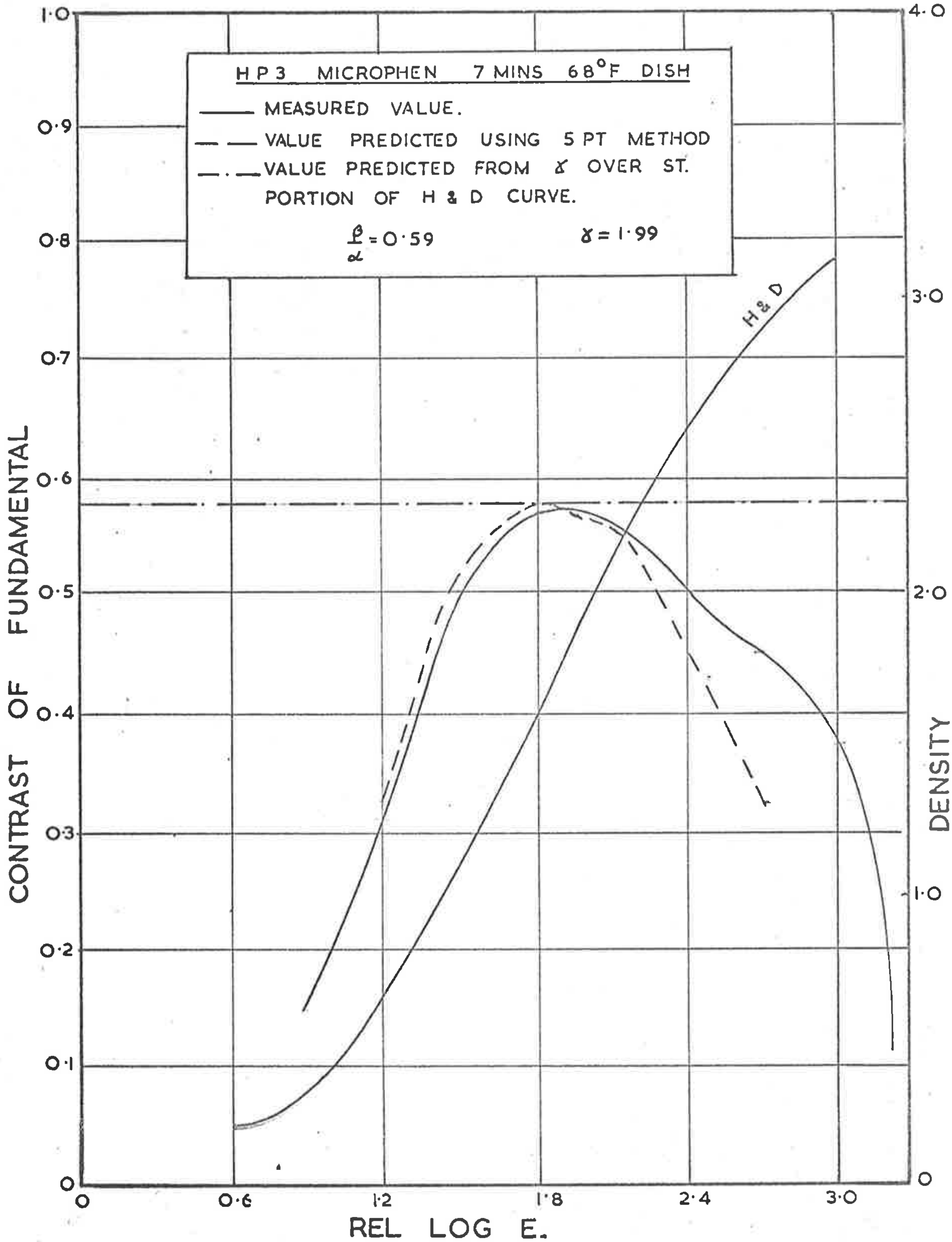

HP3 MICROPHEN 7 MINS 68°F DISH
MEASURED VALUE.
VALUE PREDICTED USING 5 PT METHOD
VALUE PREDICTED FROM γ OVER ST. PORTION OF H & D CURVE.
β/α = 0·59
γ = 1·99
H & D
CONTRAST OF FUNDAMENTAL
DENSITY
REL LOG E.
1·0
0·9
0·8
0·7
0·6
0·5
0·4
0·3
0·2
0·1
0
0·6
1·2
1·8
2·4
3·0
4·0
3·0
2·0
1·0

FIGURE 3.30.

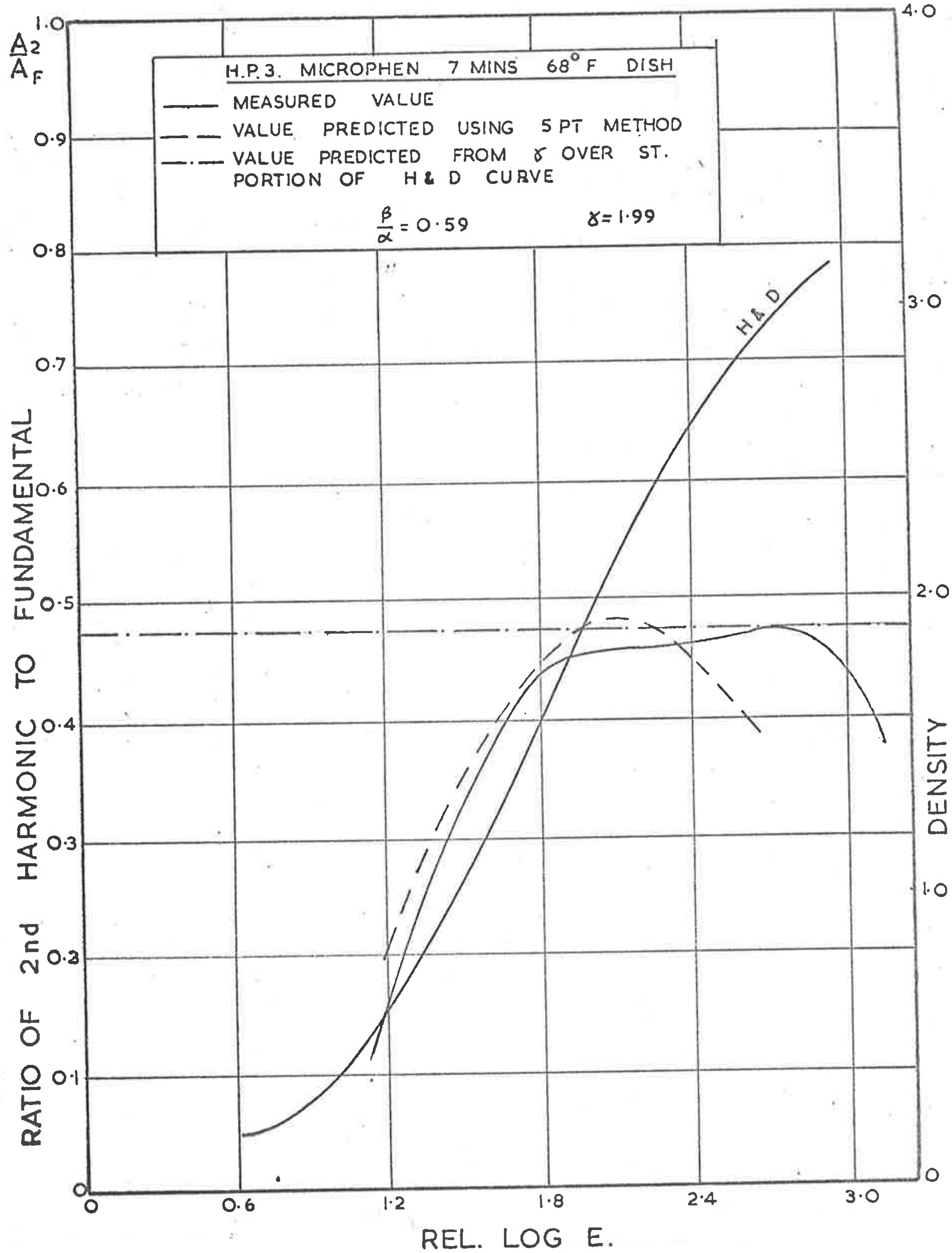

H.P.3. MICROPHEN 7 MINS 68° F DISH
MEASURED VALUE
VALUE PREDICTED USING 5 PT METHOD
VALUE PREDICTED FROM γ OVER ST. PORTION OF H & D CURVE
$\frac{\beta}{\alpha} = 0 \cdot 59$
$\gamma = 1 \cdot 99$
$\frac{A_2}{A_F}$
RATIO OF 2nd HARMONIC TO FUNDAMENTAL
DENSITY
H & D
1.0
0·9
0·8
0·7
0·6
0·5
0·4
0·3
0·2
0·1
0
4.0
3·0
2·0
1·0
0
0·6
1·2
1·8
2·4
3·0
REL. LOG E.

FIGURE 3.31.

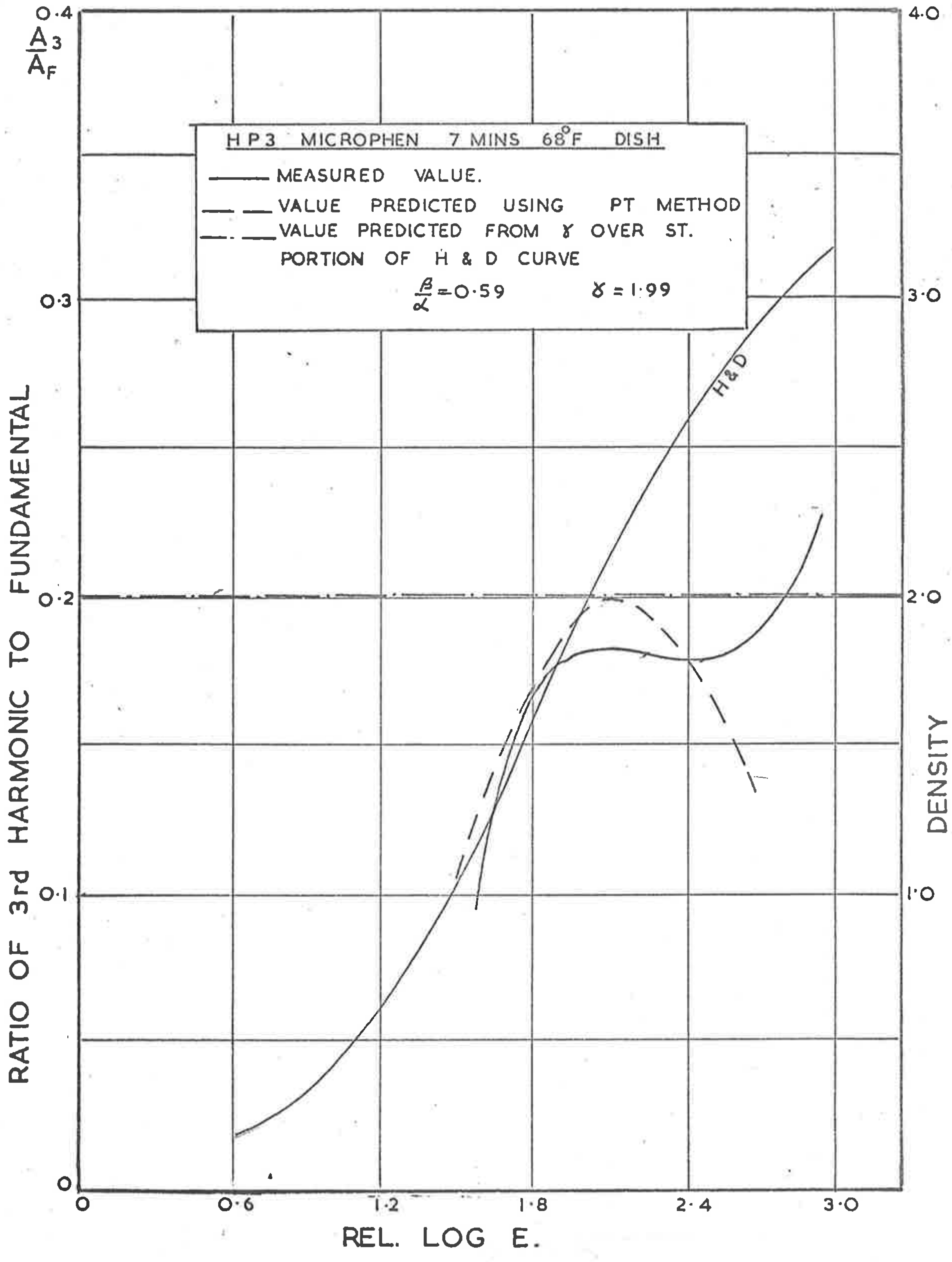
HP3 MICROPHEN 7 MINS 68°F DISH
MEASURED VALUE.
VALUE PREDICTED USING PT METHOD
VALUE PREDICTED FROM γ OVER ST. PORTION OF H & D CURVE
β/α = 0·59
γ = 1·99
H&D
$\frac{A_3}{A_F}$
RATIO OF 3rd HARMONIC TO FUNDAMENTAL
DENSITY
REL. LOG E.
0
0·1
0·2
0·3
0·4
0·6
1·2
1·8
2·4
3·0
1·0
2·0
3·0
4·0

FIGURE 3.32.

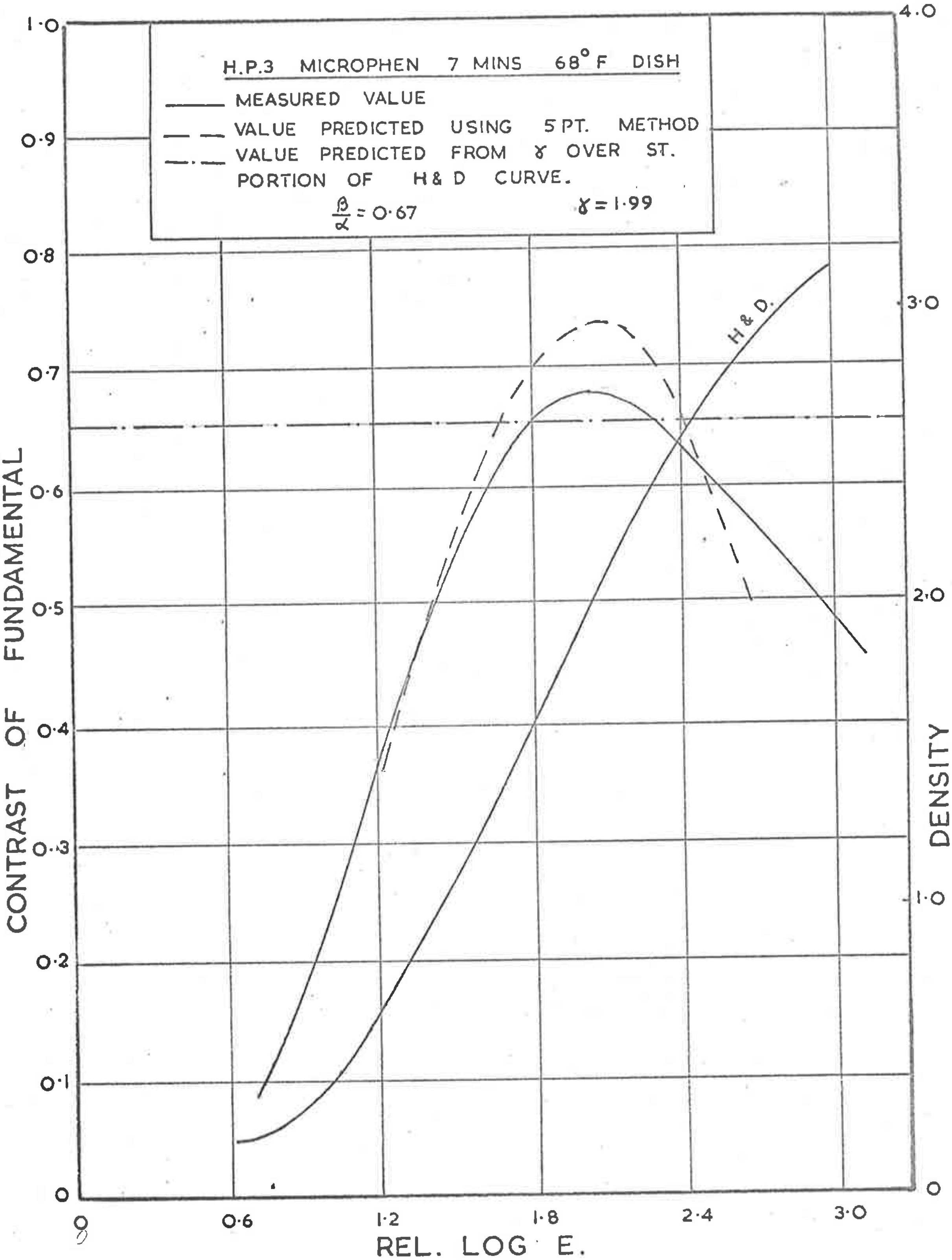
H.P.3 MICROPHEN 7 MINS 68° F DISH
MEASURED VALUE
VALUE PREDICTED USING 5 PT. METHOD
VALUE PREDICTED FROM γ OVER ST. PORTION OF H & D CURVE.
β/α = 0·67
γ = 1·99
H & D.
CONTRAST OF FUNDAMENTAL
DENSITY
REL. LOG E.
1·0
0·9
0·8
0·7
0·6
0·5
0·4
0·3
0·2
0·1
0
4.0
3·0
2·0
1·0
0
0
0·6
1·2
1·8
2·4
3·0

FIGURE 3.33.

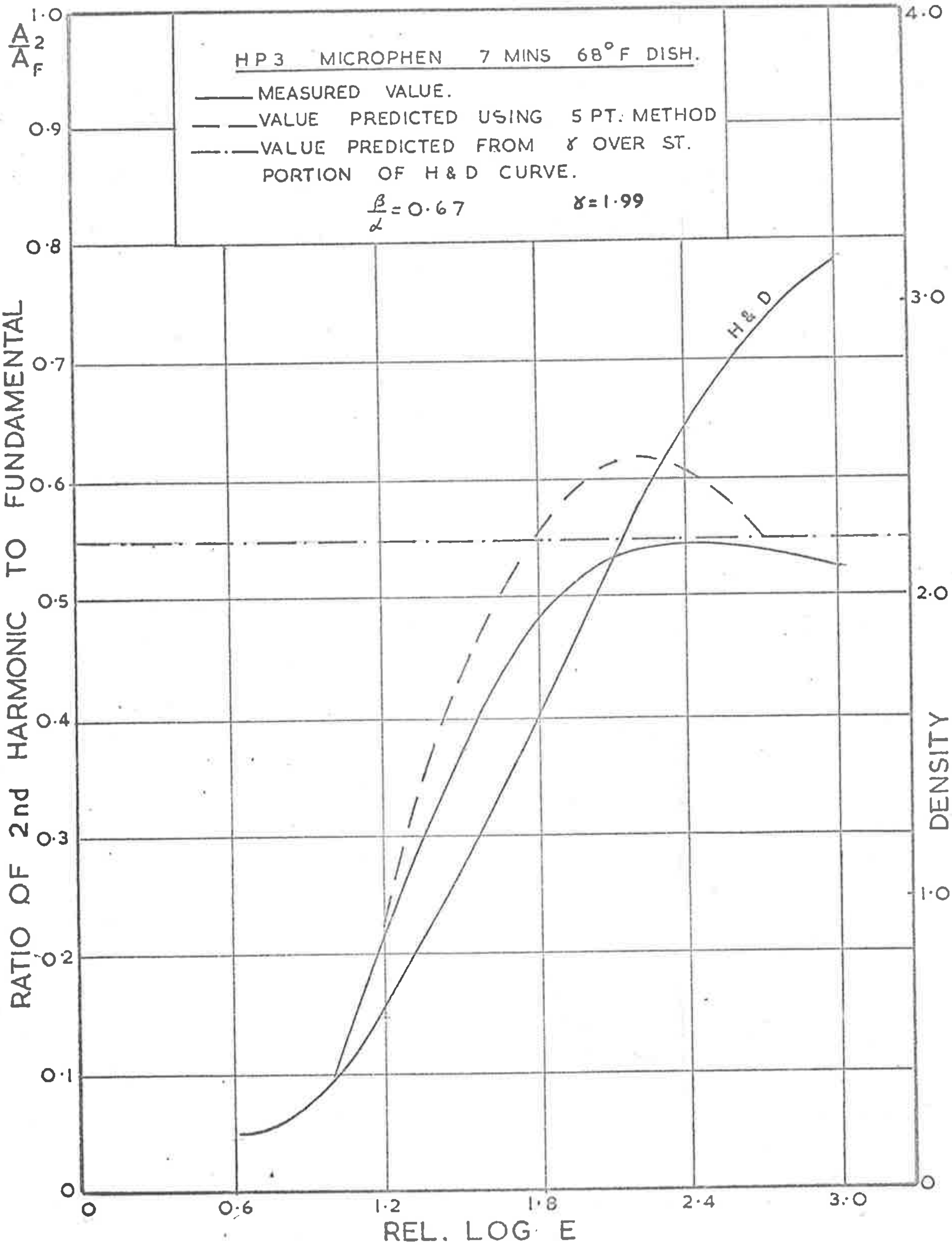
HP3 MICROPHEN 7 MINS 68°F DISH.
MEASURED VALUE.
VALUE PREDICTED USING 5 PT. METHOD
VALUE PREDICTED FROM γ OVER ST. PORTION OF H & D CURVE.
β/α = 0·67
γ = 1·99
H & D
A2/AF
RATIO OF 2nd HARMONIC TO FUNDAMENTAL
DENSITY
REL. LOG E
0
0·1
0·2
0·3
0·4
0·5
0·6
0·7
0·8
0·9
1·0
0·6
1·2
1·8
2·4
3·0
1·0
2·0
3·0
4·0

FIGURE 3.34.

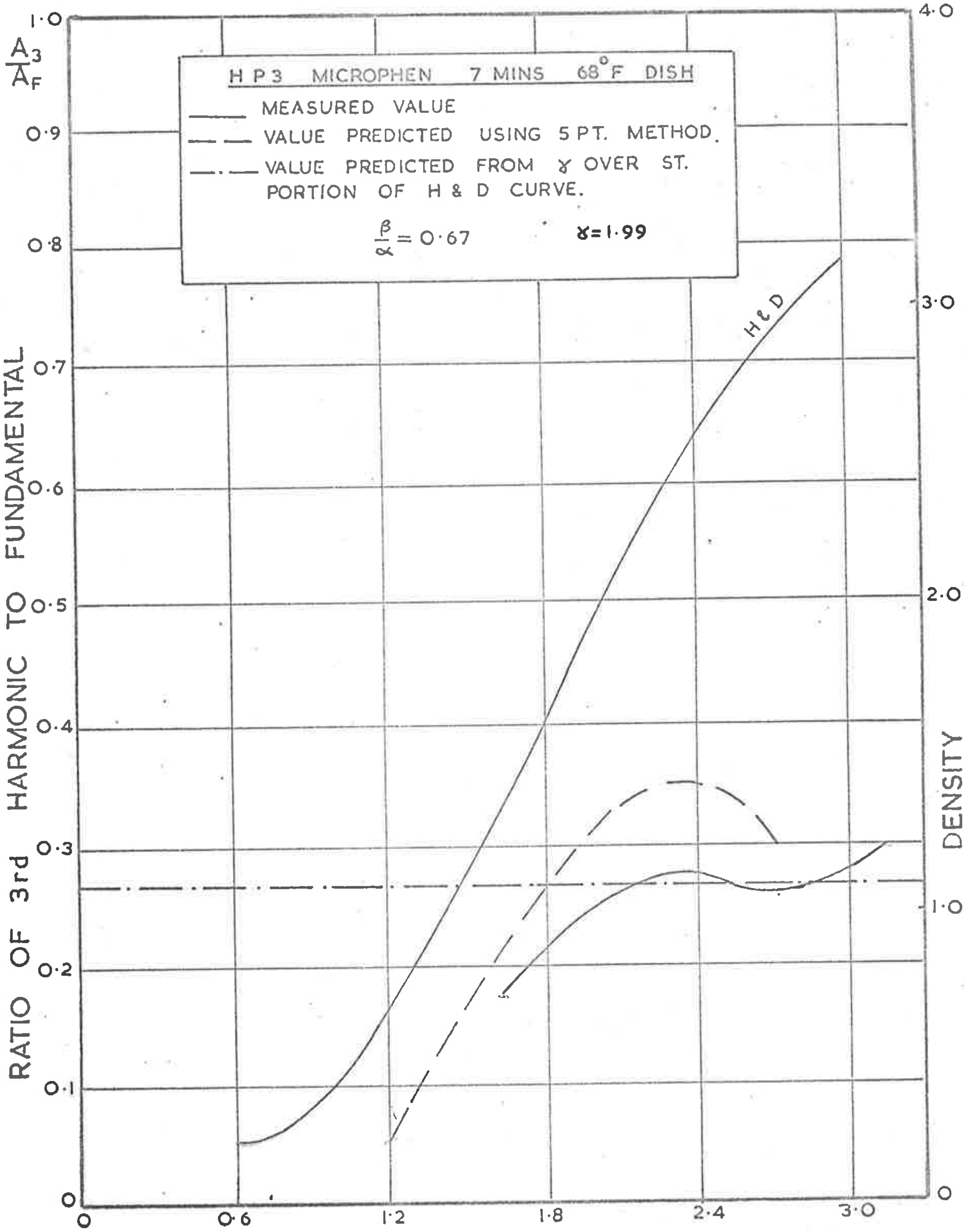

H P 3 MICROPHEN 7 MINS 68°F DISH
MEASURED VALUE
VALUE PREDICTED USING 5 PT. METHOD.
VALUE PREDICTED FROM γ OVER ST. PORTION OF H & D CURVE.
β/α = 0·67
γ=1·99
H & D
RATIO OF 3rd HARMONIC TO FUNDAMENTAL
A_3/A_F
DENSITY
REL. LOG E.
0
0·1
0·2
0·3
0·4
0·5
0·6
0·7
0·8
0·9
1·0
0·6
1·2
1·8
2·4
3·0
1·0
2·0
3·0
4·0

FIGURE 3. 35

the measured values by neighbourhood effects. This tends to agree with conclusions from the comparison of the five point method and the harmonic analysis method which were that the five point method loses accuracy as the contrast increases especially for high gammas.

If we restrict our attention to the fundamental contrast curves it is a significant observation that as the effective exposure contrast increases the optimum exposure tends to move up the H & D curve, thus the optimum exposure for sine waves of contrast 0.45 is around 1.8 where for a contrast of 0.67 it is around 2.1. The reason for this is that if we plot out a sine wave in logarithmic units, the log exposure interval from the mean level to the minimum is greater than that from the mean to the maximum and this difference is more marked as the contrast increases. Thus if we wish to get as much of the exposure on the straight part of the H & D curve as possible we must move up it as the contrast increases. This also means that the contrast of the fundamental in the transparency is much more critical to exposure for high contrast objects than for low contrast ones. This can be clearly seen by comparing figures 3.9 and 3.15. Another factor which is observed is that the contrast of the fundamental is more critical to under exposure than over exposure. This is especially obvious from figure 3.24 where a change in exposure about the optimum position of 0.6 logarithmic units (equivalent to two stops) gives a change in contrast from 0.62 to 0.38 on the under exposure side and from 0.62 to 0.54 on the over exposure side. Again the reason for this is found in the way that the sine wave is distributed about its mean level when plotted in logarithmic units as would be expected the position of maximum contrast in all cases is found to be on the straight part of the H & D curve. This is contrary to the findings of Wilczynski (1960), and McKenzie (1931), who clearly state that "a signal recorded on the toe portion of the characteristic curve leads to the highest contrast in the image." The author feels that this difference in view comes about from a misuse of the word "contrast" by the above mentioned authors but that some explanation is required to clarify the position.

If one denotes the fundamental amplitude in the transparency by β and the mean level by α then, by definition, the contrast is given by the ratio, β/α. Using the five point method it is easy to show that β maximises in the toe region of the characteristic curve and is significantly greater than that deduced on the straight part of the curve. This might lead one to think that the contrast is greater in the toe region but a factor which must be borne in mind is that the value of α is also greater in the toe region. Thus the important variable to calculate is β/α and when this is done it is found that "a signal recorded on the straight part of the characteristic curve leads to the highest contrast in the image". This is a satisfying result in that it agrees with what one experiences when visually examining the transparencies.

III.4.6 Conclusions from experiment with low frequency sine waves

From the results of this experiment it is possible to make a number of conclusions:-

(a) The five point method may be used to estimate the harmonic distortion in sine wave images provided that the contrast or gamma are not too high. We can set approximate maximum values on these two variables of 0.6 for contrast and 1.6 for gamma.

(b) If we restrict our exposure to the straight part of the characteristic curve, the magnitude of the harmonic distortion occurring in images of sine waves can be estimated by using the graphs deduced in III.2. This treatment holds for contrasts up to 0.8 and gammas up to 2.0 but could easily be extended.

(c) The optimum position of exposure is on the straight part of the H & D curve, the exact location depending upon the contrast of the object, as the contrast increases the optimum position moves up the characteristic curve.

(d) The contrast of the image is more critical to exposure for high contrast objects than ones of low contrast.

(e) The contrast of the image is more critical to under exposure than over exposure about the optimum position.

III.5 Experiments to determine the frequency response of emulsions

III.5.1 General discussion

Using the apparatus described there are two methods of determining the frequency response of a photographic emulsion.

In the first method sine waves of known frequency and contrast are exposed and developed together with a density step wedge. The transparencies are analysed with the apparatus and the mean intensity and harmonic amplitudes found. From these measurements the five values of I_T in equations 3.10 are deduced. Using these five values of I_T and the H & D curve five values of effective exposure are found. From these five values of effective exposure the contrast of the effective exposure is calculated and the ratio of this contrast to the original "printed-on" contrast is the frequency response of the emulsion at that particular frequency.

Besides being a rather lengthy process, once having made the necessary measurements, there are difficulties in the measurement which make this method a little cumbersome. One of the difficulties is that measurements have to be made of the contrast of the harmonics which say, in the case of 30 lines/mm, means extending our measurements into the 100 lines/mm region. This necessitates a change of prisms or using the coarse (2^{o}) prisms throughout which is undesirable from the point of view of accurate setting. However, bearing in mind the results of the previous experiment we can, by careful choice of exposure, restrict ourselves to measurements of the contrast of the fundamental frequency only. This is the basis of the second method which has been established and used to measure the response functions of four Ilford emulsions. It can be seen from figure 3.12 that if we give an exposure around the 1.5 Rel Log E position, the contrast of the fundamental measured agrees well with that predicted from the measured gamma of the H & D curve. Thus if we have a graph of measured fundamental contrast against effective exposure contrast for that particular gamma and restrict our exposure to the predetermined level, all we have to do is measure the fundamental contrast and read off the effective exposure contrast to determine the response function.

III.5.2 Experimental procedure

The experimental procedure was as follows; exposures were made of fringes of known contrast (0.59 in this case) in steps of 6 lines/mm up to a maximum frequency of 48 lines/mm. The exposure was predetermined to give us the above discussed condition. A density wedge was also exposed on the plate. The gamma of the H & D curve was measured and, using figure 3.6, the graph of fundamental contrast in the transparency against effective exposure contrast for this particular gamma was plotted. The developed plate was now returned to the apparatus and the fundamental contrast in each exposure measured as described in the previous experiment. Using these measured contrasts and the above mentioned graph, the effective exposure contrast for each frequency was determined. This value divided by the printed on contrast (0.59 in this case) gives the response of the emulsion for the particular frequency being considered.

This procedure was repeated using four different Ilford emulsions namely, H.P.3, F.P.4 (plate version of F.P.3), R20, and G30 (Chromatic Plate). It was not possible to obtain any information from the manufacturers to test the accuracy of this method but a curve, appearing in a paper by Shaw[4] (Ilford 1962) for H.P. 3 agrees very well with that determined by this method.

The four response functions are presented in the usual form of contrast transfer factor versus frequency in lines/mm and can be seen in figures 3.36 - 3.39.

III.5.3 Discussion of results

From the results obtained F.P.4 has a superior response over the frequency range considered than any of the other three emulsions which all have similar response functions. A significant factor is that for three of the emulsions the response is greater than unity for low frequencies. This arises because the contrast measured is greater than it theoretically should be due probably to neighbourhood effects[2]. Unfortunately there is not a method available for taking into account these effects and arriving at the true response functions; it suffices to say that at these frequencies the response is high and of the order of unity.

It is interesting to consider how the frequency response of an emulsion can effect the choice of emulsion when the frequency content of the subject to be photographed is known. A short experiment was conducted using H.P.3 and F.P.4 which have significantly different response functions. On each plate sine waves of contrast 0.59 and frequency 3.0 lines/mm and 30 lines/mm were exposed with exposures covering the complete range of the H & D curve. In figures 3.40 and 3.41 the experimental results are presented in the form of fundamental contrast in the transparency as a function of exposure. From figure

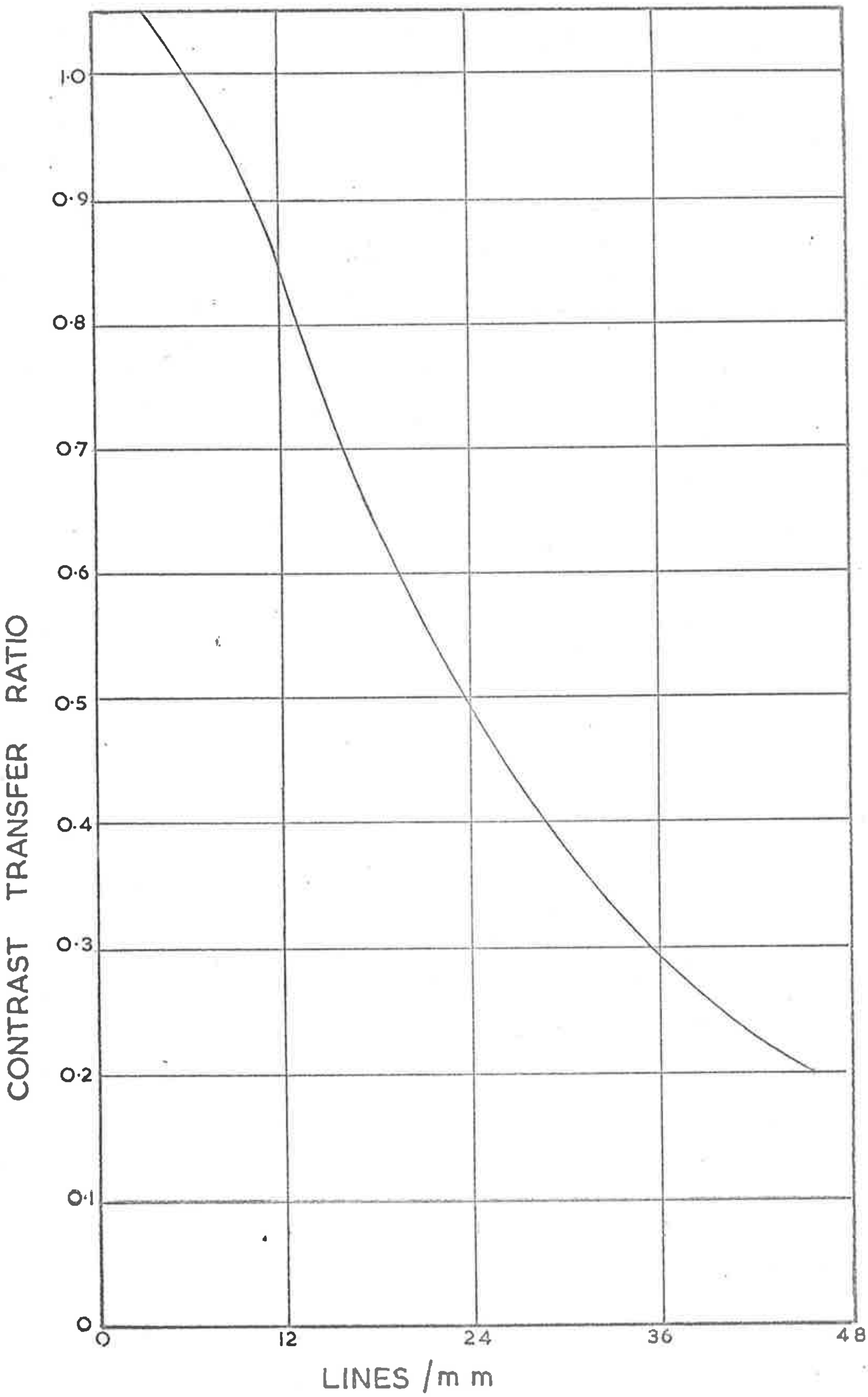

FIGURE 3.36 EMULSION H.P. 3.

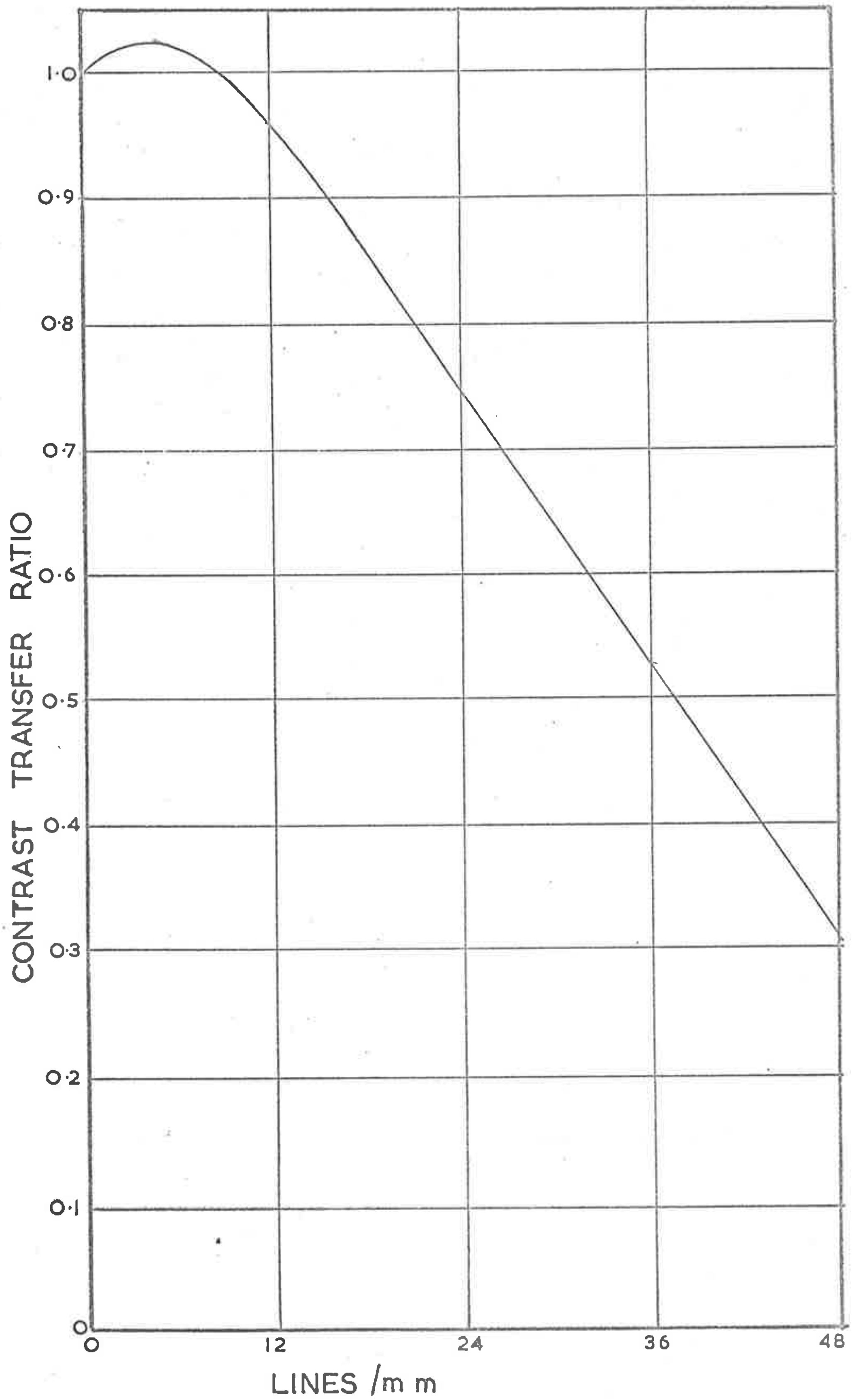

FIGURE 3.37. EMULSION F.P. 4

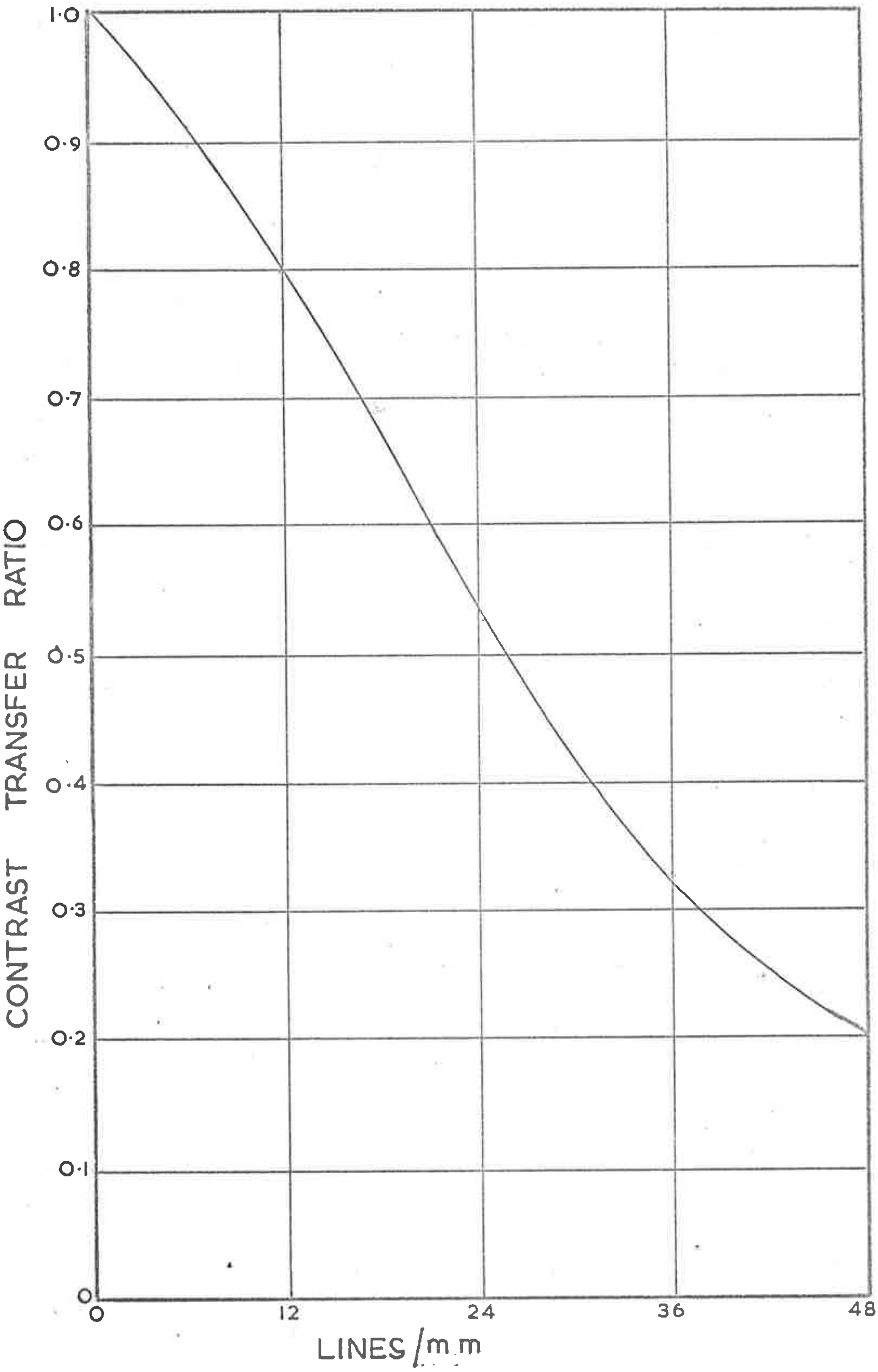

FIGURE 3.38 EMULSION R 20

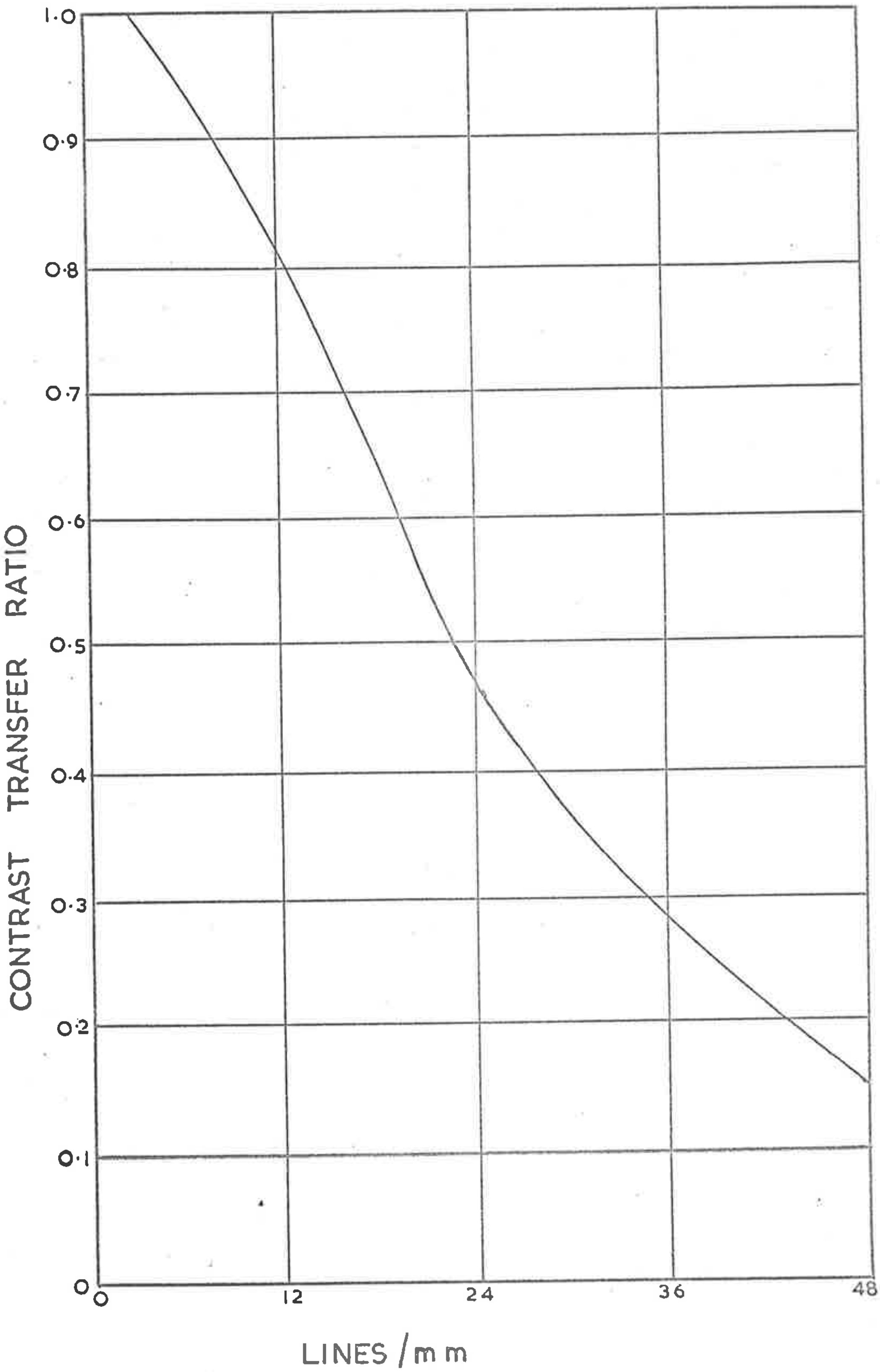

FIGURE 3.39 EMULSION G.30 CHROMATIC PLATE.

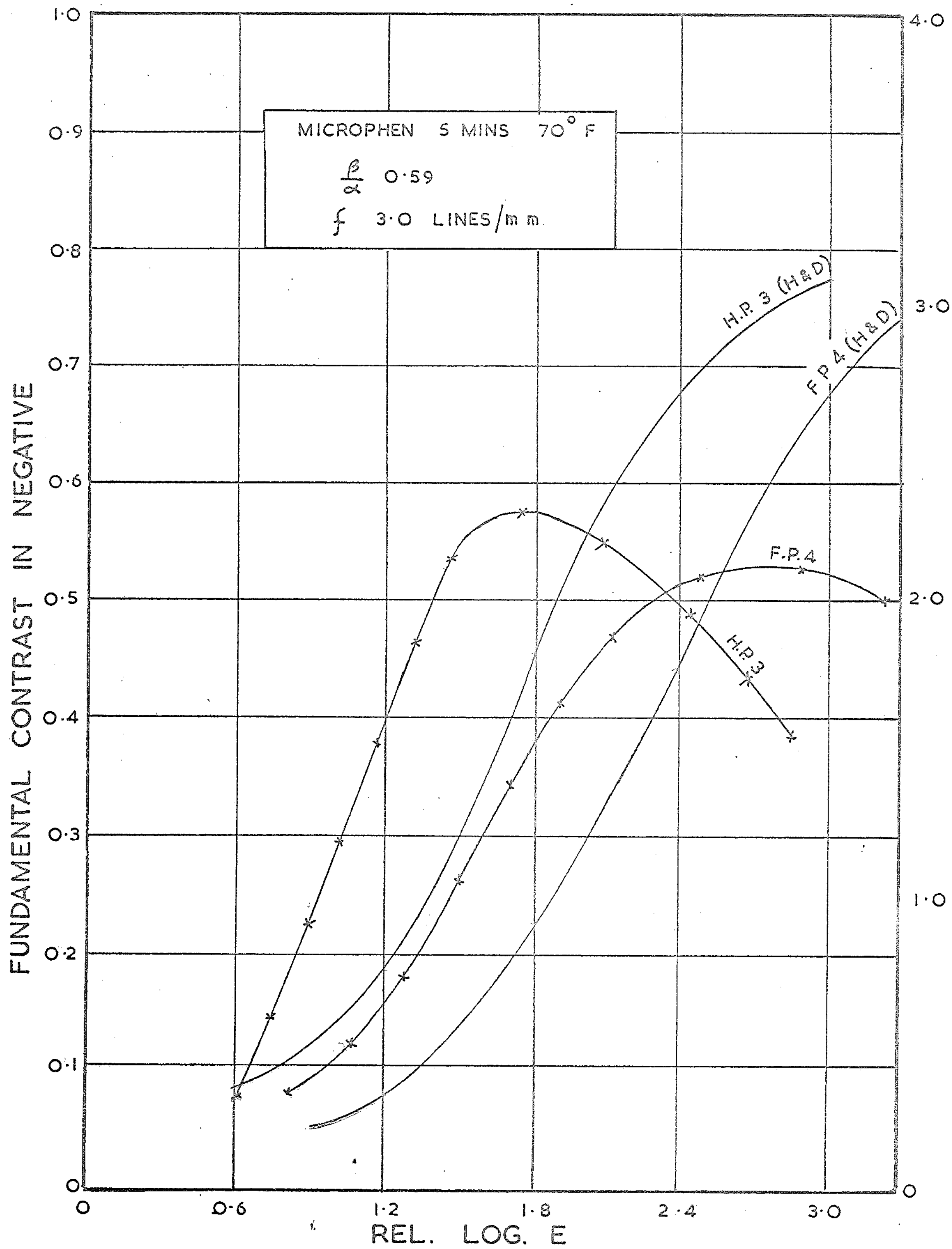

MICROPHEN 5 MINS 70° F
β/α 0·59
f 3·0 LINES/mm
H.P. 3 (H&D)
F.P. 4 (H&D)
F.P. 4
H.P. 3
FUNDAMENTAL CONTRAST IN NEGATIVE
REL. LOG. E
1·0
0·9
0·8
0·7
0·6
0·5
0·4
0·3
0·2
0·1
0
0·6
1·2
1·8
2·4
3·0
4·0
3·0
2·0
1·0
0

FIGURE 3. 40.

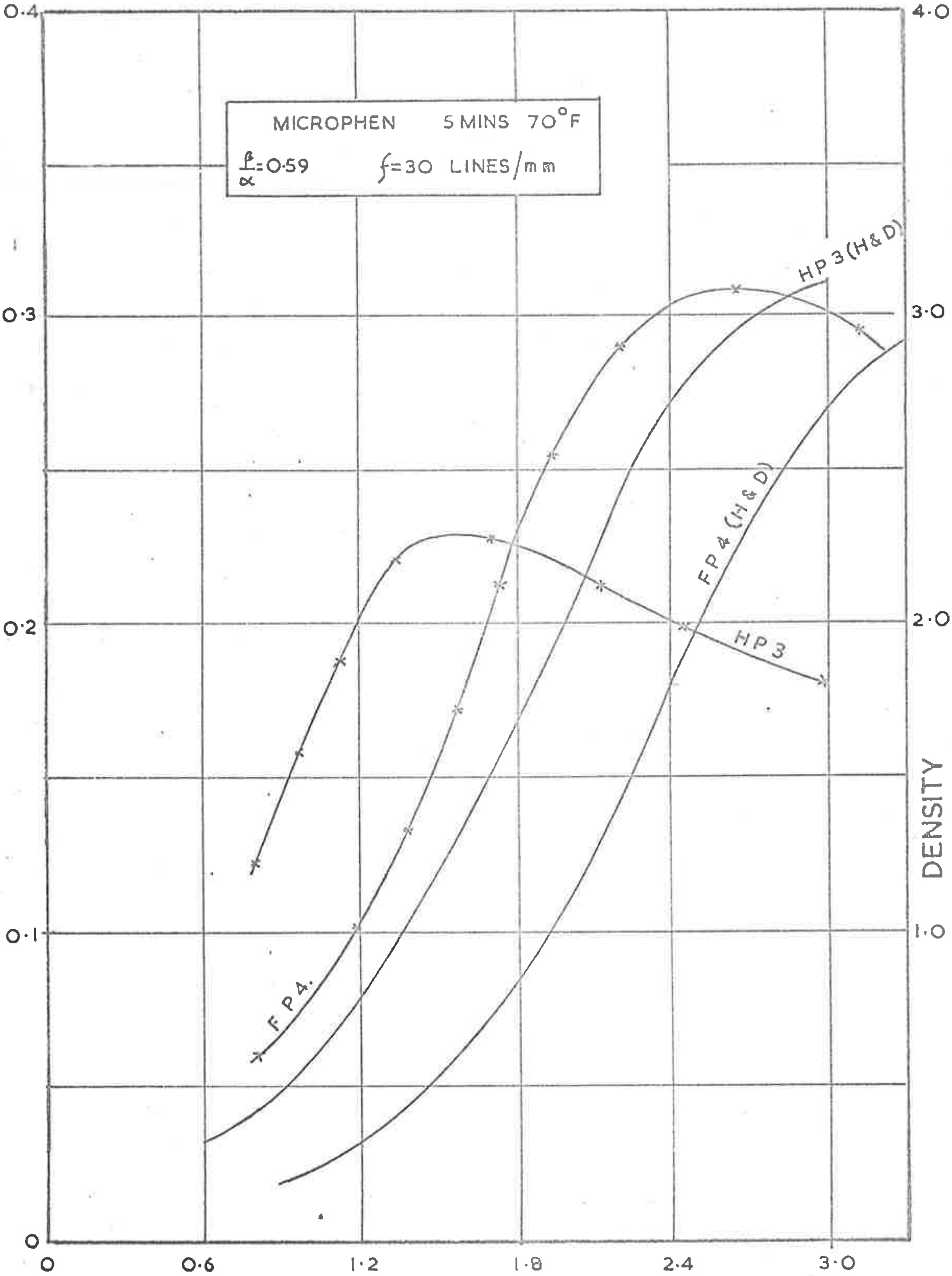

REL. LOG E.

FIGURE 3. 41.

3.40 it can be seen that for a frequency of 3.0 lines/mm and the development conditions stated, which were the same for each plate, it would be preferable to use H.P.3 up to an exposure level of about 2.3 but that, if the frequency is 30 lines/mm, it would only be preferable to use H.P.3 up to a level of 1.8. This change is brought about purely by the superior response of F.P.4 at this particular frequency.

From this short experiment we can conclude that for a certain fixed exposure level and development conditions, there is an optimum emulsion to use depending on the frequency content of the subject. Consider the exposure level 2.1 in the experiment; for 3.0 lines/mm it is preferable to use H.P.3 but for 30.0 lines/mm F.P.4 presents itself as the better emulsion. The importance of the frequency response function of an emulsion as a contributing factor in the final observed image is obvious from the above experiment.

It would seem reasonable to expect that the emulsion with the best response function is capable of recording most information and should, if possible, be used. Thus if we have control over the exposure level, we can adjust this so that the emulsion with the highest response can be used and providing it can be developed to a sufficiently high gamma the best results will be obtained.

REFERENCES

1.	Espley, D.C.	(1933)	Proc. I.R.E. 21 1439
2.	Wilezynski, J.	(1960)	Thesis, P.125 **University of London**
3.	McKenzie, D.	(1931)	J.S.M. PE, 17 172
4.	Shaw, R.	(1962)	P.S. & E. 6 284

CHAPTER IV

POSSIBLE APPLICATIONS OF APPARATUS AND RESULTS SO FAR OBTAINED

It has been shown that, when photographing an object of known contrast, an optimum exposure exists for a particular emulsion and development. This treatment could be extended to any emulsion - developer combination, results given in this paper only refer to H.P.3 developed in Microphen.

Two methods have been outlined for determining the frequency response function of an emulsion and again these could be extended to emulsions other than the four investigated here.

The optimum exposure, referred to above, has so far been assumed to be that exposure which gives the greatest contrast of the original fundamental frequency in the transparency function. Assuming that we restrict ourselves to negatives and have methods at our disposal of filtering out the harmonics, this would be the best exposure for reading information from the recorded image about the aerial image.

If we now consider making a positive from the negative we encounter the possibility of making the overall process linear. Denoting the gamma of the negative by γ_1 and that of the positive γ_2, it is easy to arrive at the condition that, if $\gamma_1 \gamma_2 = 1$, the process is linear and the transmission of the positive is linearly related to the original object brightness. The apparatus described would lend itself well to an investigation of how linear the process could be made and over what range of exposure it could be considered linear. This could be done by exposing sine waves over the complete range of the negative characteristic curve and analysing the transparencies obtained when forming positives of these exposures. If the process was completely linear the transparencies would contain only the fundamental frequency with exactly the same contrast as the original. Any deviations from linearity would be detected by the presence of harmonics in the transparencies. The range over which the process could be considered linear would obviously vary with the contrast of the object and to some extent with the frequencies involved. The light transmitted by the negative will contain the fundamental frequency and harmonics and the positive material must have a response which is high over a range sufficient to cover all the harmonics presented to it. If these harmonics are attenuated before the positive development process then distortion in the negative will not be completely compensated for by the positive and distortion will remain in the final image. This immediately leads one to the conclusion that the negative should be developed to a relatively low gamma to keep distortion down to a low level at this stage, and that the positive should be developed to a relatively high gamma to arrive at the condition $\gamma_1 \gamma_2 = 1$. This is the usual procedure when making positives but the range over which the process is linear is not always known. Of course fidelity of tone reproduction is not always the prime objective and development of negatives to a low gamma not always advantageous. For instance if detection of some object is the aim, definition is the important factor. Usually negatives are used and as harmonic distortion invariably goes hand in hand with better definition, a high gamma is sought. The tolerance of exposure is tighter because with high gammas the range of exposure over which the H & D curve is straight is usually not great. In practical cases probably some compromise has to be arrived at because of lack of control over exposure.

The instrument could also be used in an attempt to study the effect of frequency content on acceptability of images. Initially the frequency content of a picture (transparency) could be determined. The transparency could then be placed in an image enhancer, which is effectively a spatial frequency filter, and its spectrum altered by attenuating certain frequencies. A positive could be made of this altered image, analysed and then compared with the original. This could possibly be done a number of times and we would then have a series of pictures, basically the same, but differing in frequency content. These could be judged by an audience and perhaps some correlation between frequency content and acceptability arrived at. Similar experiments[1] to this have been performed by various authors but, although the transfer function of the imaging system has been known and altered (in the above case the image enhancer), the content of the final image has not been measured and thus the experiments have been incomplete, with consequent difficulty in assessing the significance of the results. It is felt that an experiment designed upon the previously discussed procedure would not suffer from this defect and that a more complete understanding of the significance of the frequency content of images would be arrived at.

REFERENCES

	Higgins, G.C.	Reprints of the 5th
1.	Lambert, R.L.	meeting and conference
	Wolfe, R.N.	of I.C.O.

ACKNOWLEDGEMENTS

The author would like to thank the Chief Scientist, Australian Department of Supply, for permission to submit this thesis which is based on work carried out by him as part of a research project at the Weapons Research Establishment, Salisbury.

He would also like to thank Mr F.A. Dixon for guidance and helpful criticism offered to him concerning the substance of this thesis.

APPENDIX

VALUES OF COMPONENTS IN THE SELECTIVE AMPLIFIER CIRCUIT

Diagram 2.5

Valves

1. 12AU7
2. CV 5080

3.)
) 12AU7
4.)

5. 12AU7

6.)
) 12AU7
7.)

Condensers

1. 0.1μF
2. 8μF Electrolytic
3. 5000pF
4. 0.05μF
5. 0.05μF
6. 8μF Electrolytic
7. 8μF Electrolytic
8. 0.1μF
9. 10μF Paper
10. 0.1μF
11. 0.05μF
12. 10μF Paper
13. 0.05μF
14. 50μF Electrolytic

Resistors

1. 1 M ohm H.S.
2. 270K ohm
3. 30K ohm
4. 40K ohm
5. 5M ohm
6. 2.2K ohm
7. 500K ohm
8. 220K ohm
9. 1M ohm
10. 1M potentiometer
11. 820K ohm
12. 1.2M ohm
13. 80K ohm
14. 20K ohm
15. 1M ohm
16. 270K ohm
17. 820K ohm
18. 200K ohm
19. 1.2M ohm
20. 80K ohm
21. 20K ohm
22. 1M ohm
23. 270K ohm